RELATIONSHIP BETWEEN COMMUNITY STRUCTURE AND THE BIO-OPTICAL PROPERTIES OF MARINE PHYTOPLANKTON

by

Heather Alison Bouman

Submitted in partial fulfilment of the requirements
for the degree of Doctor of Philosophy

at

Dalhousie University
Halifax, Nova Scotia
July 2003

National Library
of Canada

Bibliothèque nationale
du Canada

Acquisitions and
Bibliographic Services

Acquisisitons et
services bibliographiques

395 Wellington Street
Ottawa ON K1A 0N4
Canada

395, rue Wellington
Ottawa ON K1A 0N4
Canada

Canada

DALHOUSIE UNIVERSITY

DEPARTMENT OF BIOLOGY

The undersigned hereby certify that they have read and recommend to the Faculty of Graduate Studies for acceptance a thesis entitled "Relationship between Community Structure and the Bio-Optical Properties of Marine Phytoplanton" by Heather Alison Bouman in partial fulfillment for the degree of Doctor of Philosophy.

Dated: July 18, 2003

External Examiner:

Research Supervisor:

Examining Committee:

Departmental Representative:

DALHOUSIE UNIVERSITY

Date: **18 July 2003**
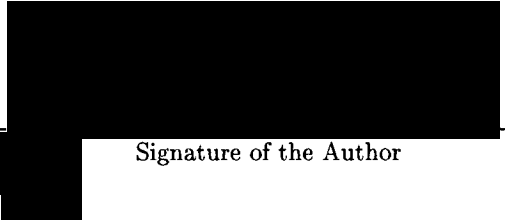
Author: **Heather Alison Bouman**

Title: **Relationship between Community Structure and the
           Bio-Optical Properties of Marine Phytoplankton**

Department: **Biology**

Degree: **Ph.D.**   Convocation: **October**   Year: **2003**

Permission is herewith granted to Dalhousie University to circulate and to have copied for non-commercial purposes, at its discretion, the above title upon request of individuals or institutions.

Signature of the Author

To my supervisor, Dr. Trevor Platt, for his constant support, guidance and encouragement.

TABLE OF CONTENTS

Chapter 4: Seasonal Variations in the Bio-optical Properties of Bedford Basin

Chapter 5: Summary and Conclusions

LIST OF FIGURES

LIST OF TABLES

ABSTRACT

In the marine environment it is often observed that changes in the absorptive and photosynthetic properties of marine phytoplankton are accompanied by changes in temperature. Since temperature is accessible to remote sensing, it is a possible proxy for the absorptive properties of phytoplankton, but its utility in this regard is relatively untested. Although temperature has been incorporated into several primary production models that use ocean colour data, such models have limited success in predicting primary production on regional scales. In this study, I assess the value of temperature as an indicator of the photosynthetic and absorptive properties of marine phytoplankton and consider how it might be applied to refine algorithms for retrieval of algal biomass and primary production from remotely-sensed data on ocean colour.

In the first part of the study, the use of temperature as a predictor of the absorptive characteristics of phytoplankton is assessed for a broad range of oceanic regimes. Using temperature as an independent variable, nearly half of the variance in the specific absorption coefficient of phytoplankton ($a_\phi^*(\lambda)$) at wavelengths (λ) 676 and 443 nm is explained. Using HPLC pigment and flow cytometric data, I demonstrate that our results are consistent with the view that the size structure and the taxonomic composition of phytoplanktonic communities are regulated by physical processes, for which temperature is often a suitable proxy.

In the second part, variability in the absorptive and photosynthetic properties of marine phytoplankton is examined in two regions: the Scotian Shelf and Bedford Basin. At both study sites, a strong correlation was found between phytoplankton size structure (indexed by the chlorophyll-a specific absorption coefficient at 676 nm) and primary productivity (indexed by the parameters of the photosynthesis-irradiance (P-E) response curve). The P-E parameter P_m^B was also strongly correlated with temperature. The results also show, however, that using temperature as a surrogate for P_m^B and $a_\phi^*(\lambda)$ in global algorithms of primary production will require a greater understanding of the underlying processes driving the relationships between temperature, phytoplankton community structure and light-saturated photosynthesis.

LIST OF SYMBOLS

Notation	Quantity [Units]
A	Clearance area of the filter used to measure particulate absorption [m^{-2}].
a_d	Absorption coefficient of detritus [m^{-1}].
$a_d(\lambda)$	Absorption coefficient of detritus at wavelength λ [m^{-1}].
a_t	Absorption coefficient of total particulates [m^{-1}].
a_x	Absorption coefficient of detritus or CDOM [m^{-1}].
$a_x(\lambda)$	Absorption coefficient of detritus or CDOM at wavelength λ [m^{-1}].
a_y	Absorption coefficient of CDOM [m^{-1}].
$a_y(\lambda)$	Absorption coefficient of CDOM at wavelength λ [m^{-1}].
a_ϕ	Absorption coefficient of phytoplankton [m^{-1}].
$a_\phi(\lambda)$	Absorption coefficient of phytoplankton at wavelength λ [m^{-1}].
$a_\phi^*(\lambda)$	Chlorophyll-a-specific absorption coefficient of phytoplankton at λ [m^2 mg^{-1}].
$\bar{a}_\phi^*$	Spectrally-averaged mean value of $a_\phi(\lambda)$ [m^{-1}].
B	Phytoplankton biomass, as chl-a concentration [mg m^{-3}].
C	Chlorophyll-a [mg m^{-3}].
$< D_s >$	Average mean equivalent spherical diameter of ultraphytoplankton cells ($<20\,\mu$m).
F_{dv}	Ratio of divinyl chl-a to total chl-a [dimensionless].
E	Available irradiance [W m^{-2}].
E_k	Irradiance at which the onset of saturation occurs, calculated as the ratio of P_m^B to α^B [W m^{-2}].
E_d	Direct component of available irradiance [W m^{-2}].
F_p	Ratio of the sum of diagnostic pigments associated with large cells to the sum of total diagnostic pigments [dimensionless].
n	Number of data points.
O_d	Optical density of detrital materials on the filter [dimensionless].
O_e	Optical density of extracted pigments in solution [dimensionless].

O_p	Optical density of particulate matter on the filter [dimensionless].
O_s	Optical density of particulate matter in suspension [dimensionless].
P	Instantaneous rate of primary production [mg C m^{-3} h^{-1}].
P^B	Production normalized to phytoplankton biomass [mg C (mg chl-a)$^{-1}$ h^{-1}].
P_m^B	Rate of photosynthesis at saturating irradiance, normalized to phytoplankton biomass [mg C (mg chl-a)$^{-1}$ h^{-1}].
P_{opt}^B	Maximum rate of photosynthesis in the water column [mg C (mg chl-a)$^{-1}$ h^{-1}].
S_d	Exponential coefficient describing the wavelength dependence of detrital absorption [nm^{-1}].
S_x	Exponential coefficient describing the wavelength dependence of detrital or CDOM absorption [nm^{-1}].
S_y	Exponential coefficient describing the wavelength dependence of CDOM absorption [nm^{-1}].
T	Water temperature at a given sampling depth [°C].
z	Depth [m].
V	Volume of seawater filtered [m^{-3}].
z_N	Distance between the sampling depth and the top of the nitracline [m].
z_m	Depth of the mixed layer [m].
α^B	Rate of photosynthesis at low irradiance, that is, the initial slope of the photosynthesis-irradiance curve, measured in broad-band light [mg C (mg chl-a)$^{-1}$ h^{-1} (W m^{-2})$^{-1}$].
λ	Wavelength [nm].
μ_m	Light-saturated maximum growth rate of phytoplankton [d^{-1}].
ϕ_m	Maximum quantum yield of photosynthesis [mol C (mol photons)$^{-1}$].
σ_T	Water density at a given sampling depth [kg m^{-3}].

ACKNOWLEDGEMENTS

incredibly useful in the interpretation of the dataset. The help and enthusiasm offered by Bill Li greatly advanced the development of the central theme of this work, namely the relationship between temperature and phytoplankton community structure. Programming has always been my achilles heel; however the assistance provided by Carla Caverhill, Heidi Maass and Cathy Porter helped me overcome (slightly) my fear of Fortran. Mary Kennedy helped me fill in the missing pieces of data which would have taken me a lifetime of rummaging through old log books to recover. I am forever indebted to Venetia Stuart, for her tremendous support and encouragement and for answering my innumerable questions about the absorption and pigment data. I would also like to thank Marilyn Landry for her help and support during my time at BIO.

Apart from the help I received for my thesis-related problems, I also experienced unexpected and touching moral support during my stint at the QEII and afterwards. Without the kindness, patience and understanding of my co-workers I honestly believe that I would not have been able to complete this work. I would especially like to thank Trevor and Shubha for their constant support. I would also thank my loving family and friends for sticking by me through it all.

CHAPTER 1

General Introduction

One of the principal goals of ecology is to relate ecological function to the structure of biological communities (Odum 1959). In studies of phytoplankton ecology the ecological function of interest is primary production. Over the past century many advances have been made in measuring both the structure of phytoplankton assemblages and their productivity. The structure of natural algal assemblages was first examined by light microscopy and this remains a common method used to obtain detailed information on the taxonomic composition of phytoplankton. The development of the ^{14}C technique by Steemann Nielsen (Steemann Nielsen 1952) provided oceanographers with the sensitivity required to measure the primary production in the open ocean. For over half a century, the ^{14}C technique has remained the conventional method of assessing primary production of natural waters.

It may seem paradoxical that the problem of assessing community structure of microalgae has proven to be more of a challenge than assessing their primary productivity. Although light microscopy has been used routinely to examine the species composition and abundance of preserved algal cells in natural waters, it fails to account fully for organisms that are either not preserved or too small for easy detection or identification. In the late 1970s epifluoresence microscopy was used to enumerate phytoplankton cells based on their fluorescent properties. Cell counts obtained by epifluorescence microscopy revealed the numerical dominance of picoplankton cells, especially of the cyanobacterial genus *Synechococcus*, in the marine environment. The importance of picoplankton in marine ecosystems was confirmed when flow cytometry was applied to the problem of enumerating picoplankton cells in the early 1980s (Li 1986). The most abundant photoautotroph in the ocean, however, the cyanobacterium *Prochlorococcus*, remained undetected by epifluorescence microscopy until 1988, when this important algal prokaryote was

1

first discovered using flow cytometry (Chisholm et al. 1988). At present, flow cytometry is the standard method of quantifying the abundance of picoplankton in the marine environment because it is more sensitive and less time-consuming than epifluorescence microscopy .

Although flow cytometry is capable of providing information on the abundance and size of algal cells that are too small to be observed by microscopic analysis, its ability to discriminate between the various groups of phytoplankton is limited at present. Conventional flow-cytometric methods rely on two criteria to attempt to identify algal cells: the scattering properties of the cells, which are a function of their size, and their fluorescence properties which are related to their pigment complement (Li 1986). Unfortunately, many taxa of eukaryotic cells overlap in their scattering and fluorescence characteristics and thus cannot be separated from one another by flow-cytometric analysis. Moreover, standard flow cytometric methodology uses only small volumes of seawater, thus excluding the larger cells, which although fewer in number can contribute substantially to the overall algal biomass (Li and Dickie 2001).

The attraction of using pigments and their optical properties rather than conventional microscope analysis to assess phytoplankton community structure is that these measurements account for the entire autotrophic biomass (Yentsch and Phinney 1989, Claustre 1994). Furthermore, since several of the accessory pigments are restricted to a few groups of phytoplankton, information on the pigment composition can provide useful information on the taxonomic composition of marine algae (Mackey et al. 1996, Jeffrey and Vesk 1997). Margalef (1965) first proposed using pigments and their optical properties as a surrogate for phytoplankton community structure. His rationale for deriving an index of community structure is that variability in primary production was related not only to the concentration of chlorophyll-a but is also dependent on the taxonomic composition of the phytoplankton assemblage. Thus, explaining the variability in primary production requires some quantitative measure of the structure of the phytoplankton community.

Assessment of the biotic diversity of phytoplankton assemblages by microscopy as pointed out above is highly biased in favour of larger cells and is time-consuming. The other proxy of community structure presented was the ratio of absorbance of extracted pigments (O_e) at two wavelengths: 430 nm and 665 nm. By analysing phytoplankton samples collected in both marine and freshwater systems, Margalef (1965) found a strong correlation between the $O_e(430)/O_e(665)$ ratio and the biotic diversity of net phytoplankton. He suggested that the shape of the absorption spectrum of algal pigments contained important information on the photosynthetic machinery and taxonomic composition of marine algae and that this information should be incorporated in studies that examine the variability in marine primary production. It is important to note that this work was conducted at a time when the determination of pigment composition and concentrations by thin layer chromatography was prohibitively time consuming and the potential use of optical properties of phytoplankton to assess algal community structure was not yet realised.

With the development of optical sensors to monitor changes in the phytoplankton standing stock came a renewed interest in the examination of the absorptive properties of marine phytoplankton. Numerous studies on both phytoplankton cultures and natural assemblages have shown that the absorptive properties of phytoplankton cells are linked not only to the pigment complement, but also to the size and intracellular pigment concentration of phytoplankton cells (Morel and Bricaud 1981, Sathyendranath et al. 1987, Bricaud et al. 1995, Stuart et al. 1998). The decrease in the absorptive efficiency of pigments when they are packaged within algal cells compared with that when they are dispersed homogeneously in solution is termed the package effect (Duysens 1956). The degree with which the absorptive efficiency is reduced is a function of both the concentration of pigment molecules within the cell and the diameter of the cell (Morel and Bricaud 1981). Thus, unlike the early work of Margalef (1965, 1967), which used the absorbance of extracted pigments in solution to obtain information on phytoplankton community structure, more recent studies have employed the absorptive properties of intact algal cells

to provide a proxy of community structure that is influenced by both the pigment composition and the size structure of the algal cells.

In a study by Yentsch and Phinney (1989), a clear link between the size structure of phytoplankton communities and their absorptive properties was made. Using measurements of the chlorophyll-a specific absorption coefficients of phytoplankton along with information on the size spectrum of algal cells obtained by flow cytometry, they examined the relationship between the size structure of natural communities of phytoplankton and their optical properties. They showed that variability in specific absorption was strongly related to algal cell size. Yentsch and Phinney (1989) proposed that the observed changes in the size structure of phytoplankton are related to nutrient availability. The paper concluded by emphasising the importance of phytoplankton community structure in the interpretation of ocean-colour data. Subsequent studies have also shown that variation in phytoplankton community structure can have a marked effect on the optical properties of marine systems (Bricaud and Stramski 1990, Bricaud et al. 1995, Stuart et al. 1998, Carder et al. 1999, Sathyendranath et al. 2001).

Since the absorptive properties of phytoplankton are embedded in the reflectance signal of natural waters, it may be possible to retrieve information not only on the concentration of chlorophyll-a, but also on the spectral structure of phytoplankton absorption from remotely-sensed data. A preliminary algorithm already exists that attempts to derive information on the size structure of phytoplankton assemblages from ocean-colour data (Ciotti et al. 1999). This may make it possible to observe changes in phytoplankton community structure over large spatial and temporal scales.

Sea-surface temperature is another important variable of the marine ecosystem that is accessible to remote sensing on the same temporal and spatial scales as ocean-colour data. In remote-sensing algorithms of new production (Sathyendranath et al. 1991) and ocean colour (Carder et al. 1999), temperature has been used as an index of nutrient availability. The rationale for the use of temperature as an indicator

of nutrient status is that one of the principal sources of nutrient supply to the surface waters of the ocean is the vertical transport of cool, nutrient-rich waters from depth to the sea surface. Thus, locally or temporally, lower temperatures are often associated with well-mixed, high-nutrient conditions, whereas higher temperatures are generally associated with highly-stratified, nutrient-poor conditions.

The link between physical forcing and community structure is part of a well-established paradigm in the field of plankton ecology (Margalef 1978, Cullen et al. 2002). Well-mixed and nutrient-replete waters tend to be dominated by diatoms, whereas highly-stratified, nutrient-poor conditions tend to support algal communities dominated by small algal cells (Cullen et al. 2002). Shifts in community structure with changes in water-column stability are known to occur both temporally, for example in the seasonal cycle of temperate marine ecosystems, and geographically. These gradients in nutrient status, stratification and community structure are reflected not only in the magnitude of productivity, but also in the fraction of production that is fuelled by the supply of nitrate compared with that fuelled by ammonia (Platt et al. 1992). The fraction of the total production that is 'new' versus 'regenerated' will dictate the amount of autotrophic biomass that is available to higher trophic levels or that will be exported to the deep ocean (Platt et al. 1992). If temperature could be used as an indicator of the physicochemical status of the marine environment and the absorptive characteristics of phytoplankton could be used as an index of phytoplankton community structure, then remote sensing might help oceanographers to understand better the relationship between phytoplankton succession and the marine environment. The use of remote sensing to provide marine scientists with a synoptic view of changes in algal size structure could have many applications in the field of marine ecology, such as improving the assignment of biogeographical provinces and the modelling of biogeochemical cycles and food webs.

In this work, I examine the geographic and temporal variability in the absorptive characteristics of marine phytoplankton as they relate to changes in phytoplankton community structure. In Chapter 2, I begin by examining the relationship between temperature and phytoplankton absorption using data collected over a wide range of oceanic regimes. The result will be useful in the elaboration of improved algorithms for the retrieval of chlorophyll-a from remotely-sensed data. Two proxies of phytoplankton community structure were used: pigment composition by HPLC (High Performance Liquid Chromatography) analysis and cell size by flow-cytometric analysis. Changes in the values of these proxies are indicators of corresponding change in the community structure of the phytoplankton.

Using the Scotian Shelf as a case study, in Chapter 3 I examine the relationships amongst the physicochemical environment, phytoplankton community structure and primary production. Correlations between both temperature and water-column stability and phytoplankton community structure are examined. The relationships amongst temperature and community structure, and the photosynthesis-irradiance (P-E) parameters are discussed and the problem of co-variability between these factors is addressed. The implication of the findings on modelling primary production from space-borne optical sensors is explored.

The optical characteristics and physicochemical dynamics of coastal waters are markedly different from those of the open ocean. In Chapter 4, I use data collected at a single location (Bedford Basin, Nova Scotia, Canada) to examine the temporal variation in physical forcing, nutrient availability, phytoplankton absorption and primary production in a coastal inlet over an annual cycle. Temporal changes in the absorptive properties of non-algal particulates and coloured dissolved organic matter (CDOM) were also examined since these optical components account for a significant fraction of the variability in both light attenuation and total absorption in turbid waters.

In Chapter 5 a general summary and some concluding remarks are given.

CHAPTER 2

Temperature as an Indicator of the Optical Properties and
Gross Community Structure of Marine Phytoplankton

2.1 Introduction

One of the leading issues in contemporary biological oceanography is to understand the factors that drive the regime shift in phytoplankton communities from picoplankton (prokaryotic)-dominated to diatom (eukaryotic)-dominated assemblages, with a concomitant increase in ratio of new production to total primary production (Legendre and LeFevre 1989) and decrease in the importance of the microbial loop (Longhurst 1998, Karl 1999). It is known that such transitions are often associated with a change from oligotrophic, stratified water columns to eutrophic, vertically-mixed ones with a corresponding increase in phytoplankton biomass (Margalef 1978, Cushing 1989, Cullen et al. 2002). Seasonal and regional changes in vertical stratification are usually accompanied by changes in water temperature and nutrient concentration.

The optical properties of the upper ocean contain latent information on the gross community structure in the pelagic ecosystem. Among these, the chlorophyll-a specific absorption coefficient of phytoplankton $a_\phi^*(\lambda)$ (the absorption coefficient of phytoplankton at wavelength λ divided by the chlorophyll-a concentration), required for the interpretation of remotely-sensed data on ocean colour, is especially informative (Yentsch and Phinney 1989, Bricaud and Stramski 1990, Hoepffner and Sathyendranath 1993, Lutz et al. 1996, Stuart et al. 1998, Sathyendranath et al. 1999). Variations in $a_\phi^*(\lambda)$ are related to changes in the size of the cells, to their taxon-specific pigment complement, and to the quantity of pigment per cell (Morel and Bricaud 1981, Sathyendranath et al. 1987). Several studies have shown how $a_\phi^*(\lambda)$ varies either with trophic status (Yentsch and Phinney 1989, Bricaud

7

et al. 1995, Lazarra et al. 1996) or with season (Sathyendranth et al. 1999). Such variations in the relationship between pigment concentration and phytoplankton absorption are known to lead to significant errors in the estimation of chlorophyll-a concentration from ocean colour data (Carder et al. 1999, Sathyendranath et al. 2001). Therefore, knowledge of the sources of the variability in $a_\phi^*(\lambda)$ is crucial for models of the remote estimation of chlorophyll concentration.

Bricaud et al. (1995) examined the relationship between trophic status, as indexed by chlorophyll-a concentration, and chlorophyll-a specific absorption using data collected from a variety of oceanic regimes. The rationale behind the selection of chlorophyll-a concentration as an indicator of phytoplankton community structure is based on the view that much of the variability in chlorophyll-a concentration is caused by fluctuations in the abundance of microphytoplankton (mainly diatoms) superimposed on a ubiquitous and more constant background of nano- and picoplankton biomass (Yentsch and Phinney 1989). Yet, in temperate regions, diatoms may still be abundant at low chlorophyll concentrations, and small cyanobacteria have been observed at moderate (1.25 mg chl-a m^{-3}) chlorophyll concentrations (Morel 1997). Furthermore, in the context of improving chlorophyll-retrieval algorithms based on ocean-colour data, it is desirable to use an environmental predictor of $a_\phi^*(\lambda)$ that is independent of the reflectance signal, yet is accessible on the same synoptic scales. Sea surface temperature is one variable that meets these criteria.

The dynamics of plankton communities are forced by the physical system in which they are embedded: temperature can be a useful indicator of the physicochemical properties of the marine environment, such as water-column stability and nutrient availability (Carder et al. 1999, Sathyendranath et al. 2001). The association between temperature and phytoplankton species composition has been established since the birth of biological oceanography as a discipline (Gran and Braarud 1935). More recently, Sosik and Mitchell (1995) observed a relationship

between temperature and the absorptive characteristics of phytoplankton off the California coast.

In this work, I examine the relationship between $a_\phi^*(\lambda)$ and temperature based on optical and pigment data collected from oceanographic cruises covering a wide range of oceanic conditions. The roles of phytoplankton community structure, nutrient availability and water-column stability as potential factors influencing this relationship are examined and the results are placed in the context of improving our understanding of phytoplankton community structure in marine systems and its implication in remote sensing of ocean colour.

2.2 Data Collection and Analysis

The field observations were made on a number of oceanographic cruises covering numerous oceanic regimes, from eutrophic upwelling regions to strongly-stratified oligotrophic waters (Fig. 2.1). For each station, measurements of temperature were made using a CTD (Conductivity, Temperature, Density) profiler. Chlorophyll-a concentrations were determined fluorometrically from pigment extracts before and after acidification using a Turner Designs fluorometer (Holm-Hansen et al. 1965). In addition, pigment composition was determined for most samples using reverse-phase, high-performance liquid chromatography analysis (HPLC) as described in Head and Horne (1993). HPLC chlorophyll-a concentrations were computed as the sum of concentrations of chlorophyll-a, chlorophyll-a allomers and epimers, divinyl chlorophyll-a and chlorophyllide-a. Ancillary data on the nitrate concentration were also available for the majority of stations sampled.

Absorption was measured using the filter technique. Briefly, between 0.5 and 1 L of seawater was filtered through a 25 mm GF/F filter. The optical density of total particulates retained on the filter was measured using a Shimadzu UV-2101 spectrophotometer with a split-beam, dual detector optical system with an integrating sphere. To determine the spectral absorption by detrital material, pigments
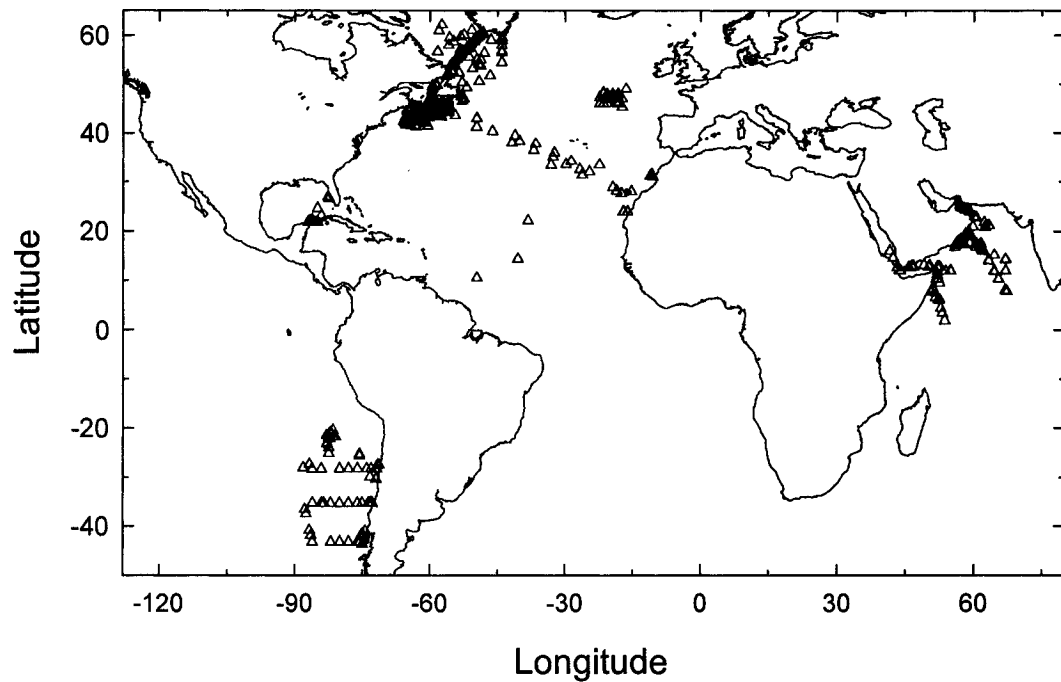
Figure 2.1. Map showing the location of the station where phytoplankton absorption, pigment concentrations and temperature were measured. All samples were analysed by the Biological Oceanography Group of the Bedford Institute of Oceanography. Flow cytometric measurements were confined to the Scotian Shelf and the Labrador Sea.

were extracted from the filter using a mixture of (6:4 vol:vol) 90% acetone and dimethyl sulfoxide (Hoepffner and Sathyendranath 1992, 1993) for all samples analysed prior to October 1998. After this date, pigments were extracted using hot methanol (Kishino et al. 1985). Unpublished data show no significant difference between extraction methods. The extracted filters were scanned from 350 to 750 nm to measure the optical density of the detrital component.

Since the samples were collected over a wide range of trophic conditions, care had to be taken with the choice of the pathlength-amplification factor, which corrects for scattering by the filter. Moore et al. (1995) reported that significant errors might result if a conventional correction factor is applied to samples containing *Prochlorococcus*. To address this problem, I used the following formula presented in Kyewalyanga et al. (1998):

$$O_s(\lambda) = F_{dv}\{A_1 O_p(\lambda) + B_1 [O_p(\lambda)]^2\} + (1 - F_{dv})\{A_2 O_p(\lambda) + B_2 [O_p(\lambda)]^2\}. \quad (1)$$

where $O_s(\lambda)$ is the optical density of the particulate material in suspension at wavelength λ. Two sets of coefficients were applied to the contributions of *Prochlorococcus* (A_1 and B_1) and the rest of the phytoplankton population (A_2 and B_2) to transform the total optical density measured on the filter ($O_p(\lambda)$) to the optical density in suspension, based on F_{dv}, the ratio of divinyl chlorophyll-a to total chlorophyll-a. The transformation (Mitchell and Kiefer 1988)

$$a_t(\lambda) = 2.3 O_s(\lambda)(A/V) \quad (2)$$

converts $O_s(\lambda)$ to absorption coefficients of total particulates $a_t(\lambda)$ (m^{-1}), where A is the clearance area of the filter, V is the volume of seawater filtered and the constant 2.3 converts from base 10 logarithms to natural logarithms. Absorption coefficients of phytoplankton $a_\phi(\lambda)$ were obtained by subtraction the absorption coefficients of detrital material $a_d(\lambda)$ from the absorption by total particulates $a_t(\lambda)$.

For consistency, since HPLC pigment data were not available for all cruises, each absorption spectrum was normalised to Turner chlorophyll-a concentration, to obtain the chlorophyll-a specific absorption spectrum $a_\phi^*(\lambda)$.

The abundance and volume of picoplankton and nanoplankton cells (0.5 - 20 μm) were measured on 8387 samples collected during 23 cruises to the Nova Scotia Shelf and the Labrador Sea (Li and Harrison 2001) and covered seven ecological provinces as defined by Longhurst (1998). Chlorophyll autofluorescence was used to enumerate phytoplankton cells from samples collected at 10 m depth intervals throughout the photic zone using a FACSort (Becton Dickson, San Jose) flow cytometer, as described in Li (1995). Estimates of cell biovolume and mean equivalent spherical diameter ($< D_s >$) for each sample were derived from measurements of cytometric forward light scatter (Li 1995).

Satellite data from the SeaWiFS ocean-colour sensor were obtained from the Remote-Sensing Unit of the Bedford Institute of Oceanography for the period April 8, 1998 to October 14, 2000, corresponding to the dates of *in situ* sampling on the Nova Scotia Shelf. Chlorophyll-a concentrations were determined by fluorometric analysis. Using SeaDAS software (version 4.1) the satellite images were corrected for atmospheric influences using regional near-real-time meteorological and ozone data. Satellite-derived values of chlorophyll-a were calculated using the standard OC4v4.1 algorithm (O'Reilly et al. 2000).

2.3 Results and Discussion

The chlorophyll-a specific absorption coefficent $a_\phi^*(\lambda)$ is a spectral property. The blue (λ=443 nm) and red (λ=676 nm) wavelengths correspond to the two absorption peaks of chlorophyll-a. I have examined the relation between $a_\phi^*(\lambda)$ and temperature at 443 nm and 676 nm in 1187 samples collected from various depths over a wide range of seasons and regions (Fig. 2.2). The measured fluorometric chlorophyll-a concentrations ranged from 0.01 to 25 mg chl m^{-3} and the temperatures varied from -0.5 to 30°C.
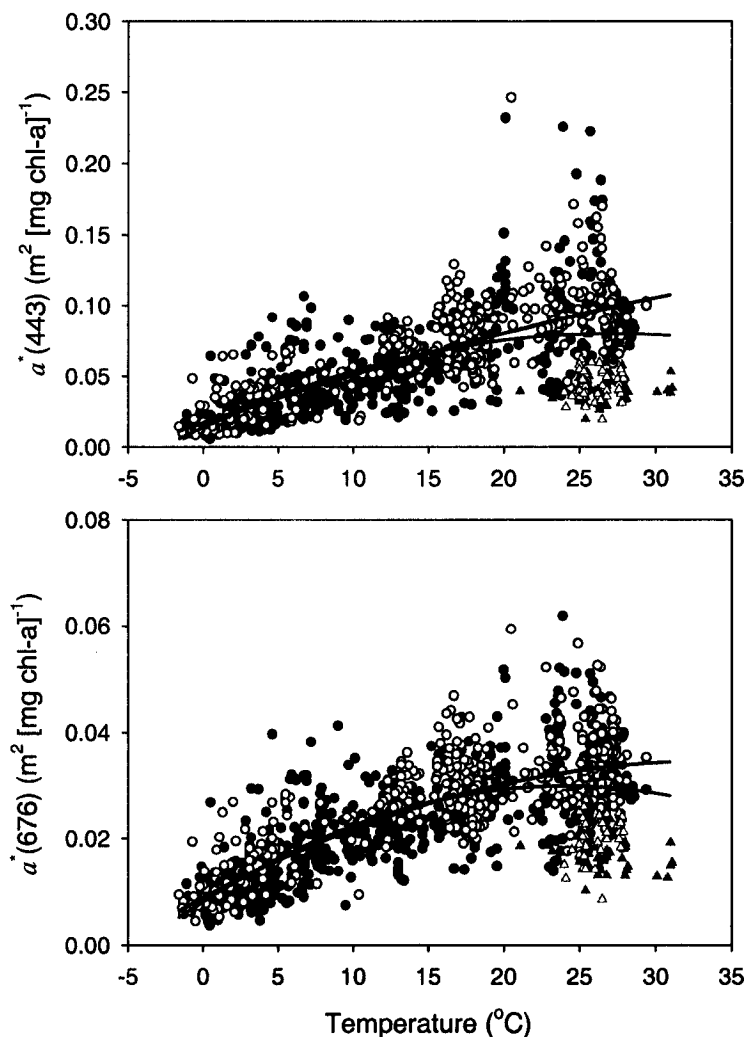
Figure 2.2. Plots of the correlation between specific absorption coefficients at the blue ($a_\phi^*(443)$) and red ($a_\phi^*(676)$) peaks of chlorophyll absorption and temperature T (°C) for some 1187 samples analysed at the Bedford Institute of Oceanography. Filled symbols represent samples collected within the top 20m and empty circles represent samples collected at depths greater than 20m. The green regression lines are second order polynomial fits to the entire dataset at 443 nm and 676 nm. When data collected in the Arabian Sea during the SW monsoon (green triangles) are excluded, the resulting polynomial fit to the remaining dataset (black circles) for 443 nm and 676 nm is shown by the red line.

The plots reveal significant correlations between $a_\phi^*(\lambda)$ and temperature at 443 nm ($a_\phi^*(443) = 0.0138 + 0.0049T - 0.00010T^2$, r^2=0.43, p<0.0001) and 676 nm ($a_\phi^*(676) = 0.0081 + 0.0018T - 0.00010T^2$, r^2=0.49, p<0.0001) (Fig. 2.2). The cluster of points with low specific absorption coefficients at high temperature (in green) corresponds to one cruise conducted during the SW monsoon in the Arabian Sea. When this cruise was removed from the analysis, ca 58% of the variance in $a_\phi^*(443)$ ($a_\phi^*(443) = 0.0171 + 0.0036T - 0.000022T^2$, r^2=0.58, p<0.0001) and 61% of the variance in $a_\phi^*(676)$ ($a_\phi^*(676) = 0.0089 + 0.0015T - 0.000022T^2$, r^2=0.61, p<0.0001) could be explained by temperature alone.

When I tried to explain the substantial fraction of the total variance in both $a_\phi^*(443)$ and $a_\phi^*(676)$ explained by temperature, three hypotheses present themselves. Temperature may be responsible directly for changes in optical properties; a covariate of temperature may be responsible; or the same physical processes that correspond to changes in ocean temperature, such as stratification of the water column, may also regulate phytoplankton community structure.

2.3.1 Environmental factors causing variability in $a_\phi^*(\lambda)$

Amongst the environmental properties known to modify the absorptive properties of phytoplankton cells are temperature itself, light history and nutrients, especially nitrogen. In several studies the effects of these three factors on the specific absorption coefficient of phytoplankton have been examined using phytoplankton cultures under controlled growth conditions. In studies of the effect of temperature on *Dunaliella tertiolecta* and *Thalassiosira pseudonana* grown under light-saturating and nutrient-replete conditions (Sosik and Mitchell 1994, Stramski et al. 2002), a response was observed directly counter to that shown in Figure 2.2 (i.e. $a_\phi^*(\lambda)$ decreased with temperature). Thus, a direct effect of temperature can be ruled out.

Photoacclimation is another possible explanation for our results. Cells grown under high light intensities have lower intracellular pigment concentrations than

those grown at low light (Falkowski and LaRoche 1991), resulting in a corresponding increase in specific absorption due to a decrease in the package effect (Geider and Platt 1986). Given that our samples generally represent conditions where density is dominated by temperature, we suppose that stations sampled in different parts of the wide temperature range covered in this study represent different light regimes (surface irradiance, vertical mixing). In the range from -2 to 5°C say, we could expect significant vertical mixing and low surface irradiance leading to low values of $a_\phi^*(443)$ and $a_\phi^*(676)$, whereas at temperatures greater than 12°C we would expect highly stratified conditions with high surface irradiance and high values of $a_\phi^*(443)$ and $a_\phi^*(676)$, as observed in our dataset (Fig. 2.2). However, if photoacclimatory change in intracellular pigment concentration was the only mechanism operating, we would also expect that surface samples would show higher values of $a_\phi^*(443)$ and $a_\phi^*(676)$ than deep samples, but this was not the case. Analysis of covariance (ANCOVA) revealed that adjusted mean values of $a_\phi^*(443)$ and $a_\phi^*(676)$ were significantly higher for samples collected below 30 m than those collected within the top 30 m ($p<0.001$).

Changes in nutrient regime offer another potential explanation for our results. In phytoplankton grown under steady-state nitrogen limitation (Sosik and Mitchell 1991, Stramski et al. 2002), higher rates of nutrient supply led to lower $a_\phi^*(\lambda)$. To examine whether availability of nitrate may explain some of the variability in phytoplankton optical properties, both $a_\phi^*(443)$ and $a_\phi^*(676)$ were plotted against the corresponding ambient nitrate concentration for the subset of our data (N=860) (Fig. 2.3) for which information on nitrate concentration is available. Again, the Arabian Sea showed anomalous results, with the some of the highest observed values of $a_\phi^*(443)$ and $a_\phi^*(676)$ occurring at nitrate concentrations in excess of $10\,\mu$M (Fig. 2.3). The high degree of scatter in the relationship between ambient nitrate concentration and chlorophyll-a specific absorption, especially at low levels of nitrate, is not surprising. Ambient nutrient concentrations are governed by both physical and biological mechanisms. Hence, during periods of rapid algal growth, such as
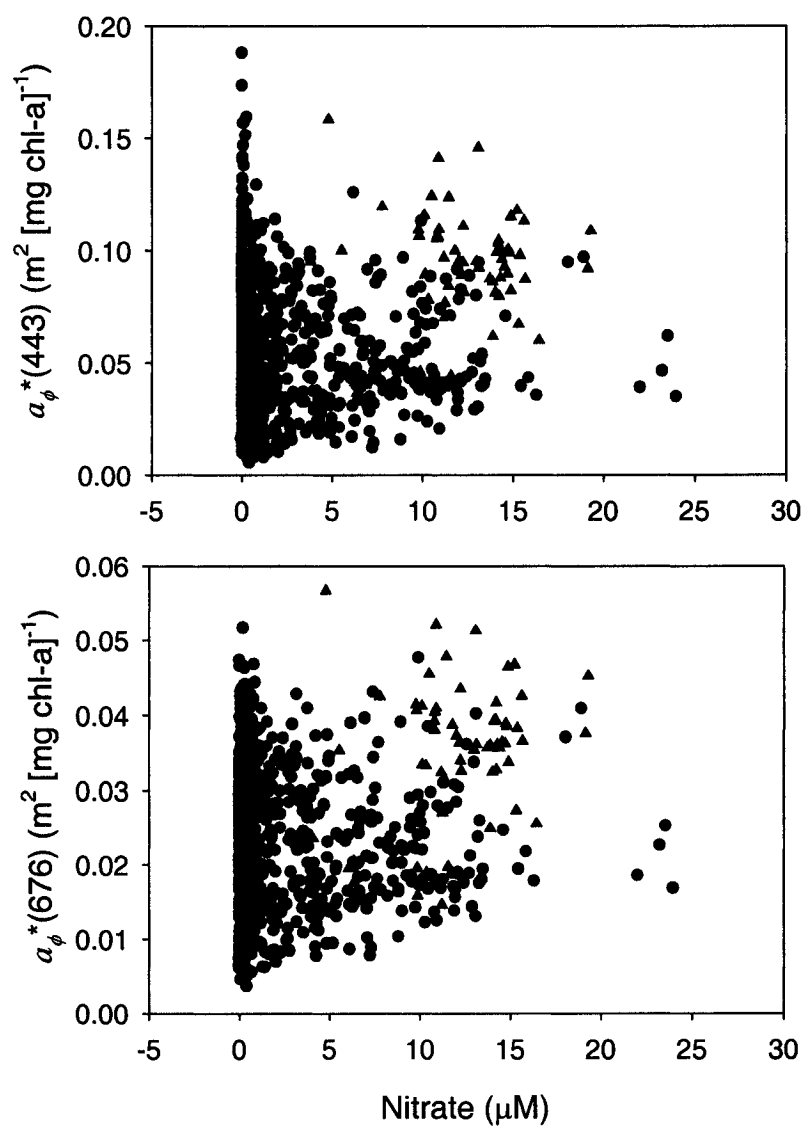
Figure 2.3. Plots of $a_\phi^*(443)$ and $a_\phi^*(676)$ against nitrate concentration (μM). These data are a subset (N=860) of the absorption samples presented in Fig. 2.2, since not all of the 1187 absorption measurements had corresponding nutrient observations. The red triangles represent samples collected in the Arabian Sea during June and July, 1997.

the North Atlantic spring bloom, we would not expect the correlation between temperature and nitrate to be robust, since nitrate depletion would occur at a much faster rate than the vernal warming of the sea surface by solar heating. It can be argued that some indicator of nitrate supply would be a more suitable variable to approximate nutrient availability than would ambient nitrate concentration. For example, Sosik and Mitchell (1995) showed a strong relationship between $a_\phi^*(440)$ and the distance from the nitricline. Unfortunately, for most of the cruises examined in this study our nutrient data were not sufficiently resolved in the vertical to establish a nitricline depth to test this relationship.

2.3.2 Effect of phytoplankton community structure on $a_\phi^*(\lambda)$

Pigment markers allow us to classify algal samples according to the relative abundance of taxa present (Mackey et al. 1996) and, indirectly, give some indication of size composition (Claustre 1994). Cell counts, on the other hand, often do not cover the entire phytoplankton size spectrum. For example, conventional microscope counts often exclude or incorrectly estimate cells in the picoplankton ($<2\,\mu$m) size range, whereas conventional flow cytometry measurements often exclude microphytoplankton ($>20\,\mu$m) due to the small sample volumes used in the analysis (Li 2002). In contrast, provided that HPLC pigment analysis is of samples retained by GF/F filters, the entire phytoplankton community will be included (Claustre 1994).

I used 19'-hexanoyloxyfucoxanthin as an indicator of prymnesiophytes, which generally fall into the nanoplankton (2-20 μm) size range (Jeffrey and Vesk 1997), and zeaxanthin as an indicator of cyanobacteria (*Synechococcus* and *Prochlorococcus*), which typically fall in the picoplankton ($<2\,\mu$m) size range (Claustre 1994). Fucoxanthin is often considered to be an indicator of diatoms, which frequently fall into the microphytoplankton class ($>20\,\mu$m). However, fucoxanthin is also a dominant accessory pigment of prymnesiophytes (Jeffrey and Vesk 1997). When

the HPLC chlorophyll-a-normalised pigment ratios are plotted against temperature, clear patterns emerge (Fig. 2.4A). In general, diatoms (as indicated by fucoxanthin) dominated mostly at low temperatures -2 to 2°C. Prymnesiophytes coexisted with diatoms in the range from 2 to 10°C. At temperatures between 10 and 18°C, 19'-hexanoyloxyfucoxanthin was the principal accessory pigment, indicating the prevalence of prymnesiophytes. The importance of picoplankton (as indicated by zeaxanthin) increased directly with temperature.

Analysis of accessory pigments also allows us to explain the anomalous SW Monsoon cruise, where $a_\phi^*(\lambda)$ values were low at high temperatures. During this cruise, intensive wind mixing did not change the sea temperature, yet the introduction of nutrient-rich water from depth produced blooms of diatoms (Sathyendranth et al. 1999), as indicated by high concentrations of fucoxanthin relative to HPLC chlorophyll-a at temperatures ranging from 20-29°C.

Another way of looking at the change in taxonomic composition with temperature is to use a pigment index that reflects the fraction of large and small cells in a sample. I adopted the ratio F_p proposed by Claustre (1994), which takes the ratio of the sum of diagnostic pigments associated with large cells (diatoms and dinoflagellates) to the sum of diagnostic pigments associated with both large and small cells. The ratio is calculated as follows:

$$F_p = (fuco + per)(fuco + per + 19'HF + 19'BF + zea + Chlb + allox)^{-1} \quad (3)$$

where fuco, per, 19'HF, 19'BF, zea, Chl$b$ and allox represent the concentrations of fucoxanthin, peridinin, 19'-hexanoyloxyfucoxanthin, 19'-butanoyloxyfucoxanthin, zeaxanthin, chlorophyll-b and alloxanthin, respectively. The plot of the ratio F_p against temperature (Fig. 2.4B) shows very clearly that the Arabian Sea falls into its own grouping. In the Arabian Sea dataset, ratios of F_p varied between 0 and 1 with most points falling within a narrow temperature range of between 24 and 30°C. Thus, it would appear that in this particular region, temperature would be a poor predictor of phytoplankton community structure. For the remaining dataset,
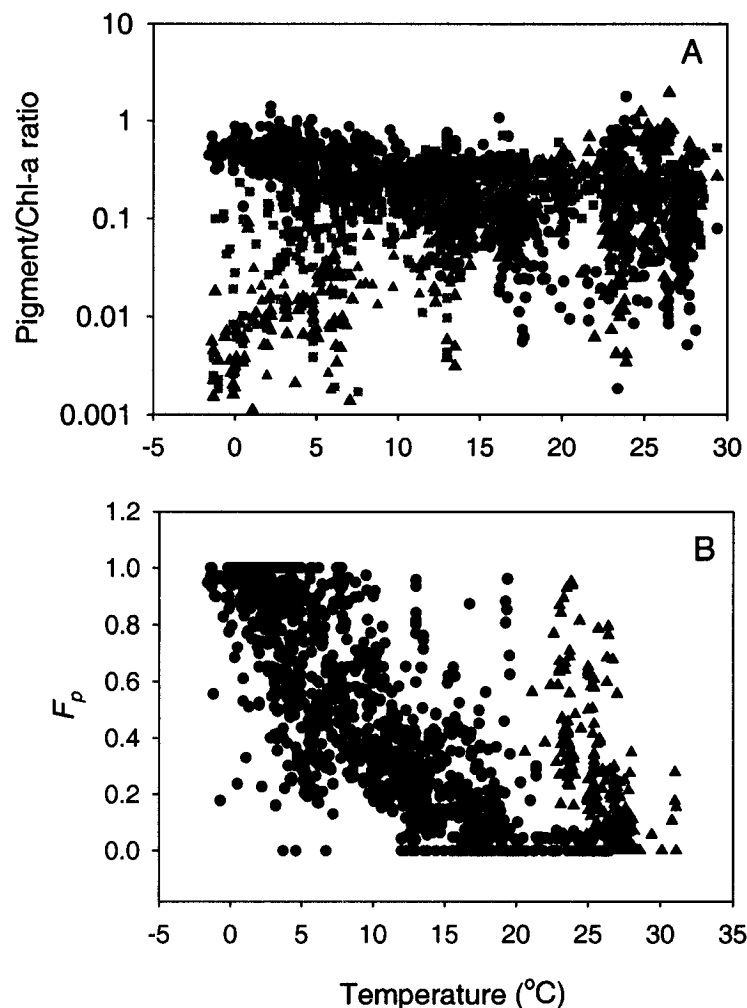
Figure 2.4. A) The relationship between the chlorophyll-a normalised concentrations of three major accessory pigments and temperature. The black circles represent fucoxanthin/chlorophyll-a values: fucoxanthin is a conventional indicator of the presence of diatom cells. The green squares denote the chlorophyll-a-normalised concentrations of 19'-hexanoyloxyfucoxanthin, which indicates the presence of prymnesiophytes. The red triangles signify the chlorophyll-a normalised zeaxanthin concentration, which indicates the presence of cyanobacteria. B) Relationship between the ratio F_p (see text) and temperature. The red triangles represent data collected in the Arabian Sea. The black circles show data collected in the remaining oceanic regimes.

however, F_p decreased gradually with increasing temperature. The ratio F_p was also used to examine the relationship between taxonomic structure and phytoplankton optical properties. I plotted $a_\phi^*(443)$ and $a_\phi^*(676)$ against the F_p for the entire dataset (Fig. 2.5) and found a strong negative relationship for both wavebands (r^2 = 0.49 at 443 nm (p<0.0001) and r^2=0.43 at 676 nm (p<0.0001)).

The relationship between the size structure of natural phytoplankton assemblages and temperature was also examined using flow cytometric data. The average equivalent spherical diameter of cells less than $20\,\mu$m in diameter for the top 100 m of the water column $<D_s>$ was computed for each of the 645 stations on the Nova Scotian Shelf and the Labrador Sea. The semi-log plot of $<D_s>$ against the temperature at 10 m shows a clear linear pattern (Fig. 2.6).

The specific absorption coefficient of phytoplankton is sensitive to both cell size and pigment composition. The two peaks in phytoplankton absorption are associated with the wavebands of chlorophyll-a absorption, one located at around 443 nm and the other at 676 nm. Although pigment packaging affects the specific-absorption coefficient in both wavebands, the influence of pigment composition on the absorption differs markedly in the two wavebands. Absorption in the 676 nm waveband is due primarily to chlorophyll-a, although the contribution of chlorophyll-b can be important in samples containing low-light acclimated *Prochlorococcus* cells. However, in the 443 nm waveband the influence of accessory pigments, especially photoprotective carotenoids, can be significant. Based on a study of six species of phytoplankton cultures grown under a range of irradiance levels, Fujiki and Taguchi (2002) reported that under high light conditions, the influence of photoprotective pigments weakened the relationship between cell size and specific absorption at 440 nm, whereas under low-light conditions, the relationship between $a_\phi^*(440)$ and cell size was significant. In the red region of the visible spectrum the relationship between cell size and $a_\phi^*(\lambda)$ was significant at all growth irradiances. Based on their observations, it would appear that the absorptive characteristics of phytoplankton in surface waters, which are detected by the satellite optical sensors, may be related
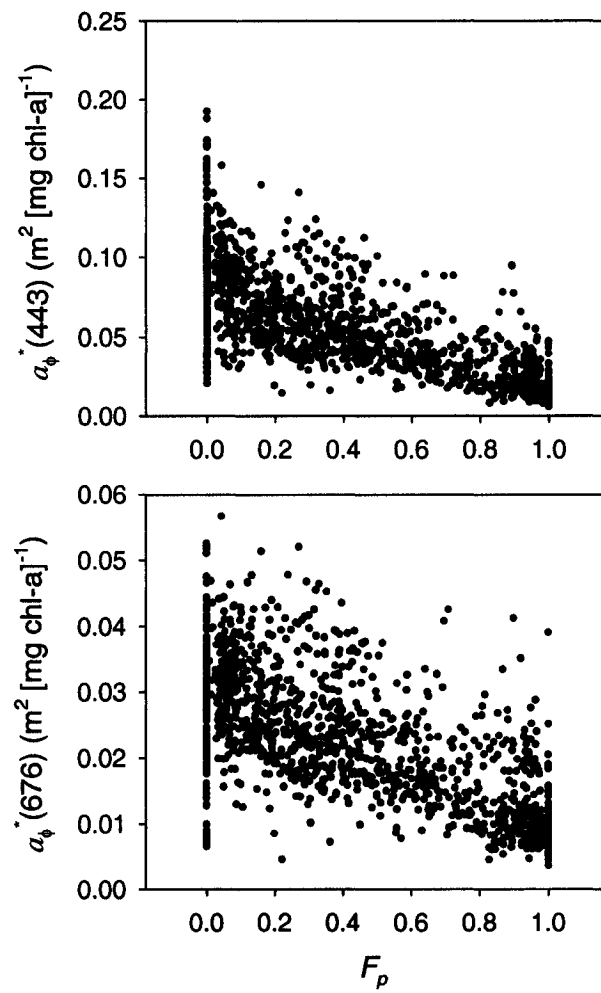
Figure 2.5. Plot of the ratio F_p versus chlorophyll-specific absorption coefficients at the blue (443 nm) and red (676 nm) absorption maxima.
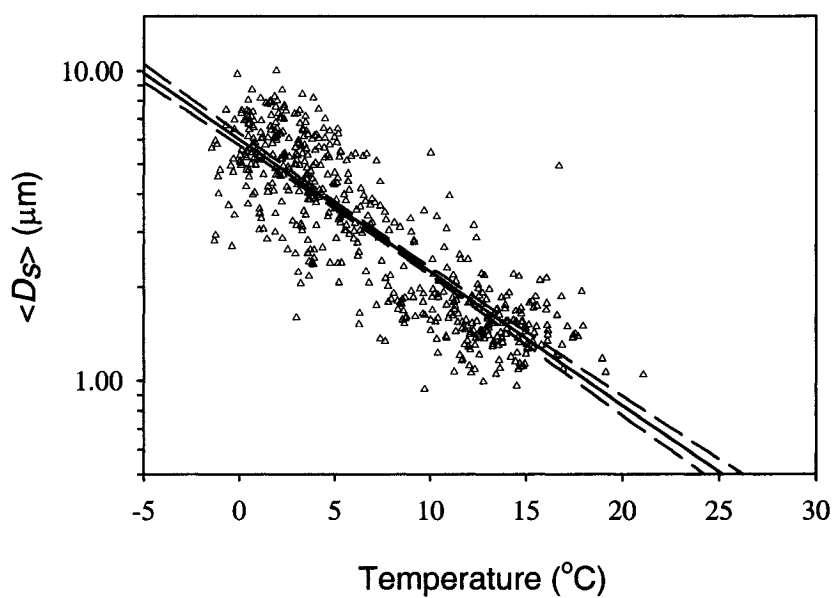
Figure 2.6. Plot of the water-column average values of the mean equivalent spherical diameter ($<D_s>$) for nano- and picoplankton cells and temperature (T) at 10 m. Samples were collected at 645 stations on the Nova Scotia Shelf and in the Labrador Sea. The solid line represents the linear regression equation $\log<D_s> = 0.778 - 0.042T$ ($r^2=0.73$). The dashed lines represent the 95% confidence limits.

more strongly to photoprotective pigment composition than to cell size. Yet, in this study, a strong relationship was observed between the absorptive properties in both the blue and red regions of the spectrum and phytoplankton size structure (Fig. 2.5). The reason for this strong correlation between specific absorption at the 443 and 676 nm wavebands and cell size maybe caused by a relative increase in the concentration of photoprotective pigments as we move from diatom-dominated waters to cyanobacteria-dominated waters. Zeaxanthin, a photoprotective carotenoid that is a chemotaxonomic indicator of cyanobacteria *Synecoccocus* and *Prochlorococcus*, is a dominant accessory pigment in oligotrophic tropical and subtropical waters. In surface waters, this pigment contributes up to approximately half of the total absorption at 440 nm (Babin et al. 1996, Bouman et al. 2000). It is therefore fortuitous that picoplanktonic cells exhibit both lower pigment packaging and higher relative concentrations of photoprotective pigments than larger cells, which allows the size-dependent change in chlorophyll-a specific absorption to be similar at both wavebands. The results obtained from two independent analyses (HPLC and flow cytometry) thus provide strong support for the view that broad changes in community structure of phytoplankton from the global ocean, as indexed by pigment composition and size composition, are associated with the distribution of temperature. Moreover, cell size is an important determinant of the optical properties of phytoplankton. I believe that these factors offer the most plausible explanation for the robust relation between $a_\phi^*(\lambda)$ and temperature.

The principal result may be presented in a simpler way. The general increase in absorption by phytoplankton with increasing concentration of chlorophyll-a is well known (Prieur and Sathyendranath 1981, Sathyendranath and Platt 1988). Indeed, it provides the basis for the remote sensing of phytoplankton biomass (Morel and Prieur 1977, Gordon and Morel 1983). When phytoplankton absorption at 676 nm is plotted against fluorometric chlorophyll-a concentration and then partitioned according to temperature (Fig. 2.7A), the significance of temperature, and therefore

of community structure as a modulator of bio-optical characteristics, becomes very clear.

2.3.3 Implications to remote sensing of ocean colour

Can these results be exploited to improve the synoptic census of phytoplankton by ocean-colour remote sensing? They certainly can. Chlorophyll retrieval by remote sensing depends on the reflectance at certain wavelengths in the visible part of the spectrum (Gordon and Morel 1983). Reflectance is a function of absorption (Gordon and Morel 1983). Cell size (Duysens 1956) and pigment complement (Bidigare et al. 1988, Hoepffner and Sathyendranath 1991, Hoepffner and Sathyendranath 1993), both of which I have shown to be significantly correlated with temperature, are known to influence the magnitude and shape of $a_\phi^*(\lambda)$. I have established (Table 2.1) that residual variance about the regression of chlorophyll-a specific absorption on fluorometric chlorophyll-a concentration is reduced significantly for all SeaWiFS wavebands when temperature is included as an independent variable. The low r-square values for regressions of chlorophyll-a and temperature against $a_\phi^*(555)$ are due to the minimal amount of variability in specific absorption caused by accessory pigment absorption and pigment packaging at this region of the spectrum. Both the r-square values and regression coefficients show strong wavelength dependence, similar to the findings of Bricaud et al. (1995). What is also important to note is that the predictive ability of temperature as a single independent variable is nearly equal to that of chlorophyll-a for all the SeaWiFS wavebands as indicated by the similar r-square values obtained from the regression analysis (Table 2.1). More directly, I have examined the regression of the remotely-sensed estimate of chlorophyll (NASA OC4 V4.1 algorithm) (O'Reilly et al. 2000) against chlorophyll concentrations measured on 192 samples collected by ship on the Nova Scotia shelf. In the ideal case, this regression should have unit slope. Instead samples separate distinctly into groups depending on the temperature regime from which they were taken (Fig. 2.7B). Thus, sea-surface temperature could be used to select
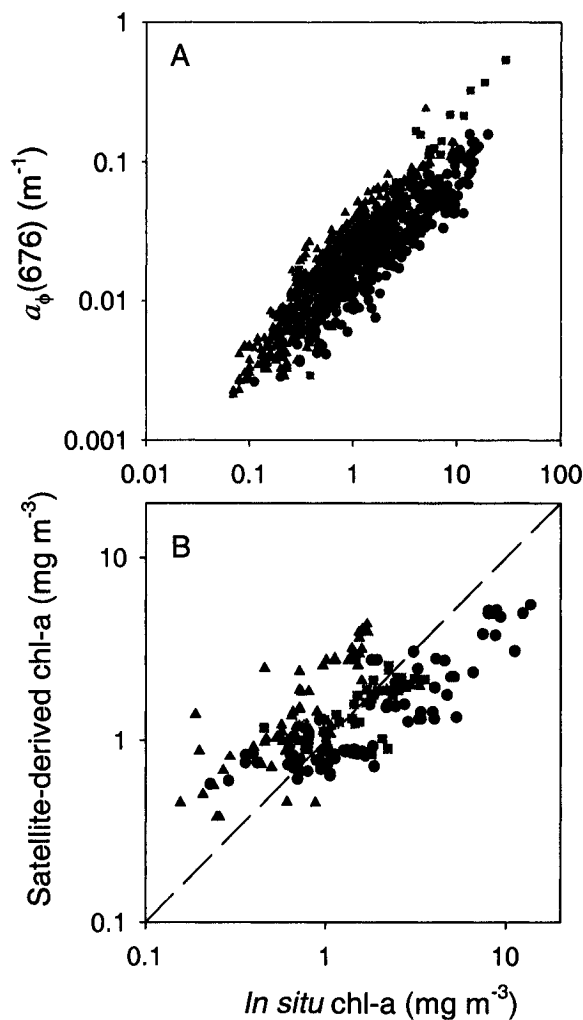
Figure 2.7 A) Log of the absorption coefficient of phytoplankton at 676 nm $a_\phi(676)$ (m^{-1}) versus the log of the *in situ* chlorophyll-a concentration. The black circles represent samples collected at temperatures less than 5°C, the green squares represent samples collected at temperatures between 5 and 12°C, and the red triangles represent samples collected at temperatures greater than 12°C. The total number of observations is 1187. B) Log of the satellite-derived chlorophyll-a concentration using the SeaWiFS OC4 algorithm against the corresponding log of *in situ* chlorophyll-a concentration for samples collected on the Scotian Shelf (N=192). The black circles, green squares and red triangles mark observations made at temperatures less than 5°C, between 5 and 12°C and greater than 12°C, respectively.

Table 2.1: Linear regressions* of the log-transformed chlorophyll- specific absorption coefficient $\log_{10}(a^*_\phi(\lambda))$ against log- transformed chlorophyll-a concentration $\log_{10}(C)$ and temperature T, and the multiple-linear regression of $\log_{10}(a^*_\phi(\lambda))$ on both $\log_{10}(C)$ and temperature (T). The coefficients of the equations $\log_{10}(a^*_\phi(\lambda)) = b\log_{10}(C)+d$; $\log_{10}(a^*_\phi(\lambda)) = bT+d$ and $\log_{10}(a^*_\phi(\lambda)) = b\log_{10}(C)+eT+d$ and their corresponding r^2 values are presented for the six SeaWiFS wavebands in the visible. The number of observations in each case equals 1187.

λ	$\log_{10}(a^*_\phi(\lambda)) = b\log_{10}(C) + d$			$\log_{10}(a^*_\phi(\lambda)) = bT + d$			$\log_{10}(a^*_\phi(\lambda)) = b\log_{10}(C) + eT + d$			
	b	d	r^2	b	d	r^2	b	d	e	r^2
412	-0.332	-1.404	0.49	0.017	-1.624	0.42	-0.235	-1.538	0.010	0.58
443	-0.397	-1.346	0.54	0.021	-1.609	0.46	-0.280	-1.506	0.012	0.65
490	-0.424	-1.554	0.56	0.021	-1.817	0.42	-0.317	-1.702	0.011	0.64
510	-0.346	-1.745	0.48	0.017	-1.966	0.39	-2.252	-1.873	0.009	0.56
555	-0.162	-2.176	0.12	0.010	-2.309	0.14	0.090	-2.276	0.007	0.17
670	-0.275	-1.735	0.43	0.016	-1.945	0.47	-0.166	-1.885	0.011	0.58

chlorophyll-retrieval algorithms to account for changes in the optical characteristics of phytoplankton caused by changes in phytoplankton community structure, thereby reducing potential errors in the estimation of sea-surface chlorophyll (see also Carder et al. 1999).

2.3.4 Temperature as an index of environmental conditions

Although it is not difficult to be convinced that both the size and taxonomic composition of phytoplankton cells govern most of the variability in $a_\phi^*(\lambda)$, we also need to understand why temperature is such an effective indicator of phytoplankton community structure for such a diverse group of oceanic provinces. Yentsch and Phinney (1989) proposed that variability in the chlorophyll-a normalised absorptive properties of phytoplankton is caused by changes in the availability of new nitrogen. Water-column stability is known to influence both nitrogen availability and temperature within the photic zone. The transport of cold, nutrient rich water to the surface layers is one of the major sources of new production in the open ocean. It is this link between temperature and new nitrogen supply that has been exploited to estimate new production from surface temperature fields obtained from satellite (Sathyendranath et al. 1991).

Apart from its role in supplying nutrients from depth to well-lit surface layers, vertical mixing will also favour the presence of larger cells by allowing them to remain suspended within the photic zone. Species succession in phytoplankton communities has been attributed to changes in the physical environment: namely advection and turbulence (Margalef 1978, Cullen et al. 2002). A recent study by Rodriguez et al. (2001) showed that mesoscale vertical motion was important in regulating the size structure of marine phytoplankton. However, it is important to point out that the relationship between temperature and vertical stability is not always a robust one. For example, in coastal and polar regions, salinity can play a dominant role in controlling water-column stability due to terrestrial runoff and ice melt, respectively. We have also seen, in the case of the Arabian Sea, that high

levels of vertical mixing can sometimes result in negligible changes in sea surface temperature.

The limited ability of temperature as an indicator of turbulence in the Arabian Sea region may explain the poor correlation found there between temperature and phytoplankton community structure. Another potential cause for the poor relationship is that biotic rather than abiotic factors may play an important role in regulating phytoplankton community structure in this region. Results from a study by Goericke (2002) in the monsoonal Arabian Sea suggest that phytoplankton community structure is regulated primarily by zooplankton grazing rather than by the prevailing physical and chemical conditions. Thus, in regions such as the Arabian Sea, where top-down control of phytoplankton community structure may occur at least some of the time, the use of temperature as a predictor of seasonal changes in community structure may be less robust than elsewhere. The importance of planktonic micrograzers in controlling phytoplankton biomass in high-nitrate, low-chlorophyll (HNLC) regions (Strom et al. 2000) suggests that the microalgal community structure in these regions may also be regulated in part by microzooplankton.

The regions examined in this study generally fall across the two turbulence-nutrient regimes: low turbulence and low nutrients, which in general are associated with high temperatures, and high turbulence and high nutrients, which are generally associated with low temperatures. There are two other regimes of turbulence and nutrient availability, however, that are not represented in this study (Margalef et al. 1979, Cullen et al. 2002). The first regime is low turbulence and high nutrient conditions in coastal regions. In this regime, there are two mechanisms by which these conditions can be attained: vertical migration of cells from low-nutrient surface waters to high-nutrient deep waters and the introduction of low-salinity, high-nutrient waters from terrestrial runoff and riverine inputs (Margalef et al. 1979, Cullen et

al. 2002). Since coastal regions are optically complex, more detailed chlorophyll-retrieval algorithms are required: variability in the concentrations of coloured dissolved organic matter and non-algal particulate material limits the applicability of open-ocean algorithms.

The second turbulence-nutrient regime is high-turbulence and low-nutrient conditions, associated with high-latitude, high-nitrate, low-chlorophyll (HNLC) regions (Cullen et al. 2002). The mechanisms responsible for regulation of phytoplankton community structure in these regions are still debated. In such regimes the relationship between temperature and community structure may not be as clear as those found in the oceanic regions examined in this study. Thus, additional study is required on the principal mechanisms responsible for change in phytoplankton community structure.

2.4 Concluding Remarks

It is becoming increasingly accepted that regionally-specific algorithms for chlorophyll retrieval are likely to replace globally-universal ones (Carder et al. 1999, Sathyendranath et al. 2001). The principal obstacle has been to find a continuous variable (ideally, one that is accessible to remote sensing) to use as the basis for definition of the regional algorithms (Platt and Sathyendranath 1999). Carder et al. (1999) used sea surface temperature (SST) to improve chlorophyll estimates on global scales, by dividing the world ocean into bio-optical domains and by comparing SST with the temperature at which nitrate levels are below the limit of detection, favoring the presence of small cells. Our results also point clearly to temperature as a viable indicator for algorithm selection for many of the regions examined in this study. The advantage of using temperature to approximate the initial estimate of chlorophyll-a specific absorption, instead of chlorophyll-a concentration, is that it provides a value of $a_\phi^*(\lambda)$ that is independent of the optical signal detected by the satellite. Furthermore, our study shows that using both temperature and chlorophyll concentration would improve significantly estimates of $a_\phi^*(\lambda)$

for all cruises examined in this study, more than if chlorophyll were used alone. As additional studies on the relationship between temperature and the absorptive properties of phytoplankton are conducted within other oceanic regions the utility of this approach will become clearer. On a cautionary note, however, the application of temperature in regional algorithms must be made with an awareness of the main factors governing the variability in the taxonomic composition of the phytoplankton assemblage, as we have seen in the example of the Arabian Sea.

This chapter has shown that the gross community composition and therefore size structure of the autotrophic plankton, as revealed by pigment markers and flow cytometric analysis, vary in a regular way according to the temperature distribution of the upper ocean for many of the regions examined in this study. The associated changes in optical properties of the plankton are of immediate relevance to ocean bio-optics in general. The results demonstrate the potential use of sea-surface temperature to improve regional algorithms of chlorophyll-retrieval (and subsequently, primary production) on synoptic scales by remote sensing, tasks of central significance to major contemporary issues such as the ocean carbon cycle (climate change) and interannual variability in the ocean ecosystem (fisheries). Given the fundamental importance of temperature as an ocean observable, these findings will be also be of broad applicability in the analysis and modelling of marine ecosystems.

CHAPTER 3

Community Structure and Photosynthetic Characteristics
of Marine Phytoplankton on the Scotian Shelf

3.1 Introduction

Understanding the principal mechanisms responsible for changes in photosynthetic performance of marine phytoplankton has been an important aim of biological oceanographic research for over four decades. Early field studies revealed that marine primary production varied considerably in space and time (Steemann Nielsen 1952). One obvious explanation for the observed changes in primary production was that the phytoplankton standing stock also exhibited spatial and temporal variation. By normalising production measurements to the concentration of chlorophyll-a, the influence of changes in microalgal biomass was much reduced, allowing for the examination of other potential factors affecting primary production. The rationale behind the choice of this photosynthetic pigment as a proxy for autotrophic biomass was that it was easily measured, is found in all photosynthetic organisms, and is the first-level interface between available light and photosynthesis.

The other principal factor regulating the rate of photosynthesis in the water column is the light available for absorption by photosynthetic pigments. This varies according to the time of day, season and latitude, as well as the concentration of optically-significant material in the water (Jerlov 1968, Kirk 1994). In addition to the concentration of pigments and the flux of photons, there are other factors that may contribute to variation in primary production in the World Ocean (Platt and Jassby 1976, Harris 1978, Harrison and Platt 1980). To examine the contribution of secondary factors to the overall variability in marine photosynthesis requires that variation in production caused by the primary factors (biomass and light) be accounted for in some quantitative way. The photosynthesis-irradiance (P-E)

response curve is used to parameterize the light-saturated and light-limited rates of photosynthesis over the range of light intensities that phytoplankton encounter in the marine environment (Jassby and Platt 1976). A variety of functional forms can be used to describe the P-E curve, but all can be expressed using two parameters, one representing the rate of photosynthesis at light saturation, P_m^B, and the other representing the initial slope of the curve, α^B (Jassby and Platt 1976).

Photosynthesis-irradiance (P-E) experiments provide a means of comparing the physiological characteristics of different microalgal populations (Platt and Jassby 1976). Instead of exposing the phytoplankton sample only to the depth from which the sample was collected, the P-E experiment introduces the algal cells to a range of light intensities from zero to surface irradiance values. Numerous P-E experiments have been done on both cultures and natural assemblages of marine algae. These studies have shown that nutrient concentration, temperature, light history, as well as cell size and taxonomic composition, all influence the magnitudes of the P-E parameters in the ocean (Geider and Osborne 1992).

In addition to its use in studies of phytoplankton physiology, the P-E response curve plays a central role in the models of aquatic primary production (Morel 1978, Platt and Sathyendranath 1988, Platt and Sathyendranath 1989, Morel 1991). Initial models of primary production using the P-E parameters were implemented on local scales. The estimates obtained from the models were routinely compared with *in situ* production estimates measured at the same time and place as the P-E parameters. In several studies it has been found that, given accurate estimates of pigment biomass, P-E parameters and the underwater light field, the P-E model production estimates corresponded well with *in situ* measurements of primary production (Harrison et al. 1985, Côté and Platt 1984, Sathyendranath and Platt 1989).

Assessment of the role of phytoplankton in the global carbon budget has always involved the problem of extrapolation. Prior to 1978, information on the distribution of phytoplankton standing stock in the marine environment was obtained by studies conducted on ships. Since there existed such a vast area of the World Ocean

over which little was known of the changes in chlorophyll-a concentration in space and time, early calculations of global primary production were made using highly simplified representations of the physiology of algal cells and their spatial and temporal distribution (Platt and Subba Rao 1975).

The launch of ocean-colour sensors lead to the capability of producing global maps of phytoplankton biomass. Once a synoptic view of the distribution of pigment biomass in the surface ocean was available, biological oceanographers had two remaining obstacles to overcome before estimating global primary production: to estimate the shape of the chlorophyll-a profile and to assign values of the photosynthetic parameters. Knowledge of the physiological response of phytoplankton to available light has been, and continues to be, provided by experiments conducted on ships: at present there is no routine means of deriving the P-E parameters using remotely-sensed data. Two principal methods have been used to approach the problem of extrapolating the P-E parameters obtained from experiments conducted at a given location and time to synoptic scales. The first approach was to divide the ocean into biogeochemical provinces, based on their unique physical dynamics (Platt and Sathyendranath 1988, Longhurst et al. 1995, Sathyendranath et al. 1995). Information on the seasonal variability of the photosynthesis-irradiance (P-E) parameters was compiled for each region. From these data a standard suite of parameters was selected for each province and used in primary production algorithms. The principal assumption for the implementation of this approach was that, for a given season, the P-E parameters were assumed to be constant (or derivable by particular algorithms) within the provincial boundaries. The second method was to use sea-surface temperature as a predictor of photosynthetic performance, since this environmental variable is known to influence the photosynthetic parameter P_m^B and is also amenable to remote sensing (Balch et al. 1992, Antoine and Morel 1996, Behrenfeld and Falkowski 1997).

With the development of optical sensors having greater sensitivity and spectral resolution, the optical properties of the marine environment may also provide

insight into the physiological status of algal cells. The absorptive properties of phytoplankton can be considered a valuable index of phytoplankton community structure (Yentsch and Phinney 1989). Since pigments absorb within discrete windows of the visible spectrum and vary between taxonomic groups, changes in taxonomic structure of phytoplankton communities can lead to changes in the shape of the phytoplankton absorption spectrum (Hoepffner and Sathyendranath 1992, 1993). The intracellular pigment concentration and size of algal cells may also modify the shape of the phytoplankton absorption spectrum (Morel and Bricaud 1981). A decrease in the *in vivo* specific absorption of aggregated pigments compared with that of the same quantity of pigment evenly dispersed in solution is called the packaging effect (Duysens 1958). An increase in cell size and/or intracellular pigment concentration is responsible for this decrease in absorptive efficiency of a given pigment molecule (Duysens 1958, Morel and Bricaud 1981). The *P-E* parameters P_m^B and α^B have also been shown to vary across taxonomic groups (Geider and Osborne 1992) and with cell size (Taguchi 1976, Geider et al. 1986, Finkel 2001). Furthermore, shifts in community structure are commonly caused by changes in the same physical (turbulence) and chemical (nutrient availability) properties of the marine environment that are known to influence photosynthetic performance (Margalef 1978, Cullen et al. 1992).

Because the absorptive properties of phytoplankton contribute to the optical signal received by satellite ocean-colour sensors, there exists the potential to observe changes in the community structure of natural phytoplankton assemblages based on variations in their optical properties over large spatial scales (Stuart et al. 1998, Ciotti et al. 1999, 2002, Sathyendranath et al. 1999). In the future, this information may be integrated into remote-sensing algorithms of primary production. Against this background I examine the relationship between the community structure and the absorptive and photosynthetic characteristics of marine phytoplankton on the continental shelf of Nova Scotia.

3.2 Materials and Methods

The dataset consists of samples collected from nine cruises that were conducted over a five-year period (1997 - 2001) during spring and fall. The cruise transects extend across the continental shelf of Nova Scotia from approximately 12 km offshore to the shelf-slope waters (Fig. 3.1). The topography of the sampling region is diverse, including a series of banks and basins. Chlorophyll-a concentrations were determined using standard fluorometric techniques (Holm-Hansen et al. 1967). Measurements of the concentrations of chlorophyll-a and accessory pigments were determined using reverse-phase, high-performance liquid chromatography analysis (HPLC) as described in Head and Horne (1993). Temperatures corresponding to the sample depths were obtained using a Seabird CTD sensor.

Particulate absorption was measured using the filter technique. Briefly, 0.5 L of seawater was filtered through a 25 mm GF/F filter and frozen immediately in liquid nitrogen and then stored at -80°C until analysed. The optical density of total particulates was measured using a Shimadzu UV-2101 dual-beam spectrophotometer with integrating sphere. Optical densities of total particulate matter were recorded at 1 nm spectral resolution from 350 to 750 nm. Samples were extracted using a mixture (6:4 vol:vol) of 90% acetone and dimethyl sulfoxide (DMSO) according to the method of Hoepffner and Sathyendranath (1992, 1993) for samples analysed prior to October 1998, or using hot methanol according to the method of Kishino et al. (1985) for samples analysed after October 1998 to determine the spectral absorption by detrital material. Unpublished data show no significant difference between extraction methods. The extracted filters were scanned from 350 to 750 nm to measure the optical density of the detrital component. Using the method of Hoepffner and Sathyendranath (1992, 1993) optical density measurements were corrected for path-length amplification arising from scattering by the filter. Corrected optical densities were then divided by the geometrical pathlength (the volume of seawater filtered divided by the clearance area of the filter) and multiplied by
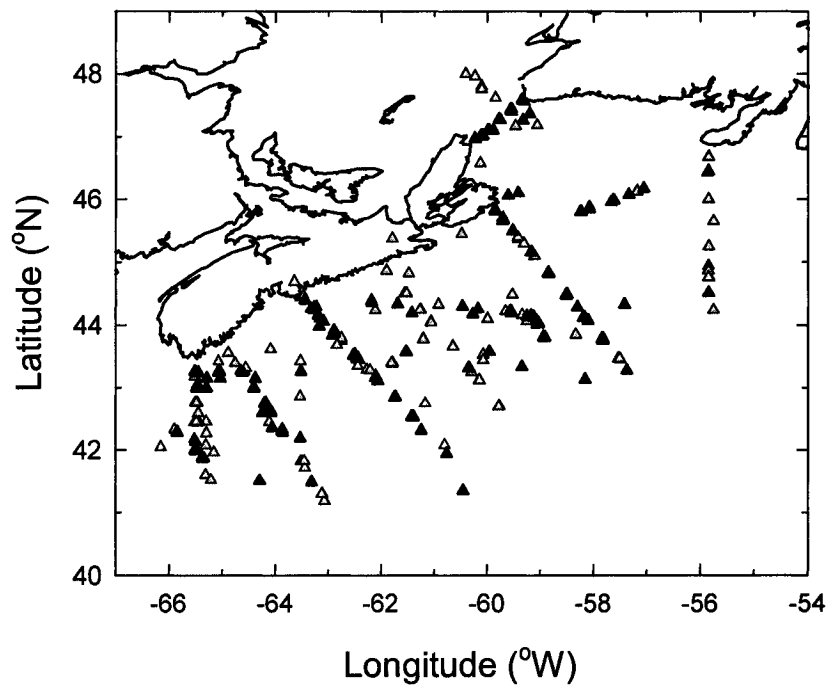
Figure 3.1. Map showing locations of the sampling stations for nine cruises
on the Scotian Shelf that were conducted over the five year period (1997-2001).
At all stations measurements of pigment composition and phytoplankton were
made. The black symbols represent stations where photosynthesis-irradiance
(*P-E*) experiments were also conducted.

the constant 2.3, which converts from decimal to natural logarithms (Mitchell and Kiefer 1988). Absorption measurements were then normalised to fluorometrically-determined chlorophyll-a concentrations to obtain chlorophyll-a specific absorption coefficients.

Flow cytometric measurements of the abundance and volume of picoplankton and nanoplankton cells (0.5 - 20 μm) were measured for all nine cruises to the Nova Scotia Shelf. A FACSort (Becton Dickson, San Jose) flow cytometer was used to enumerate phytoplankton cells from samples collected at 10 m depth intervals throughout the photic zone, as described in Li (1995). For each sample, estimates of cell biovolume and mean equivalent spherical diameter ($< D_s >$) were calculated using measurements of cytometric forward light scatter (Li 1995).

Photosynthesis-Irradiance (P-E) experiments were performed on samples collected at a variety of depths within the photic zone. To obtain a P-E curve, 30 light bottles and three dark bottles, each containing 100 ml of seawater, were inoculated with 40 μCi of sodium ^{14}C-bicarbonate. Samples were placed in a light gradient ranging from approximately 2 to 650 Wm^{-2} and incubated for 3 h. Experimental data were normalised to fluorometrically-determined chlorophyll-a concentrations and were then fitted to the equation of Platt et al. (1980) to obtain values of the initial slope (α^B) and the photosynthetic rate at saturating irradiance (P_m^B).

3.3 Results and Discussion

3.3.1 Variability in phytoplankton community structure

In this study, measurements of chlorophyll-a normalised accessory pigment concentrations, flow cytometric measurements of cell size, and the specific absorption coefficient of phytoplankton at 676 nm ($a_\phi^*(676)$) were used as indices of autotrophic community structure. One of the principal aims of the work is to determine the main environmental factors that govern changes in phytoplankton community structure on the Scotian Shelf.

Since pigments are considered to be diagnostic of certain algal taxonomic classes (Jeffrey and Vesk 1997), and chlorophyll-a and its derivative divinyl chlorophyll-a are found in all photoautotrophs (Jeffrey and Vesk 1997), total chlorophyll-a normalised pigment concentrations are useful indicators of the relative contribution of certain taxonomic groups to the total autotrophic biomass. We selected two indicator pigments to represent two major taxonomic classes of phytoplankton found on the Scotian Shelf. Fucoxanthin is an indicator pigment primarily associated with diatoms, which typically fall within the microphytoplankton size range ($>20\mu$m) (Claustre 1994, Jeffrey and Vesk 1997). 19'-hexanoylfucoxanthin is found predominantly in prymnesiophytes, which commonly fall within the nanophytoplankton size range (2-20 μm) (Claustre 1994, Jeffrey and Vesk 1997). When the chlorophyll-a normalised concentration of these pigments were plotted against temperature, clear patterns emerged (Fig.3.2A). Chlorophyll-a normalised fucoxanthin concentrations were highest at low temperatures and decreased gradually with increasing temperature, whereas chlorophyll-a normalised concentrations of 19' hexanoylfucoxanthin increased with temperature to a maximum of about 10°C.

The specific absorption coefficient of phytoplankton at 676 nm was selected as an index of the size structure of the phytoplankton community. The 676 nm waveband corresponds to the red peak of chlorophyll-a absorption, where the influence of accessory pigments is minimal (Hoepffner and Sathyendranath 1992, 1993, Allali et al. 1997, Bouman et al. 2000, Fujiki and Taguchi 2002). Thus, variability in the specific absorption coefficient in this waveband is primarily a result of pigment packaging, which is governed by two properties of the cell: its intracellular pigment concentration and its size. In a recent laboratory study by Fujiki and Taguchi (2002) a significant relationship between chlorophyll-a specific absorption at the red peak and cell size was found for a range of growth irradiances. Figure 3.2B shows $a_\phi^*(676)$ plotted against temperature. As expected, there is a positive correlation
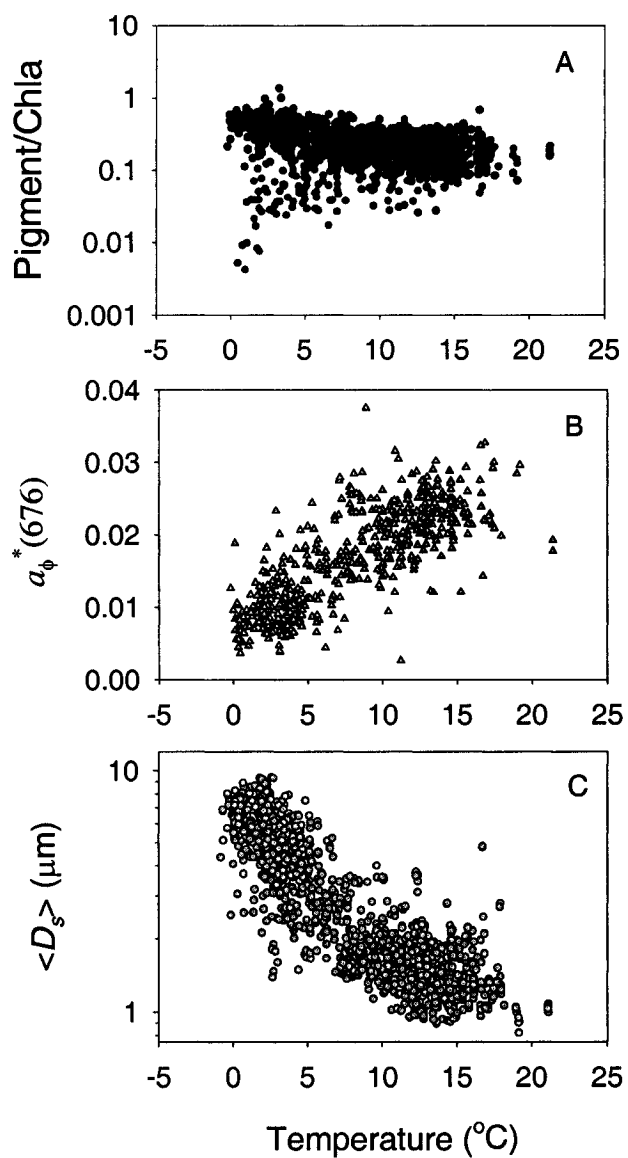
Figure 3.2. Three indices of phytoplankton gross community structure plotted against temperature. A) Chlorophyll-a normalised accessory pigment concentration. The black and red circles represent fucoxanthin and 19' hexanoyloxyfucoxanthin, respectively. B) Chlorophyll-a specific absorption coefficient at 676 nm (a_ϕ^* (676)). C) Mean equivalent spherical diameter ($<D_s>$) (μm).

between $a_\phi^*(676)$ and temperature, adding further support for the view that the relative contribution of large cells to the total phytoplankton biomass decreases with increasing temperature.

An increase in the relative contribution of small cells to total biomass with increasing temperature was also detected in flow cytometric measurements of the size distribution of ultraphytoplankton ($<20\mu$m) taken from samples collected on the Scotian Shelf. When the mean-equivalent spherical diameter ($< D_s >$) is plotted against temperature a negative correlation is found (Fig 3.2C), which provides direct evidence that the size structure of the ultraphytoplankton size range was strongly related to ambient temperature. Thus, three independent proxies of phytoplankton community structure (HPLC pigment, phytoplankton absorption and flow cytometry) are all correlated with temperature. Although temperature itself may be responsible in part for the seasonal succession of phytoplankton, it is likely that other environmental changes associated with the vernal warming of surface waters, such as an increase in water-column stratification, and a decrease in nutrient availability, also play important, if indirect, roles in determining these relationships. Therefore, I analysed vertical profiles of density (σ_T) and nitrate concentration.

Since the flux of nutrients from depth to surface waters depends partially on the strength of the density gradient ($\Delta\sigma_T/\Delta z$), one would anticipate a relationship between σ_T and the bio-optical properties of phytoplankton. The density gradient was computed as the change in σ_T from the surface to a depth of 100 m or the bottom, whichever was less, divided by the change in depth. I compared this index, a proxy for vertical stability, with another in which the gradient was computed using the difference in σ_T values measured at 30 m above and below the bottom of the mixed layer (z_m), which was defined as the depth at which σ_T has increased by a value of 1 kg m^{-3} from the surface value. The two gradients are strongly correlated with one another, despite the fact that one incorporates the depth of the mixed layer and the other does not (Figure 3.3). Thus, since little information on the general changes in vertical structure was lost by using a simple approach to computing the

density gradient and in order to compare our results with those of Li (2002), the density gradient was computed using σ_T measurements obtained from the surface and either 100 m or the bottom.

When chlorophyll-a-normalised indicator pigments were plotted against the density gradient, $\Delta\sigma_T/\Delta z$ (Fig. 3.4A), a similar pattern to that found in Figure 3.2A was observed: larger cells dominated in less stratified, well-mixed environments, whereas smaller cells contributed substantially to the overall biomass in strongly stratified waters. When $a_\phi^*(676)$ was plotted against $\Delta\sigma_T/\Delta z$, a positive correlation was found (Fig. 3.4 B). These results support the work of Li (2002), who found a strong relationship between the size distribution of the ultraphytoplankton ($<20\,\mu$m) and stratification as indexed by $\Delta\sigma_T/\Delta z$. The study showed that as stratification increased the relative abundance of picoplankton increased, the abundance of small nanoplankton cells remained relatively constant and the abundance of large nanoplankton decreased. It is important to note, however, that the relationships between the main indices of community structure and temperature (Fig. 3.2A,B) show markedly less scatter than those between the same indices of community structure and the stratification index $\Delta\sigma_T/\Delta z$ (Fig. 3.4A,B). Thus, although vertical stability may play a role in the relationship between the temperature distribution of the Scotian Shelf and phytoplankton community structure, it alone cannot account for the substantial fraction of the total variance in $a_\phi^*(676)$ explained by temperature.

Correlations between $a_\phi^*(676)$ and two indices of nutrient supply were also examined. The proxies of nutrient supply were ambient nitrate concentration (NO_3^-) and distance of the sampling depth from the depth of the nitricline (z_N), which I defined as the depth at which the nitrate concentration fell below $0.5\,\mu$M (Cleveland et al. 1989, Sosik 1996). The correlations for the two surrogates of nutrient availability with $a_\phi^*(676)$ were poor (r^2=0.03 (n=234) and r^2=0.02 (n=234) for NO_3^- and z_N, respectively).
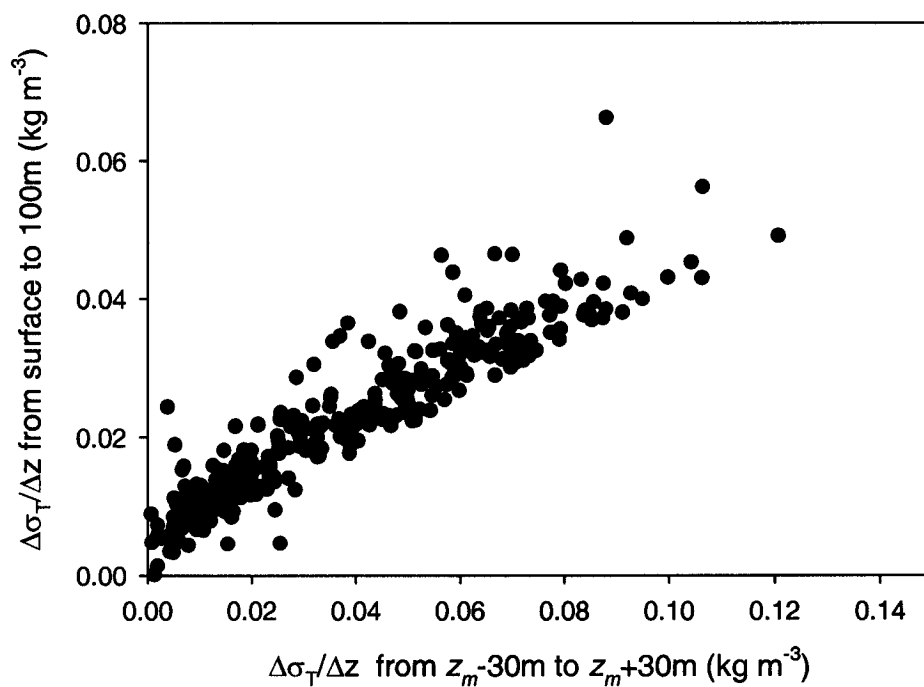
Figure 3.3. Plot of the water column density gradient computed two different ways. The difference between σ_T values measured at the surface and at 100 m or the bottom, whichever is shallower, divided by the depth interval (typically 100 m) is shown on the y-axis. The difference in σ_T values measured 30 m above and below the depth of the mixed layer (z_m) divided by the depth interval (60 m) is plotted on the x-axis.
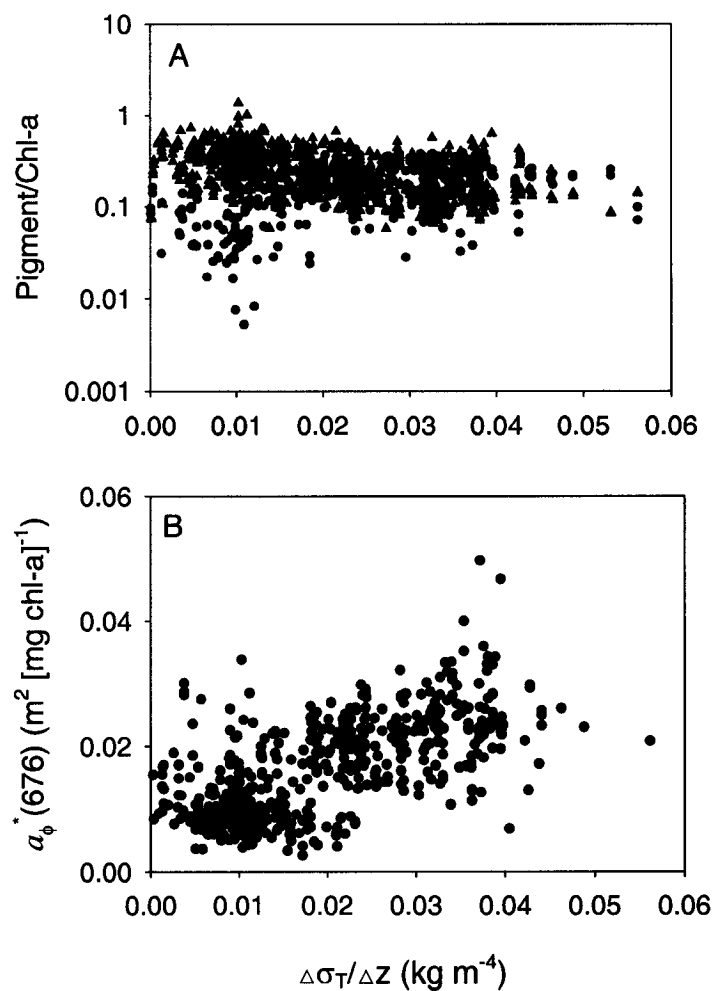
Figure 3.4. Two indices of gross phytoplankton community structure plotted against the density gradient $\Delta\sigma_T/\Delta z$. A) Chlorophyll-a normalised accessory pigment concentration of fucoxanthin and 19' hexanoyloxyfucoxanthin, represented by the black and red circles respectively. B) Chlorophyll-a specific absorption coefficient at 676 nm (a_ϕ^* (676)).

It would appear from the results presented here that shifts in phytoplankton community structure on the Scotian Shelf are in response to changes in environmental factors such as temperature and water-column stability. Several studies have proposed that nutrient supply also plays a fundamental role in the change in community composition (Yentsch and Phinney 1989, Carder et al. 1999). One of the principal advantages of small cell size is the ability to utilise low nutrient concentrations (Raven 1998). The poor correlation between $a_\phi^*(676)$ and our two indices of nutrient availability may be a result of both ambient nitrate concentration and z_N being poor indicators of nutrient supply. On the Shelf, nitrate concentrations rarely fell below $0.5\,\mu M$, which has been used in open ocean studies as a criterion for nutrient limitation (Cleveland et al. 1989, Sosik 1996). The relationship between the steepness of the density gradient ($\Delta\sigma_T/\Delta z$) and $a_\phi^*(676)$ suggests that this property of the water column may be a more useful indicator of the flux of nutrients from below the thermocline to surface waters than either ambient nitrate concentration or z_N.

3.3.2 Correlation between environmental covariates and photosynthetic performance

When the photosynthetic capacity, P_m^B, is plotted against temperature a clear positive correlation is observed (Fig. 3.5A). The plot of initial slope, α^B, against temperature shows the same pattern with markedly greater scatter (Fig. 3.5B), with deeper samples exhibiting much higher magnitudes than surface samples. The elevated values of α^B at depth are likely the combined result of low-irradiance and high-nutrient conditions, which favour high rates of light-limited photosynthesis (Cleveland et al. 1989, Sosik 1996). Based on these results, temperature can be considered a robust environmental predictor of P_m^B on the Scotian Shelf. From a physiological standpoint, these results make sense: the dark reactions of photosynthesis are enzyme-mediated and hence should exhibit temperature dependence,
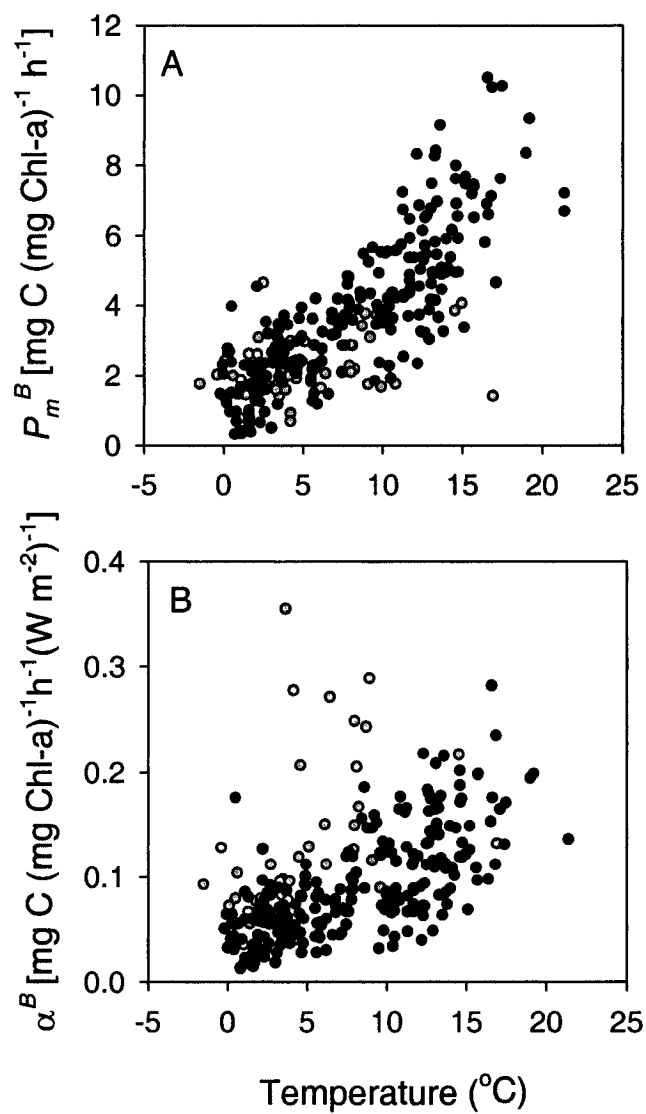
Figure 3.5. The photosynthesis-irradiance (*P-E*) parameters plotted against temperature. A) The assimilation number $P_m{}^B$. B) The initial slope of the *P-E* curve, α^B. The black and grey circles represent samples collected at or above 30 m and below 30 m, respectively.

whereas the light-harvesting reactions of photosynthesis are believed to be independent of temperature (Jewson 1976). These findings are also in agreement with other field studies that found temperature to be a strong predictor of P_m^B (Platt and Jassby 1976, Harrison and Platt 1980, Côté and Platt 1983, 1984, Kyewalyanga et al. 1998).

Some recent studies, however, have found a relatively poor correlation between temperature and P_m^B, especially in oligotrophic environments (Marañón and Holligan 1999, Siegel et al. 2001). Two hypotheses present themselves to reconcile these apparently conflicting results. The first hypothesis is that the correlation between temperature and P_m^B observed in this and other studies is coincident rather than causal: in other words a covariate of temperature is responsible for the observed relationship. The second hypothesis is that the influence of temperature on photosynthetic capacity varies in its importance relative to other environmental and/or biological covariables, (eg. nutrient availability, light history and taxonomic composition) across oceanic domains.

Using a simple correlation matrix, I examined the correlation between the main physical, chemical and biological factors known to influence phytoplankton photophysiology and the P-E parameter (Table 3.1). In addition to the positive correlation between the two P-E parameters and temperature, the matrix also shows a correlation between the P-E parameters and both the density gradient ($\Delta\sigma_T/\Delta z$) and $a_\phi^*(676)$ (see also Fig. 3.6A,B). In the following paragraphs, the results of the correlation analysis are examined in detail.

The relationship between the vertical structure of the water column and phytoplankton photophysiology was examined by plotting the P-E parameters against the strength of the density gradient, $\Delta\sigma_T/\Delta z$. The stability index $\Delta\sigma_T/\Delta z$ is an important factor controlling the rate of vertical exchange between the mixed layer and the deep water. Thus, as $\Delta\sigma_T/\Delta z$ increases, the flux of nutrient-rich water from below the thermocline diminishes. The P-E parameters were correlated with

Table 3.1: Simple correlation matrix of the photosynthesis-irradiance parameters and environmental covariates. Coefficients are based on 214 degrees of freedom.

	P_m^B	α^B	T	$\Delta\sigma_T/\Delta z$	z_m	z_N	z	$a_\phi^*(676)$
P_m^B	1.00	0.84*	0.84*	0.69*	-0.34*	-0.05	-0.30*	0.76*
α^B		1.00	0.69*	0.64*	-0.33*	0.01	-0.13‡	0.66*
T			1.00	0.73*	-0.28*	-0.11	-0.30*	0.81*
$\Delta\sigma_T/\Delta z$				1.00	-0.59*	-0.16‡	-0.28*	0.65*
z_m					1.00	0.14‡	0.22†	-0.32*
z_N						1.00	0.50*	-0.06
z							1.00	-0.25*
$a_\phi^*(676)$								1.00

* Significant at P<0.001
† Significant at P<0.01
‡ Significant at P<0.05
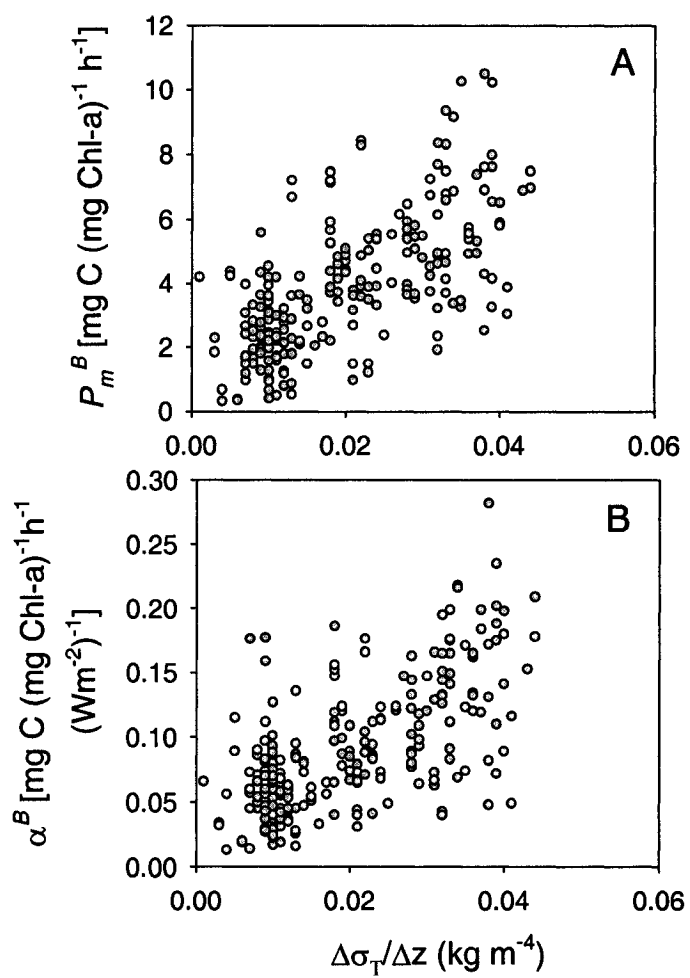
Figure 3.6. A) The light saturation parameter $P_m{}^B$ and B) the initial slope α^B plotted against the density gradient $\Delta\sigma_T/\Delta z$

the density gradient (Fig. 3.6A,B), as were the indices of community structure (Fig. 3.4 A,B).

No significant relationship between the P-E parameters and the distance of the sampling depth from the nitricline depth was found (Table 3.1). Although relationships between the distance from the nitricline and the P-E parameters have been found in other studies (Cleveland et al. 1989, Sosik 1996), these were based on observations made in regions with large vertical gradients in nitrate concentration. On the Scotian Shelf nitrate concentrations frequently were above 0.5 μM, the conventional criterion for nutrient limitation (Cleveland et al. 1989, Sosik 1996). Therefore, it seems that the distance from the nitricline may not be a suitable indicator of nutrient limitation for the Scotian Shelf.

Plots of both the light saturation parameter P_m^B and the initial slope α^B against the chlorophyll-a specific absorption coefficient of phytoplankton at 676 nm ($a_\phi^*(676)$) show clear positive correlations (Fig. 3.7). The low values of P_m^B corresponding to high values of $a_\phi^*(676)$ are likely caused by the presence of small algal cells deep in the water column during stratified conditions. The combination of low temperatures and low light conditions at depth probably led to the observed low P_m^B values. As discussed earlier, $a_\phi^*(676)$ can be considered to be a suitable proxy for phytoplankton cell size. Thus, the correlation between $a_\phi^*(676)$ and the P-E parameters may be considered as evidence that photosynthesis is governed in part by the size structure of the algal assemblage. This view is supported by several studies in which a strong correspondence between algal cell size and the P-E parameters has been found. Using cell volume measurements obtained by a Coulter counter, Harrison and Platt (1980) and Côté and Platt (1983, 1984) found strong correlations between cell volume and the P-E parameters. In laboratory studies, cell size has been shown to be negatively related to biomass-normalised rates of photosynthesis (Banse 1976, Taguchi 1976, Geider et al. 1986, Finkel 2001).

The relationship between light-limited photosynthesis and phytoplankton absorption is well known (Platt and Sathyendranath 1988, Sosik 1996). The mean
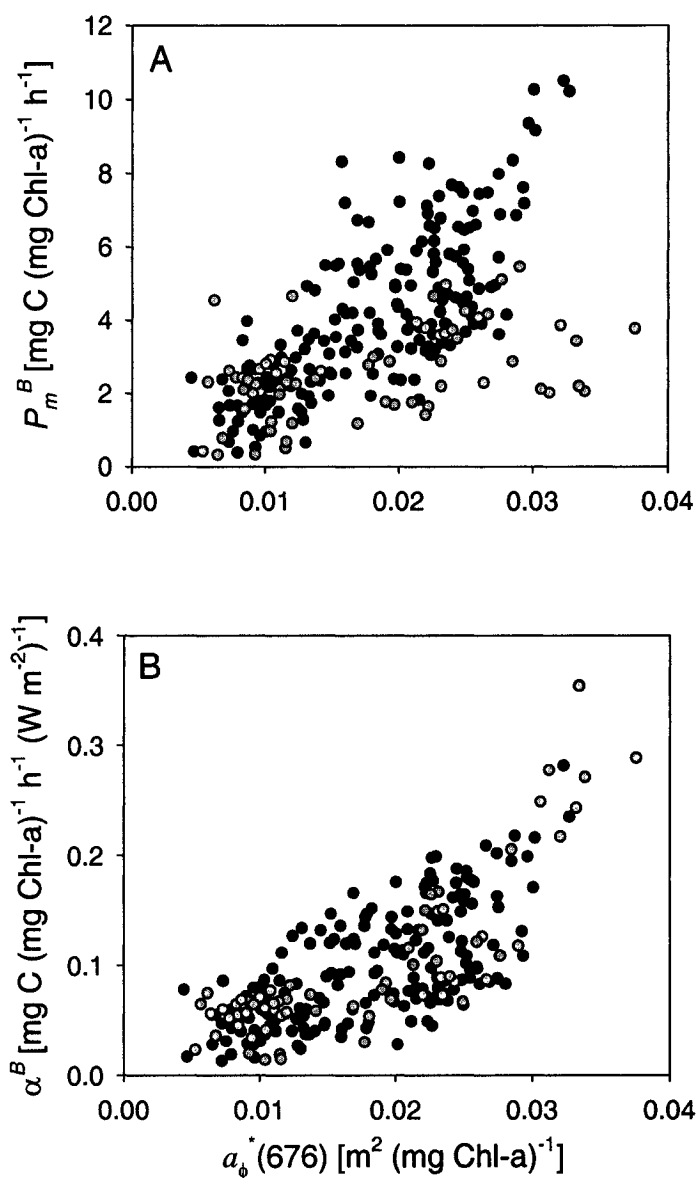
Figure 3.7. The photosynthesis-irradiance parameters, A) the assimilation number $P_m{}^B$ and B) the initial slope α^B, plotted against the chlorophyll-a specific absorption coefficient at 676 nm, a_ϕ^* (676). The black and grey circles represent samples collected at or above 30 m and below 30 m, respectively.

chlorophyll-a-specific absorption coefficient of phytoplankton, $\bar{a}_\phi^*$, averaged over the entire spectral range from 400 to 700 nm, is an important variable in bio-optical models of primary production (Geider and Osborne 1992, Sosik 1996). Specific absorption at 676 nm is influenced predominantly by pigment packaging since at this waveband chlorophyll-a is typically responsible for most of the absorption. However, in cases when chlorophytes and the cyanobacteria *Prochlorococcus* are abundant, chlorophyll-b can contribute a significant fraction of the total absorption at 676 nm. Values of $\bar{a}_\phi^*$, however, are sensitive to changes in both pigment composition and pigment packaging since they are a spectral-average of absorption by the entire pigment complement.

Understanding whether pigment packaging or pigment composition is responsible for the observed variability in $\bar{a}_\phi^*$ is important, since $\bar{a}_\phi^*$ is a central factor governing light-limited photosynthesis. The initial slope of the photosynthesis-irradiance curve (α^B) is directly related to $\bar{a}_\phi^*$ by the following relationship:

$$\alpha^B = \bar{a}_\phi^* \phi_m \tag{1}$$

where ϕ_m is the maximum quantum yield of photosynthesis (Platt and Jassby 1976, Geider and Osborne 1992). In the past it was generally assumed that most of the variability in α^B was caused by changes in $\bar{a}_\phi^*$ and that ϕ_m was relatively constant (Geider and Osborne 1992). However, in a number of field studies it has been shown that ϕ_m and $\bar{a}_\phi^*$ both contribute to the overall variability in α^B (Cleveland et al. 1989, Babin et al. 1996, Sathyendranath et al. 1996, Stuart et al. 2000). When values of α^B obtained in this study are plotted against values of $\bar{a}_\phi^*$ two things become clear (Fig. 3.8). First, the overall trend is similar to that found in Figure 3.8, suggesting that $\bar{a}_\phi^*$ is also strongly influenced by the size structure of the phytoplankton community. Second is that the scatter of this correlation, in general, falls within the ϕ_m bounds from 0.01 and 0.05 mol C (mol quanta)$^{-1}$ (Fig. 3.8). Thus, although the effect of cell size on $\bar{a}_\phi^*$ is undoubtedly an important
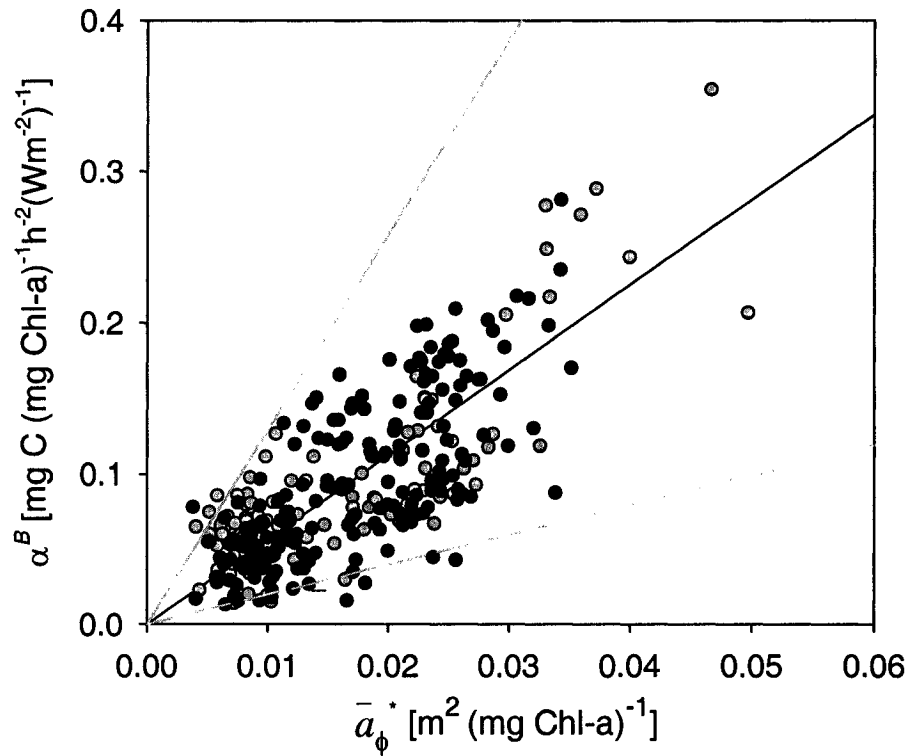
Figure 3.8. The initial slope, α^B, plotted against the mean specific absorption coefficient

of phytoplankton, $\bar{a}_\phi^*$. The black solid line is the line of best fit (maximum quantum

yield, ϕ_m, equal to 0.028 mol C (mol quanta)$^{-1}$). The upper bound of the scatter of points

represented by the solid grey line signifies ϕ_m equal to 0.05 mol C (mol quanta)$^{-1}$. The

lower bound of the scatter of points represented by the dashed grey line denotes ϕ_m equal

to 0.01 mol C (mol quanta)$^{-1}$.

factor governing the change in α^B, ϕ_m also shows a significant amount of inherent variability on the Scotian Shelf.

Multivariate linear regression analysis was performed to determine the optimal subset of environmental variables able to explain the variance in the P-E parameters. The variables used in the analysis were temperature (T), mixed layer depth (z_m), the density gradient $(\Delta\sigma_T/\Delta z)$, distance from the nitricline (zN), the chlorophyll-a specific absorption coefficient at $676\,\mathrm{nm}$ $(a_\phi^*(676))$ and depth (z). For both parameters, the best set of predictor variables at the 0.05 significance level was T, $a_\phi^*(676)$ and $\Delta\sigma_T/\Delta z$ (Table 3.2). Since temperature is accessible by remote sensing and since there exists a potential for determining the size composition of phytoplankton using high-resolution optical sensors, these results bode well for the use of satellite data to aid in the selection of the P-E parameters. It is unlikely that estimates of $\Delta\sigma_T/\Delta z$ can be obtained from remote sensing independently: estimates of this quantity would likely be derived in part from sea-surface temperature data. Nevertheless having access to information on this physical parameter will not significantly improve our ability to predict the P-E parameters since including this independent variable in the regression analysis increased the total variance explained by less than 1% in the case of P_m^B and 3% in the case of α^B.

3.3.3 Correlation between P_m^B and α^B

Because the P-E parameters represent two separate physiological processes (the light and dark reactions of photosynthesis) with different responses to temperature, the correlation between P_m^B and α^B shown in Table 3.1 is perhaps surprising. Yet studies conducted in both the field and the laboratory have shown a strong correlation between P_m^B and α^B (Platt and Jassby 1976, Taguchi 1976, Harris 1978, Côté and Platt 1983, 1984, Geider et al. 1986, Finkel 2001). Several theories, based on cell size, have been proposed to explain why the two parameters are correlated. Using data from culture studies and an energy budget of algal growth, Geider et al. (1986) demonstrated that both $\bar{a}_\phi^*$ and the light-saturated maximum growth rate

Table 3.2: Results of stepwise multiple linear regression analysis for the photosynthesis-irradiance parameters P_m^B and α^B. Input predictors were temperature (T), depth (z), nitrate concentration (NO_3^-), distance above the nitracline (z_N), the chlorophyll-a specific absorption coefficient at 676 nm $(a_\phi^*(676))$, the depth of the bottom of the mixed layer (z_m) and the density gradient $(\Delta\sigma_T/\Delta z)$. Significant biotic and abiotic variables at the 0.05 level and the amount of variance explained by the final regression are shown. Analysis is based on 234 degrees of freedom.

Parameters	Significant Predictors	P	r^2
P_m^B	T	<0.001	0.714
	$a_\phi^*(676)$	<0.001	
	$\Delta\sigma_T/\Delta z$	<0.05	
α^B	T	<0.001	0.534
	$a_\phi^*(676)$	<0.001	
	$\Delta\sigma_T/\Delta z$	<0.001	

(μ_m) decrease with an increase in cell size. Since under light saturated conditions μ_m should be proportional to P_m^B, and since $\bar{a}_\phi^*$ is proportional to α^B according to equation 1, then P_m^B and α^B should also be positively correlated. Platt and Jassby (1976) argued that cell size might be responsible for the correlation between the P-E parameters observed in coastal waters and provided theoretical justification, although no direct measurements of cell size were made. In a series of field studies conducted in Bedford Basin (Nova Scotia, Canada) strong correlations between the P-E parameters and measurements of cell volume were found (Harrison and Platt 1980, Côté and Platt 1983,1984). In this temperate coastal system, $\bar{a}_\phi^*$, temperature and cell size covary, and these three properties are known to cause variability in the magnitude of P_m^B (in the case of temperature) or α^B (in the case of $\bar{a}_\phi^*$) or both (in the case of cell size). Unfortunately, the covariation of these important factors regulating the P-E parameters makes it difficult to determine the relative contribution of each to the overall variation in P_m^B and α^B in the marine environment.

3.3.4 Relationship between P_m^B and temperature: Correlation or causation?

The relationship between P_m^B and temperature has been reported in numerous studies of temperate marine ecosystems. Using data collected from this study, as well as from two studies of the Bedford Basin (Côté and Platt (1983) and data collected as part of this thesis, see Chapter 4), P_m^B was plotted against temperature. The resulting plot (Fig. 3.9) shows that the three studies share remarkably similar trends. This was unexpected, since the coastal inlet possessed markedly different physical and chemical characteristics from those found on the Scotian Shelf. The similar trends suggest that the relationship between temperature and P_m^B observed in this study may pertain to a wider range of hydrographic regions. Thus, we compared our results with the temperature-dependent model of light-saturated photosynthesis presented in a study by Behrenfeld and Falkowski (1997). Their empirical model was based on an extensive dataset of P_{opt}^B values (the maximum
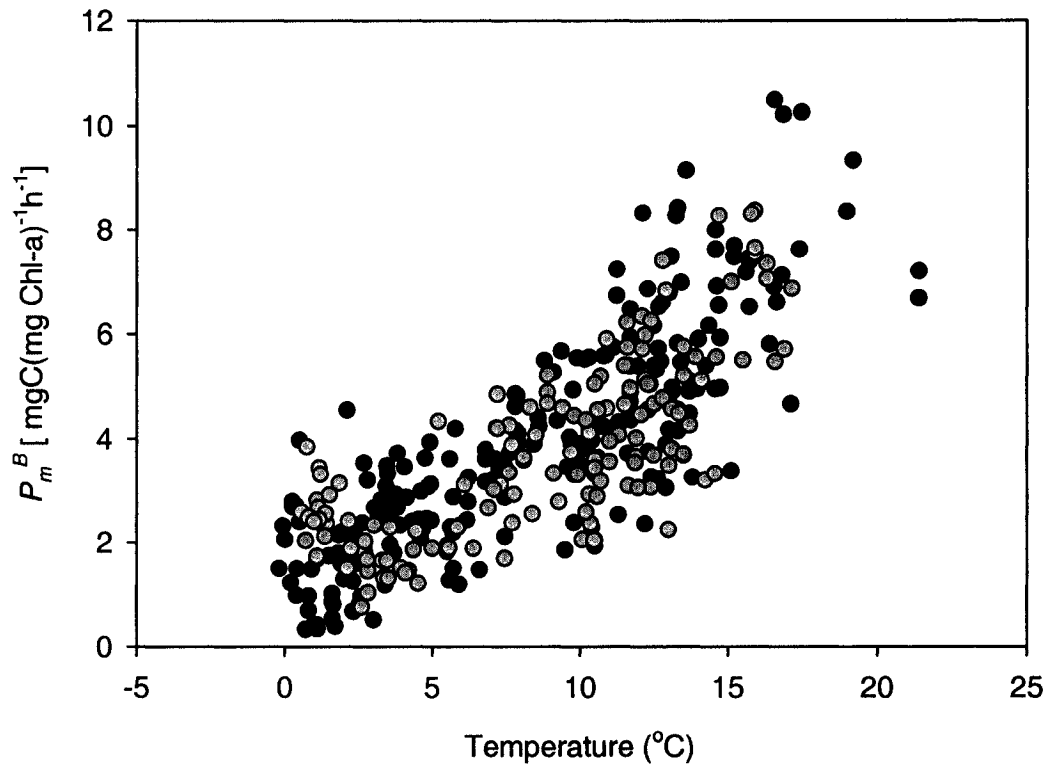
Figure 3.9. The relationship between the assimilation number, P_m^B, and temperature for three studies conducted in mid-latitude temperate waters. The grey symbols denote data collected from the study of the Bedford Basin by Côté and Platt (1983, 1984) and a year long time series study obtained from March 2000-April 2001 (see Chapter 4). The black symbols represent data collected on the Scotian Shelf. Since both of the Basin studies sampled near the surface (5m) only Scotian Shelf data obtained within the top 20m is shown for comparison.

observed rate of carbon fixation within the water column [mg C (mg Chl-a)$^{-1}$ h^{-1}]). The parameters P_{opt}^B and P_m^B are used in models of primary production to represent the biomass-normalised, maximum rate of carbon fixation. However, it is important to note that the parameters are obtained by different experimental means: P_{opt}^B is obtained from 6 to 24 h *in situ* ^{14}C incubations, whereas P_m^B is derived from short-term ($\sim$3 h) ^{14}C experiments conducted in an incubator onboard a ship. Since *in situ* experiments are conducted over a much longer time-frame than *P-E* experiments, they are strongly influenced by zooplankton grazing, respiration and excretion of labelled carbon by algal cells. Moreover, the value of P_{opt}^B is the maximum biomass-normalised production rate observed for a given *in situ* profile and whereas values of P_m^B are obtained by fitting a non-linear function to data obtained from photosynthesis-irradiance experiments conducted over a range of light intensities. *In situ* incubations usually consist of around five to ten samples spaced evenly throughout the photic zone, whereas *P-E* experiments are typically conducted over 20 to 30 light intensities. Another important distinction between the two methods is that available light is variable during *in situ* incubations, whereas irradiance levels are held constant in a *P-E* incubation experiment. Thus, P_m^B is a more stringent estimate of the assimilation number than P_{opt}^B.

To describe the relationship between P_{opt}^B and temperature, Behrenfeld and Falkowski (1997) fitted a seventh-order polynomial to median values of P_{opt}^B computed for every 1°C interval (Fig. 3.10). Given the inherent differences between P_{opt}^B and P_m^B, the empirical model of Behrenfeld and Falkowski (B-F) fits surprisingly well to the Scotian Shelf dataset for the low-to-intermediate temperature range (0-12°C). At the high end of the temperature range, however, there is a divergence between the B-F model and the Shelf data points, with the B-F model underestimating the P_m^B values. The decline in the polynomial function at around 20°C is a result of some low values of P_{opt}^B observed at high temperatures. However, if we compare the median values of P_{opt}^B that were used to obtain the high-order polynomial function with the Scotian Shelf datapoints within the temperature range that
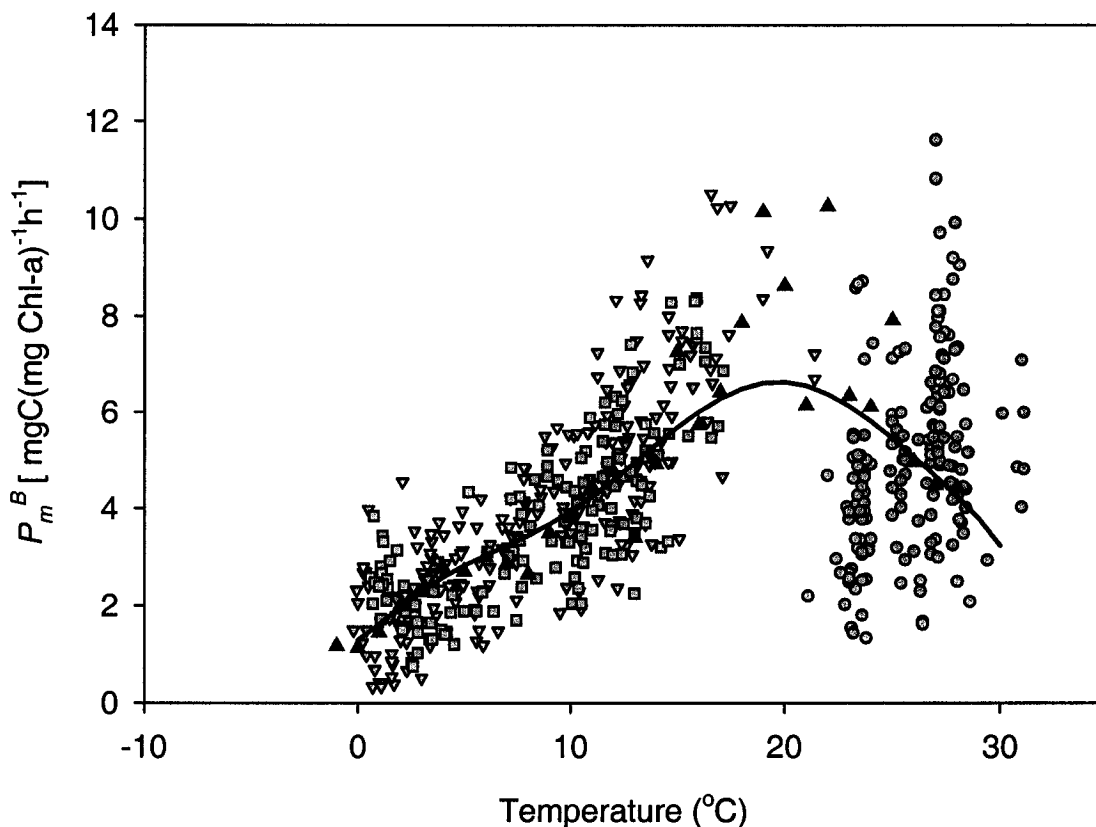
Figure 3.10. Comparison between the seventh-order polynomial proposed by Behrenfeld and Falkowski (1997) to describe the temperature dependence of the maximum observed photosynthetic rate per unit chlorophyll in the water column (P_{opt}^B), and values of the assimilation number (P_m^B) obtained by P-E experiments made in different oceanic regimes. The polynomial function is shown by the solid red line. The median points of P_{opt}^B used to obtain the polynomial fit are shown by the red triangles. The grey triangles denote data from the Bedford Basin (Côté and Platt, 1983, 1984) and additional data collected from March 2000 to April 2001 as part of this thesis work.). The grey squares represent datas obtained on the Scotian Shelf. The grey circles denote samples collected in the Arabian Sea (data obtained from the BIO optical database). For the Bedford Basin studies, samples were collected near the surface (5m), whereas for the Scotian Shelf and Arabian Sea datasets, only samples obtained within the top 20m are plotted.

both datasets share (0 - 20°C), we see that the correspondence is better. This may be caused by the high numbers of observations made in North Atlantic waters in this temperature range. In fact, over 88% of the data points used in the Behrenfeld and Falkowski model were obtained in the North Atlantic.

To examine how well the temperature-dependence of the B-F describes the photosynthetic capacity at the high temperature range, we compared data collected in the Arabian Sea with the empirical function (Fig. 3.10). It is clear that temperature is a poor predictor of P_m^B for this oceanic region. Behrenfeld et al. (2002) have reported a poor correspondence between the light-saturation parameter and temperature, especially in oligotrophic, subtropical regions. This suggests that some other environmental and/or biological co-variate may be governing the variability in P_m^B. For the Scotian Shelf dataset, the two principal covariates of temperature that were also correlated to the P-E parameters were the density gradient, $\Delta\sigma_T/\Delta z$, and the specific absorption coefficient at 676 nm, $a_\phi^*(676)$ (Table 3.1).

In the case of the Arabian Sea, temperature is a poor predictor of turbulence and vertical stability. In fact, the highest temperatures were observed during the monsoon season, when vertical mixing was strongest, whereas on the Scotian Shelf, intense mixing is associated with cooler temperatures. Since vertical mixing is one of the principal mechanisms by which nutrients are introduced from depth to the euphotic zone, one would also predict that the relationship between temperature and nutrient availability would also be markedly different in these two oceanic regions.

The specific absorption coefficient $a_\phi^*(676)$ is a proxy for the size distribution of phytoplankton. The correlation between $a_\phi^*(676)$ and both $\Delta\sigma_T/\Delta z$ and temperature in mid- and high-latitude waters can probably be attributed to changes in physicochemical factors that control the community structure of the phytoplankton. It has been shown in macroecological studies that both temperature and water-column stratification are indicators of the size structure of phytoplankton communities for a variety of oceanic regions (Li 2002, see also Chapter 2). In several studies in temperate marine ecosystems an increase in P_m^B is accompanied by a

corresponding increase in temperature and decrease in cell size. Given P_m^B has been shown to be positively correlated with both temperature and cell size, we would expect to find the highest values of P_m^B in warm, oligotrophic waters. However, we know from the example of the Arabian Sea and other studies (Marañón and Holligan 1999, Siegel et al. 2001) that this is not the case.

Taxon-specific differences in phytoplankton metabolic rates, combined with an increase in nutrient stress, may explain why in high-temperature, oligotrophic conditions, values of P_m^B are lower than at intermediate levels of temperature and nutrient concentration. In this study, as well as in those by Harrison and Platt (1980), Côté and Platt (1983, 1984), and Kyewalyanga et al. (1998), high temperatures corresponded to a high contribution to the total phytoplankton biomass of nanoflagellates, which are known to have high rates of biomass-specific production (Harris 1978, Harrison and Platt 1980). However, in warm-water, oligotrophic environments, cyanobacteria within the picoplankton size range are the dominant contributors to the total autotrophic biomass and nutrient concentrations are often at undetectable levels near the surface. Field studies conducted in picoplankton-dominated waters have reported moderate to low values of P_m^B and α^B (Babin et al. 1996, Bouman et al. 2000). In surface waters of oligotrophic regimes the accessory pigment complement of these cells is dominated overwhelmingly by the non-photosynthetic pigment, zeaxanthin, which can contribute to over 50% of the total absorption by phytoplankton cells in the blue-green region of the spectrum (Babin et al. 1996, Bouman et al. 2000). The combined effects of low nutrient availability and high contribution of non-photosynthetic pigments to the total absorption by phytoplankton leads to very low α^B values in surface waters. When P_m^B is plotted against α^B (Fig. 3.11), the scatter of points implies clear boundaries for E_k ($= P_m^B/\alpha^B$). If there is indeed a maximum value of E_k that cells can attain, then a low value of α^B, for example in picoplankton dominated nutrient-limited ecosystems, would imply a corresponding low value for P_m^B.
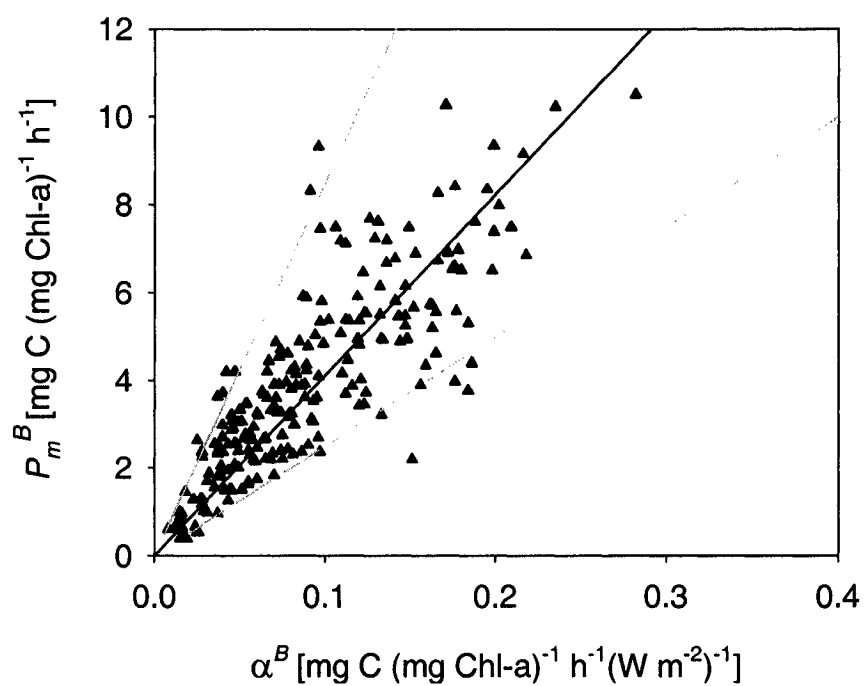
Figure 3.11. The assimilation number, P_m^B, plotted against the initial slope of the *P-E* curve α^B for samples collected within the top 20 m of the water column. The solid line denotes the line of best fit (photoadaptation parameter, $E_k = P_m^B / \alpha^B$, equals 41 W m^{-2}). The upper bound of the scatter of points represented by the solid grey line signifies an E_k value of 85 W m^{-2}. The lower bound of the scatter of points represented by the dashed grey line denotes an E_k value of 25 W m^{-2}.

It is also important to emphasize, however, that there exist regions, such as the Arabian Sea, where vertical mixing is not associated with the introduction of cooler water to the sea surface, and blooms of diatoms can occur at temperatures above 30°C. There is little doubt that the wide variation in phytoplankton community structure observed in the Arabian Sea, which is similar to that observed in temperate regions, is responsible in part for the large variation in the physiological properties within the narrow range of temperatures found in the Arabian Sea. To examine whether light-saturated photosynthesis is related to phytoplankton taxonomic composition, P_m^B was plotted against the chlorophyll-a normalised concentration of fucoxanthin, which is an indicator pigment of diatoms, for both the Scotian Shelf and Arabian Sea datasets (Fig. 3.12). The plot shows that as the relative contribution of diatoms to the total microalgal biomass increases, there is a corresponding decrease in P_m^B.

Based on the arguments presented above it is obvious that more work needs to be done to assess the value of temperature as a predictor of P_m^B. It is essential to establish whether the relationship between P_m^B and temperature is a causative or correlative one, if we are to ascertain the potential utility of this environmental co-variable in primary production algorithms for use on the global scale. The influence of phytoplankton community structure on aquatic photosynthesis should also be pursued, since there is the potential for monitoring the size distribution of phytoplankton on large scales using optical sensors (Ciotti et al. 1999).

3.5 Concluding Remarks

Phytoplankton community structure and primary productivity are ecological features of marine systems that are known to change in response to the prevailing physical and chemical conditions (Margalef 1968). In temperate regions, the evolution of phytoplankton communities from early to mature stages of succession is accompanied by transitions in the physicochemical properties of the marine ecosystem, from vertically mixed, nutrient-rich cooler waters to stratified, nutrient-poor,
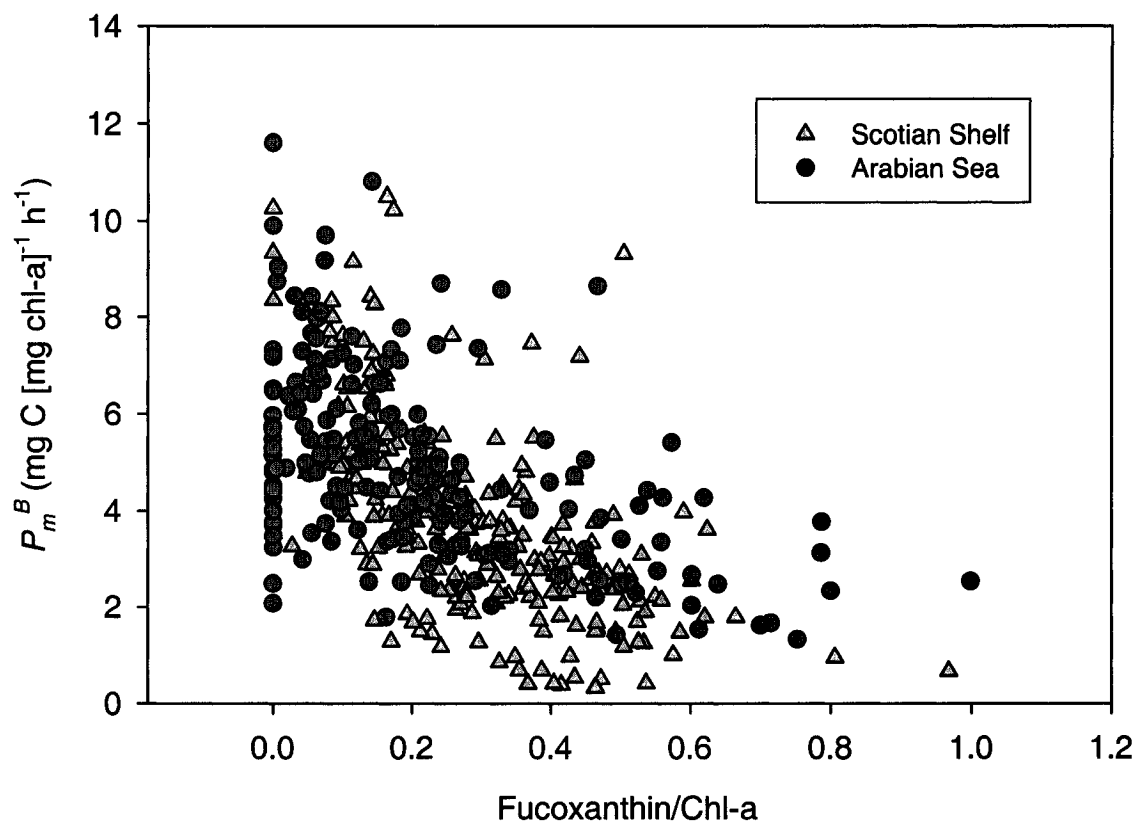
Figure 3.12. The assimilation number, P_m^B, plotted against the chlorophyll-a normalised fucoxanthin concentration. The circles represent data collected from the Arabian Sea and the triangles represent data collected on the Scotian Shelf.

warmer waters (Margalef 1978, Cullen 2002). The data presented in this paper show that across gradients of temperature and water-column stability, pronounced changes occur in the taxonomic and size structure of phytoplankton communities. In highly turbulent, nutrient-rich environments diatoms contribute overwhelmingly to the overall autotrophic biomass, whereas in stable, oligotrophic waters, smaller cells are dominant.

Temperature has been implicated as a predictor of the size structure of phytoplankton communities (Carder et al. 1999, Chapter 2). In numerous studies of temperate regions, a strong relationship between light-saturated photosynthesis and temperature has been observed (Platt and Jassby 1976, Harrison and Platt 1980, Côté and Platt 1983, 1984, Kyewalyanga et al. 1998). In these oceanic regimes, seasonal variations in nutrient availability and physical forcing result in pronounced changes in phytoplankton community structure: phytoplankton cells that are best suited to the prevailing physicochemical conditions based on their physiological characteristics will dominate. Such changes in species composition are reflected in the photosynthetic properties of the phytoplankton community. Therefore, by incorporating information on the large-scale distribution of sea-surface temperature and community structure derived from measurements obtained from remote sensing, we may be able to improve significantly our estimates of primary production using ocean-colour data.

CHAPTER 4

Seasonal Variations in the Bio-optical
Properties of the Bedford Basin

4.1 Introduction

The pigment chlorophyll-a (and its derivative divinyl-chlorophyll-a) is found in all marine photoautotrophs and therefore is a useful indicator of algal biomass. Because chlorophyll-a is so ubiquitous and is frequently the dominant pigment in marine phytoplankton, it is a major contributor to the optical characteristics of marine waters. Space-borne optical sensors can be applied to generate large-scale maps of chlorophyll concentration over near-synoptic timescales, enabling oceanographers to assess the spatial and temporal variability in phytoplankton standing stock. Such maps can be used, in combination with information on algal photophysiology, to derive maps of primary production (Platt and Sathyendranath 1988, Morel 1991).

Chlorophyll-retrieval algorithms developed for the open ocean are all based on the same fundamental assumption: variations in the reflectance signal received by the satellite are caused by variations in absorption by phytoplankton and co-varying substances (Gordon and Morel 1983). In coastal waters, however, superimposed on the optical signal of the phytoplankton are seasonal changes in the concentrations of non-algal particulate and dissolved materials. Coastal waters are heavily influenced by optical components that are terrestrial in origin. This makes it difficult to separate the contribution by phytoplankton to the optical signal from those by other optically-significant substances (IOCCG 2000). Discriminating phytoplankton from the rest of the absorptive components before optical data can be used to model primary production in coastal waters.

Accurate parameterisation of the spectral shapes of absorption by phytoplankton, detritus and coloured dissolved organic material (CDOM) is required for reli-

able estimates of pigment biomass in coastal waters (Bukata et al. 1981a,b, 1991, Doerffer and Fisher 1994, Roesler and Perry 1995, Lee et al. 1996, 1999, Garver and Siegel 1997). The absorptive properties of phytoplankton are perhaps the most studied of the optical components. Variability in the spectral shape of phytoplankton absorption is known to be influenced by three properties of the algal cell: its pigment composition, its size and its intracellular pigment concentration (Morel and Bricaud 1981, Sathyendranath et al. 1987, Hoepffner and Sathyendranath 1992, 1993). Since each pigment has a particular absorptive signature, the spectral shape of phytoplankton absorption depends on the relative concentrations of the various pigments contained within the algal cell (Bidigare et al. 1988, Hoepffner and Sathyendranath 1992, 1993). Cell size and intracellular pigment concentration also influence the spectral dependence of absorption by influencing the absorptive efficiency of the pigments found within the phytoplankton cell. Since pigments are packaged within chloroplasts, which in turn are contained within individual cells, the efficiency with which they absorb light is lower than if they were distributed uniformly in solution. This reduction in absorptive efficiency is commonly referred to as the package effect (Duysens 1956), and is highest at wavelengths where absorption is strongest. Thus pigment packaging leads to an overall flattening in the absorption spectrum (Duysens 1956, Kirk 1994). The *in vivo* absorption by algal pigments also differs from absorption *in vitro* because the absorptive properties of pigments are altered when they are embedded in protein complexes (Johnsen et al. 1994).

Compared with phytoplankton, information on the variability in the absorptive properties of detritus and CDOM is scarce. Like phytoplankton, detritus and CDOM are strong absorbers of blue light and weak absorbers of green light. This similarity in the spectral structure of absorption between algal and non-algal components is the main reason why simple chlorophyll retrieval algorithms (based on blue-to-green reflectance ratios) break down in waters heavily influenced by non-algal particulate and dissolved absorption (IOCCG, 2000). The spectral dependence

of absorption by CDOM and detritus can be described by the following exponential function (Bricaud et al. 1981):

$$a_x(\lambda) = a_x(\lambda_0) \exp[-S_x(\lambda - \lambda_0)], \tag{1}$$

where $a_x(\lambda)$ is the absorption coefficient of either detritus ($x = d$) or CDOM ($x = y$) at wavelength λ, $a_x(\lambda_0)$ is the absorption coefficient of x at reference wavelength λ_0 and S_x is the slope of the exponential curve. The slope parameter for CDOM has been shown to be heavily influenced by the chemical composition of the dissolved material. Carder et al. (1989) separated the absorption by fluvic and humic acids, which account for most of the absorption by CDOM, and found that the exponential absorption curves of the fluvic acid component had S_y values nearly two times greater than those of the humic acid component.

Information on the spectral characteristics of both particulate and dissolved components of absorption is also required to compute marine primary production. In general, three things must be known to calculate the amount of carbon fixed by marine photoautotrophs: how much photosynthetically-available light is present; second how much plant pigment is present to intercept this light; and third, with what efficiency is the light which is absorbed by these pigments converted into photosynthetic substrate (carbon). Since phytoplankton pigments and non-algal dissolved and particulate absorptive components are strong attenuators of light, estimation of the underwater light field requires knowledge of both the magnitude and spectral dependence of absorption by these materials. Moreover, since pigment biomass is a scaling factor in primary productivity models, errors in the estimation of chlorophyll-a concentration from ocean-colour algorithms will result in errors in the estimation of water-column primary production.

Estimates of the concentration of algal pigment and other attenuators of light in the water column and information on the photosynthetic response of marine phytoplankton to available light are needed before the rate of primary production can be estimated. The photosynthesis-irradiance (P-E) curve is conventionally used

in models of primary production to describe the photosynthetic response of phytoplankton to available light and can be described using two parameters: P_m^B, the assimilation number and α^B, the initial slope, where the superscript B indicates normalization to phytoplankton biomass (Jassby and Platt 1976). These so-called P-E parameters are known to vary according to cell size, temperature, nutrient availability and light history (Harris 1978, Geider and Osborne 1992). Unfortunately, the P-E parameters cannot be obtained directly through remote sensing. Thus, our ability to estimate primary production in aquatic environments relies heavily on our understanding of what physical, chemical and biological factors regulate the seasonal variability of P_m^B and α^B.

In this chapter, seasonal changes in the optical and photosynthetic characteristics of a coastal embayment (Bedford Basin, Nova Scotia) are examined. Variability in the spectral shapes and magnitudes of the absorption spectra of CDOM $(a_y(\lambda))$, detritus $(a_d(\lambda))$ and phytoplankton $(a_\phi(\lambda))$ are assessed and their relationships with the physicochemical and biological properties of the water column are examined. Variations in the optical and physical characteristics of the basin as they relate to changes in the photosynthetic properties of the phytoplankton community are explored. The implications of these findings for modelling primary production in coastal environments are addressed.

4.2 Material and Methods

Bedford Basin is a small marine inlet with a surface area of $17\,\text{km}^2$ that is separated from the sea by a $20\,\text{m}$ deep sill. Freshwater runoff, tides and wind events drive a continuous exchange of surface water between the basin and the open ocean (Platt et al. 1972). Sampling of the Bedford Basin was conducted once a week at its deepest point, $70\,\text{m}$ ($44°42.3'\text{N}$, $63°39.2'\text{W}$), from March 2000 to April 2001. During the spring bloom period the sampling frequency was increased to three times a week. Water samples were collected using a Niskin bottle at three depths (1, 5 and 10 m) for the determination of pigment concentration and composition, nutrient

concentration and absorption by particulate and dissolved material. Chlorophyll a concentrations were determined using the standard fluorometric technique (Holm-Hansen et al. 1965). In addition, pigment composition was determined using reverse-phase, high performance liquid chromatography analysis (HPLC) as described in Head and Horne (1993). Nitrate plus nitrite, silicate and phosphate concentrations were determined using an Alpken autoanalyzer (Irwin et al. 1989). Temperature and salinity profiles were recorded at 1 m intervals using a CTD sensor (Seabird, Model SBE 25).

Water samples were also collected during a red tide that occurred between August 30 and September 1, 2000. On August 30, two surface samples were collected for HPLC and absorption analysis. On September 1, samples were collected at 2 m intervals from the surface to 10 m three times during the day.

4.2.1 Optical Properties

To determine absorption by dissolved organic material, seawater was filtered through a 0.2 μm Nucleopore membrane that had been soaked in 10% HCl and pre-rinsed with 50 ml of Milli-Q water. The optical density of the filtered water was measured in a 10 cm quartz cuvette between 250 and 750 nm every 1 nm using a dual-beam spectrophotometer (Shimadzu Corp., UV-2101, Kyoto). Barnstead, UV-treated water was used as a reference. A baseline correction was applied by subtracting the optical density value averaged between 600 and 605 nm. The null value was chosen in this region of the spectrum because the absorption by CDOM is considered to be negligible and variability caused by temperature and salinity was minimal. Optical densities were converted to units of absorption by applying a multiplication factor of 2.3 to convert from base 10 to natural logarithms and dividing by the pathlength (0.1 m). Absorption spectra were then fitted to equation (1) between 350 and 500 nm to obtain values of the slope parameter for CDOM S_y.

Phytoplankton absorption was determined using the filter technique (Kishino et al. 1985). Water samples were filtered through 25-mm GF/F (Whatman) filters using a vacuum filtration pump under low pressure. The optical density of total particulates retained on the filter pad $O_p(\lambda)$ was measured using a dual-beam spectophotometer (Shimadzu Corp., UV-2101, Kyoto) equipped with an integrating sphere. Pigments were then extracted by passing 20 ml of hot methanol through the filters (Kishino et al. 1985), after which the filters were re-scanned to obtain the optical density of the detrital component $(O_d(\lambda))$. To estimate the optical density of particulate and detrital material in suspension $(O_s(\lambda))$, the pathlength amplification factor of Hoepffner and Sathyendranath (1992) was used. Finally, the optical densities were converted to absorption coefficients $(a(\lambda)$ by the following equation:

$$a(\lambda) = 2.3\,O_s(\lambda)(A/V) \tag{2}$$

where A is the clearance area of the filter, V is the volume of seawater filtered and the constant 2.3 converts from base 10 logarithms to natural logarithms (Mitchell and Kiefer 1988). Absorption by phytoplankton pigments $a_\phi(\lambda)$ was determined by subtracting the absorption by detrital material $a_d(\lambda)$ from the absorption by total particulates $a_t(\lambda)$. The chlorophyll-specific absorption coefficient of phytoplankton $a_\phi^*(\lambda)$ was calculated by dividing $a_\phi(\lambda)$ by the Turner chlorophyll concentration. Equation (1) was then fitted to the absorption spectra of detrital absorption $(a_d(\lambda))$ to obtain values of the slope parameter S_d. Data in the spectral ranges of 400-480 nm and 620-710 nm were excluded to avoid residual absorption by pigments that were not fully extracted by the hot methanol technique (Babin et al. 2003). The spectrally averaged absorption coefficient of phytoplankton was calculated as follows:

$$\bar{a}_\phi = \frac{\int_{400}^{700} a_\phi(\lambda)d\lambda}{\int_{400}^{700} d\lambda}. \tag{3}$$

To obtain values of the mean, chlorophyll-a specific absorption coefficient, $\bar{a}_{phi}$ was divided by the fluorometric chlorophyll-a concentration.

4.2.2 Photosynthesis-Irradiance Experiments

Photosynthesis-irradiance $(P\text{-}E)$ experiments were performed on water samples collected at 5 m throughout the sampling period. To obtain a $P\text{-}E$ curve, 30 light and three dark bottles, each containing 100 ml of seawater, were innoculated with 20 μCi of sodium ^{14}C-bicarbonate. To maintain the samples at *in situ* temperatures, a temperature-controlled circulating waterbath was used. Bottles were then placed in a light gradient ranging from approximately 2 to 650 W m^{-2}. At the end of the three-hour incubation samples were filtered onto GF/F filters and then fumed over a bath of concentrated HCl to remove any inorganic ^{14}C remaining on the filter. Samples were then counted in a Beckman LS 5000 CE liquid scintillation counter. Computed values of carbon uptake per unit time were then normalised to fluorometrically-determined chlorophyll-a concentrations. These data were then fitted to the equation of Platt et al. (1980) to obtain the initial slope (α^B) and the photosynthetic rate at saturating irradiance (P_m^B). Values of α^B were corrected for the emission spectrum of the tungsten-halogen lamp as described in Kyewalyanga et al. (1997).

4.3 Results and Discussion

4.3.1 Phytoplankton Biomass

Phytoplankton biomass, as indexed by *in situ* fluorescence and Turner chlorophyll concentration, fluctuated strongly over the sampling period (Fig. 4.1A,B). The spring diatom blooms in 2000 and 2001 were marked by exponential increases in pigment concentration during the month of March. During the 2000 bloom, maximum chlorophyll-a concentrations of 23 mg Chl-a m^{-3} at 1 m and 24 mg Chl-a m^{-3} at 5 m were observed on March 22 and 24, respectively. At the 10 m sampling depth,
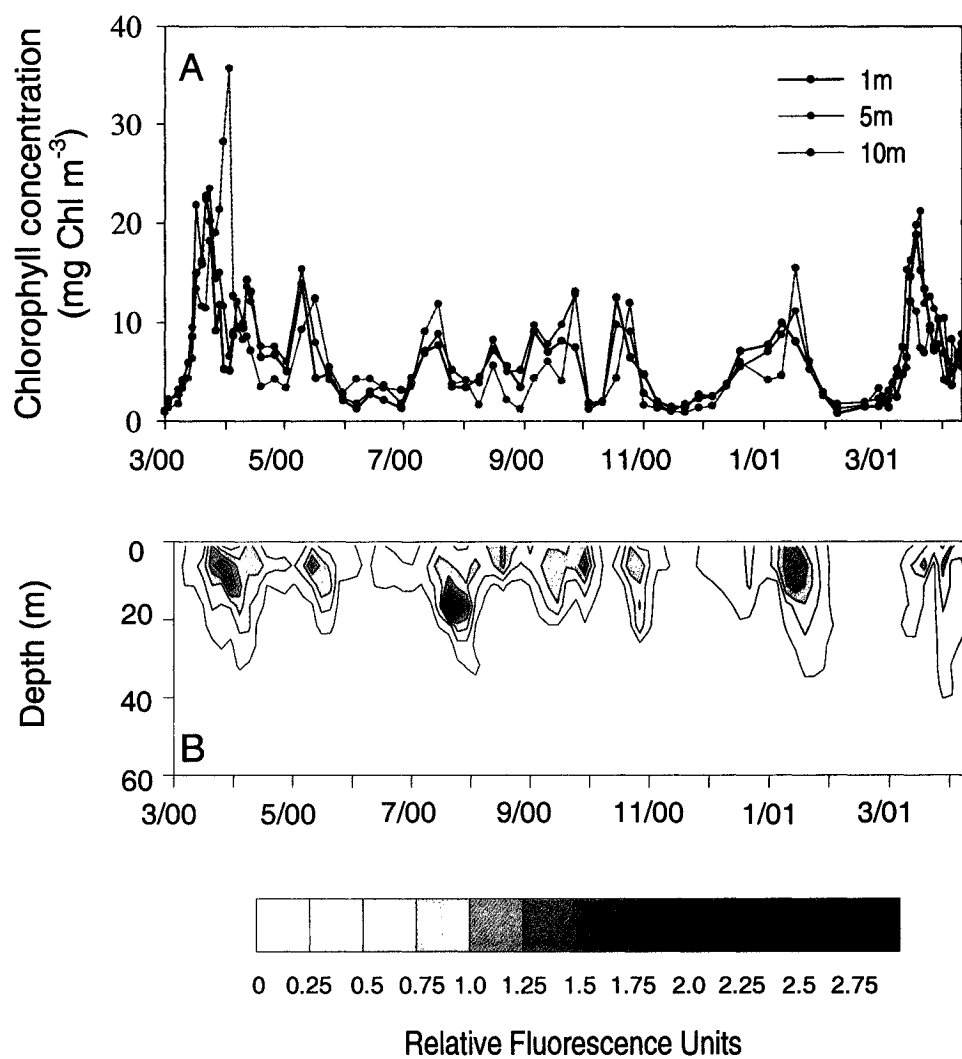
Figure 4.1. Seasonal variation in chlorophyll-a concentration in Bedford Basin from March 2000 to April 2001. A) Time series measurements of Turner fluorometric chlorophyll-a concentration at 1, 5 and 10 m. B) *In situ* profiles of fluorescence.

however, the maximum chlorophyll-a concentration of 36 mg Chl-a m^{-3} was measured more than one week later than the peak chlorophyll-a concentrations observed at 1 and 5 m. The reason for this lag is likely the combination of the deepening of the nitricline and the sinking of phytoplankton cells.

At the onset of stratification nutrient levels were high. As inorganic nutrients were utilised in cell growth and reproduction, nutrients became depleted at the sea surface (see next section). The spring bloom was each year dominated by diatoms, which have relatively fast sinking rates compared with other groups of phytoplankton due to their large size and heavy silica skeletons. The loss of phytoplankton cells from the surface due to sinking and zooplankton grazing eventually exceeded the addition of algal biomass by cell growth, resulting in a net decrease in phytoplankton biomass at the surface. The decline in pigment concentration resulted in a decrease in light attenuation, thereby allowing more photosynthetically-available radiation to reach the nutrient-rich deeper layers of the water column. Thus, phytoplankton biomass at 10 m continued to increase, until the nutrient supply became exhausted, resulting in the decrease in pigment concentration, which was observed in mid-April.

The spring bloom of 2001 was nearly identical to that of 2000 in both timing and amplitude for the upper 5 m of the water column. Maximum chlorophyll-a concentrations of 19 and 21 mg Chl-a m^{-3} were observed at 1 and 5 m on March 19 and 21, respectively. The gradual sinking of the chlorophyll maximum observed during the 2000 spring bloom did not occur in 2001. The 10 m samples attained maximum concentrations of only 12 mg Chl-a m^{-3} on March 16. The uniform vertical distribution of chlorophyll in 2001 was not the result of strong vertical mixing: winds were relatively light during this period. However, microscope analysis of water samples revealed that during the 2001 spring bloom a mixture of large diatoms and the photosynthetic ciliate *Mesodinium rubrum* was present, whereas in 2000 diatoms dominated the spring bloom almost exclusively. Since *M. rubrum* has the ability to migrate vertically within the water column, it has access to both the high light

conditions of the surface waters and the high nutrient conditions at depth. Thus the vertical distribution of the ciliate population would not be governed as strongly by vertical gradients in nutrient availability as would the diatom population, nor would the ciliates be likely to sink out of the euphotic zone.

4.3.2 Physicochemical Environment

Bedford Basin showed strong changes in its physical and chemical properties over the sampling period. The temperature-contour plot shows the onset of thermal stratification of the surface waters in late March of both years (Fig. 4.2A). Sea-surface temperatures reached a maximum of 20°C in August. An erosion of the thermocline followed in the fall months, until temperature was nearly uniform from the surface down to 60 m at the end of December. Salinity also showed marked seasonal variations, with low surface values in March and April of 2000 and 2001, which was coincident with the spring bloom for both years (Fig. 4.2B). During late October to late November another period of very low salinity values was observed, extending deep into the water column. This was a period of heavy rainfall, which resulted in an increase in freshwater runoff, and consequently, an increase in the concentration of CDOM, which will be described in the following section.

In the contour plot of oxygen, two main features are readily apparent (Fig. 4.2C). The first is that there are high levels of oxygen concentration in the surface waters, coincident with high levels of pigment biomass, during the two spring blooms (Fig. 4.1A,B). This suggests that part of the variation in oxygen concentration is caused by oxygen evolution by photoautotrophs. The second feature is the gradual depletion of oxygen in deeper waters, with oxygen concentrations reaching undetectable levels from October to late December. At the end of December, the water column was thoroughly mixed from top to bottom, allowing for oxygen-rich water from the surface to be introduced to the deep waters.
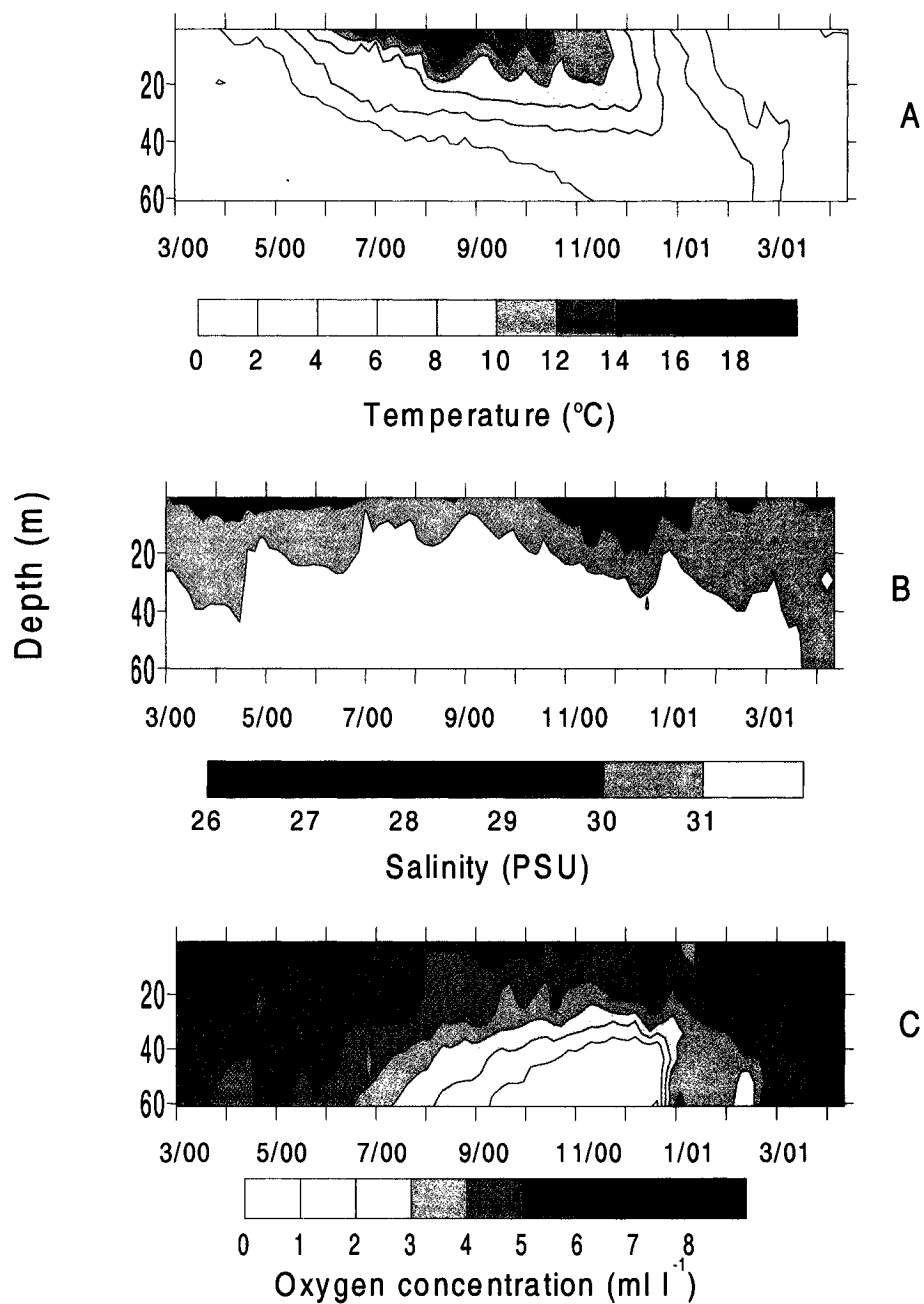
Figure 4.2. Contour plots of some physicochemical properties of the Bedford Basin measured using a Conductivity Temperature Density (CTD) profiler during March 2000 to April 2001 (A, temperature ($^{\circ}$C); B, salinity (PSU), C, oxygen concentration (ml l^{-1})).

Seasonal changes in nutrient concentrations are shown in Figure 4.3A-C. Nitrate (plus nitrite, referred to henceforth as nitrate), silicate and phosphate concentrations were high at the beginning of the sampling period. As chlorophyll concentrations began to increase in an exponential manner during the month of March 2000 (Fig. 4.1A), a strong decrease in all three nutrients was observed at 1 and 5 m. During late March to early May 2000, nitrate concentrations at 10 m samples were noticeably higher than at 1 and 5 m. Nitrate concentrations remained low during the summer stratification period and began to increase in a near-linear fashion from early October to the end of December, as thermal stratification was gradually eroded allowing for an increase in the vertical flux of nutrients from depth to the surface. Nitrate concentrations remained high during the winter months (December to February). As was the case in March 2000, a rapid decline in nitrate and silicate levels marked the onset of the spring bloom in March 2001. Silicate concentrations varied substantially more than nitrate concentration from May to mid-July. Concentrations of silicates varied from values below the limit of detection to 4.7 μM. Another prominent feature of the silicate time-series is the sharp drop in concentration during mid-January, which was coincident with an anomalous winter diatom bloom (Fig. 4.1A,B). The rapid decline in silicate concentration followed by a marked increase to maximum levels suggests that the bloom was likely the result of a short-term stratification event followed by intense wind-driven vertical mixing. Phosphate concentrations exhibited much less variability than the other nutrients and unlike nitrate and silicate did not fall below the limit of detection during the sampling period, which suggests that phosphorous was not a limiting nutrient in this coastal system.

4.3.3 Absorptive Properties

The absorption coefficients at 440 nm for phytoplankton $(a_\phi(440))$ and CDOM $(a_y(440))$ showed strong seasonal variations (Fig. 4.4). Absorption by CDOM usually exceeded that by phytoplankton and detritus at 440 nm, with the exception
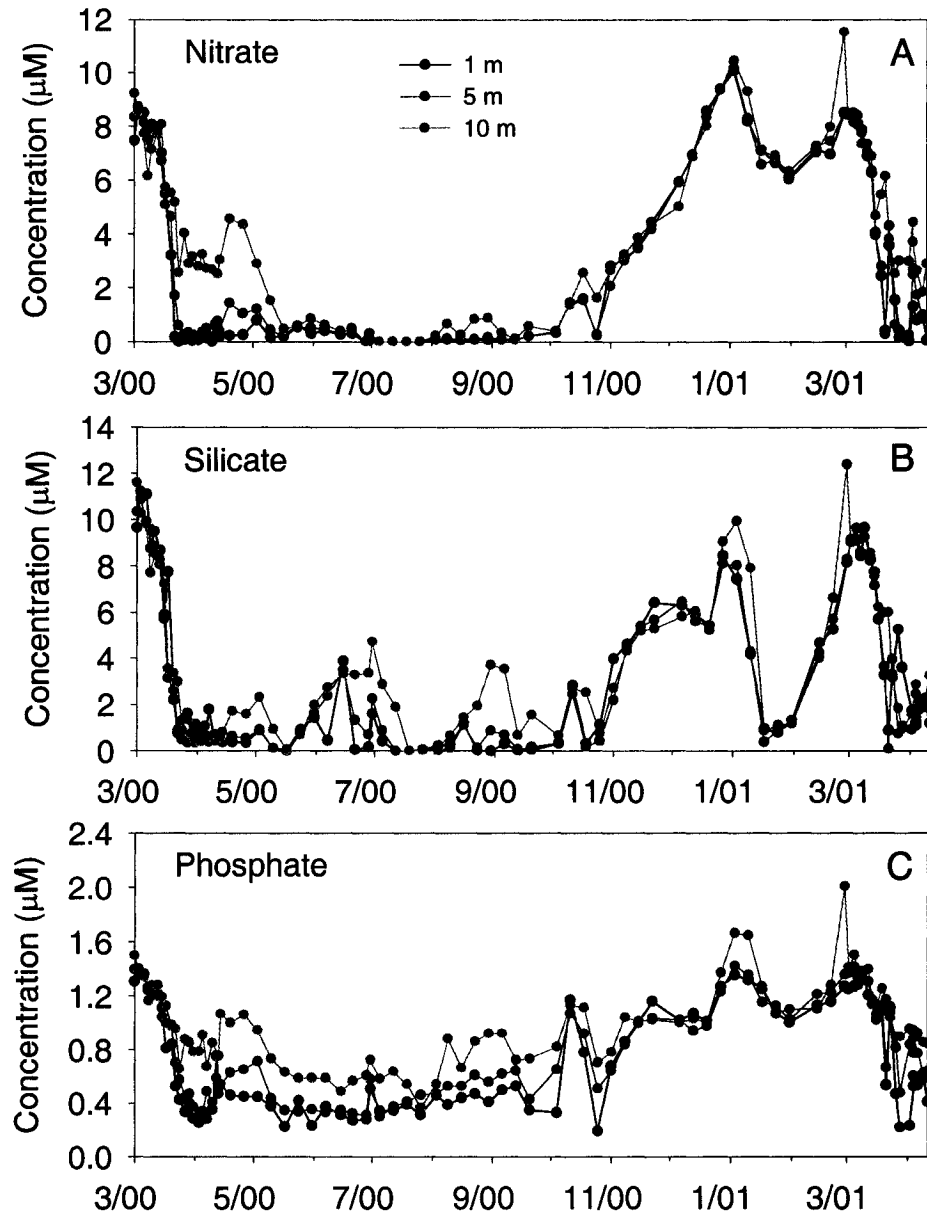
Figure 4.3. Time-series observations of nutrient concentrations collected between March 2000 and April 2001. The top (A), middle (B) and bottom (C) panels show nitrate plus nitrite, silicate and phosphate concentrations. The black, red and green symbols represent samples collected at 1, 5 and 10 m, respectively.
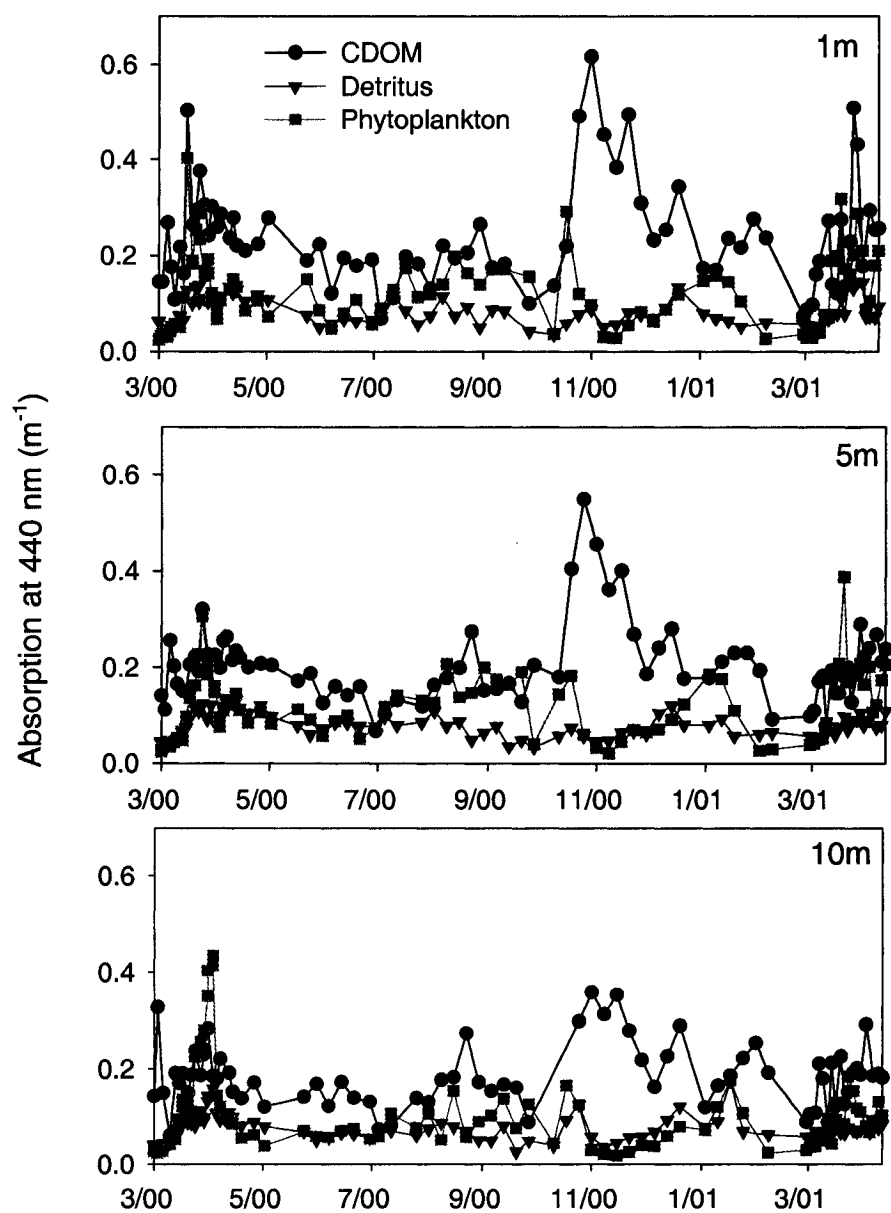
Figure 4.4. Seasonal variation in the absorption coefficients of CDOM (black circles), detritus (red triangles) and phytoplankton (green squares) at 440 nm. The top, middle and bottom panels show data from samples collected at 1, 5 and 10 m, respectively.

of a few samples collected during the spring bloom events of 2000 and 2001. Values of $a_y(440)$ were high throughout the sampling period, ranging from 0.1 to 0.6 m^{-1}. Extremely high concentrations of CDOM were observed in November, when high levels of precipitation, as evidenced by low surface salinity values (Fig. 4.2B), lead to increased inputs of coloured dissolved material from terrestrial and riverine sources. This negative correlation between surface salinity and CDOM absorption (Fig. 4.5) also indicates that the principal source of the coloured dissolved material was terrestrial. The absorption coefficient of phytoplankton also showed strong seasonal changes, with values ranging from 0.01 to 0.43 m^{-1} (Fig. 4.4). High values of $a_\phi(440)$ corresponded to a series of bloom events which punctuated the sampling period (Fig. 4.4). The absorption coefficient of detrital material remained relatively constant throughout the sampling period with absorption coefficients ranging from 0.027 to 0.172 m^{-1}.

Figure 4.6 shows the percentage contribution of the three optical constituents to the total absorption at 440nm. The ternary plot clearly shows a large variation in the relative contribution of CDOM (Y) and phytoplankton (P) to total absorption. CDOM is the dominant absorber at the 440 nm waveband, contributing from 42 to 95% of the total absorption. The contribution by phytoplankton is lower, between 5 and 58%. The percent contribution to total absorption by detritus (D) was much less variable, ranging from about 10 to 30%. Thus, it would appear that seasonal fluctuations in the relative concentrations of CDOM and phytoplankton are responsible for most of the variability in absorption in the blue region of the spectrum for this coastal system.

To assess changes in the spectral shapes of CDOM and detritus, equation (1) was fitted to each absorption spectrum. The average value of the exponential coefficient for CDOM absorption (S_y) was 0.017 nm^{-1} with a standard deviation of 0.002 nm^{-1}. This mean value of S_y was similar to those reported by Kopelevich et al. (1989), Roesler et al. (1989) and Babin et al. (2003), who found mean S_y values between 0.016 and 0.017 nm^{-1} for a wide range of marine systems. However,
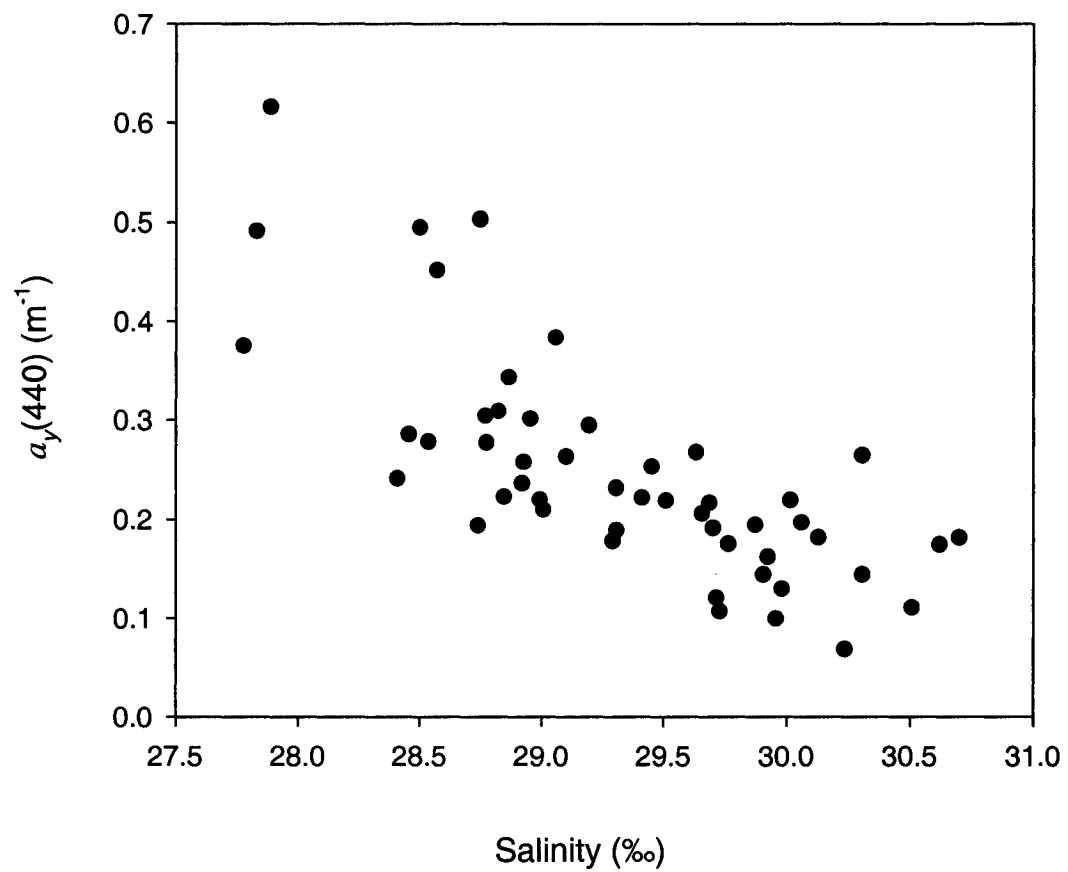
Figure 4.5. The absorption coefficient of CDOM at 440 nm plotted against salinity for samples collected at 1 m.
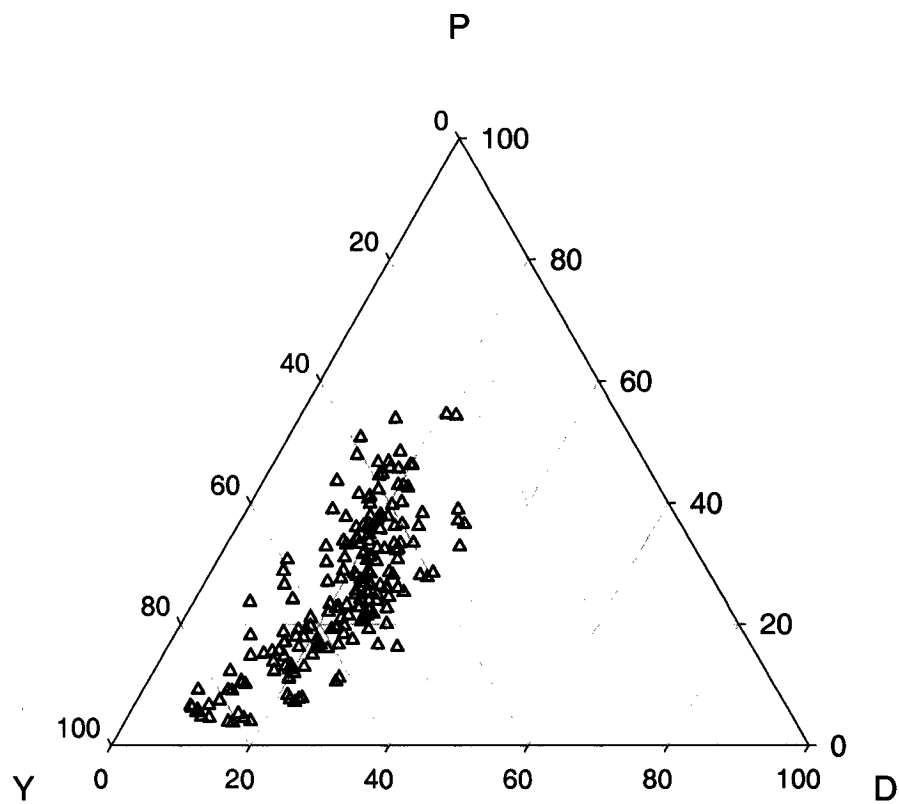
Figure 4.6. Ternary plot of the percent contribution of CDOM (Y), phytoplankton (P) and detritus (D) to the total absorption coefficient at 440 nm. Samples were collected at 1, 5 and 10 m in Bedford Basin from March 2000 to April 2001.

Højerslev (1998) showed that S_y can vary widely in coastal systems, with values ranging from 0.008 to 0.042 nm^{-1}. For the detrital absorption spectra, the average values of the exponential coefficient S_d were lower than those obtained for CDOM, with an average value of 0.011 nm^{-1} and a standard deviation of 0.002 nm^{-1}. This mean value of S_d corresponds well with mean values of 0.011 nm^{-1} (SD 0.002) and 0.012 nm^{-1} (SD 0.001) by Roesler et al. (1989) and Babin et al. (2003), respectively. Histograms of the slope parameters for both CDOM and detritus for the Bedford Basin are shown in Figure 4.7. The histograms emphasise the relatively low variation in slopes for the two optical components (Fig. 4.7). This, along with results from other studies, bodes well for the retrieval of phytoplankton biomass from hyperspectral data of light attenuation and ocean colour.

The spectral shape of phytoplankton absorption showed strong seasonal variation. To analyse the changes in spectral shape, phytoplankton absorption coefficients were normalised to the absorption coefficient at 440 nm (Fig. 4.8) and chlorophyll-a concentration (Fig. 4.9). The high variability in both normalised absorption spectra has been shown to be caused by changes in both the size of the algal cells and their intracellular pigment composition and concentration (Lutz et al. 1998). It is well known that changes in the spectral shapes are caused by seasonal shifts in community composition: as the taxonomic composition of phytoplankton changes, so do the pigment composition and size structure of the algal cells (Hoepffner and Sathyendranath 1992, Bricaud et al. 1995, Stuart et al. 1998). Pigment packaging, which is caused by an increase in either intracellular pigment concentration or cell size (Morel and Bricaud 1981), causes a flattening in regions of the absorption spectrum where absorption is strongest, typically in the blue (440 nm) and red (676 nm) wavebands (Kirk 1994), leading to high variability in the absorption coefficients at these wavebands.

An absorption spectrum with a broad absorption peak in the green region is shown in red in Figure 4.8. The absorption peak centred at 545 nm denotes the
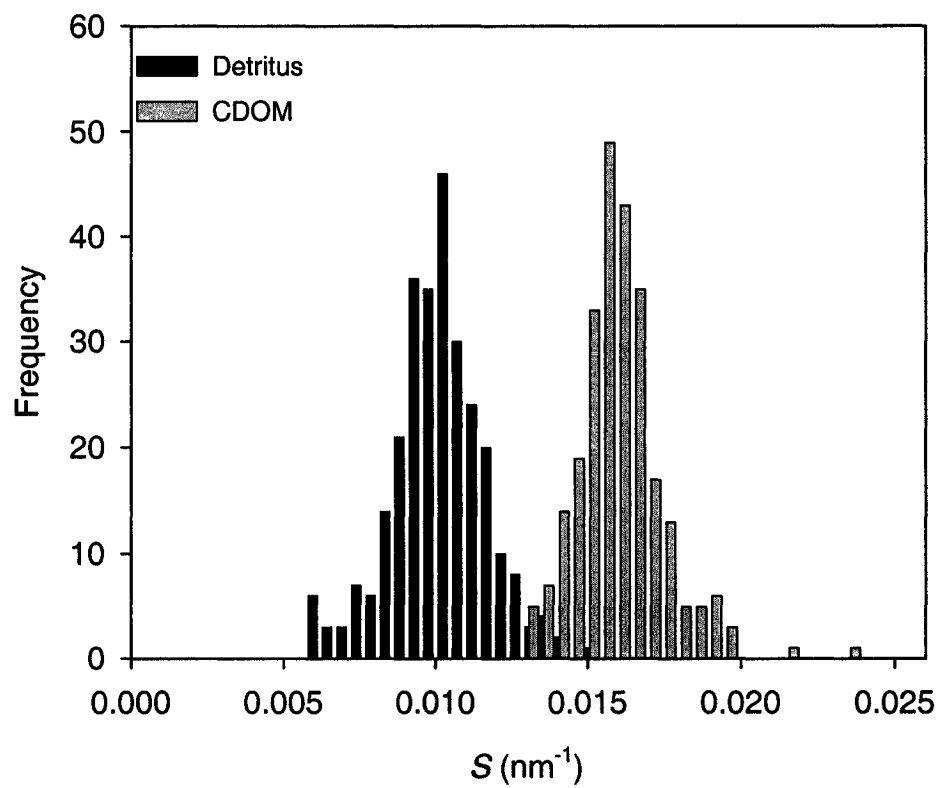
Figure 4.7. Frequency distribution of the exponential coefficient S for detritus (black) and CDOM (grey) obtained from absorption samples collected at 1, 5 and 10 m.
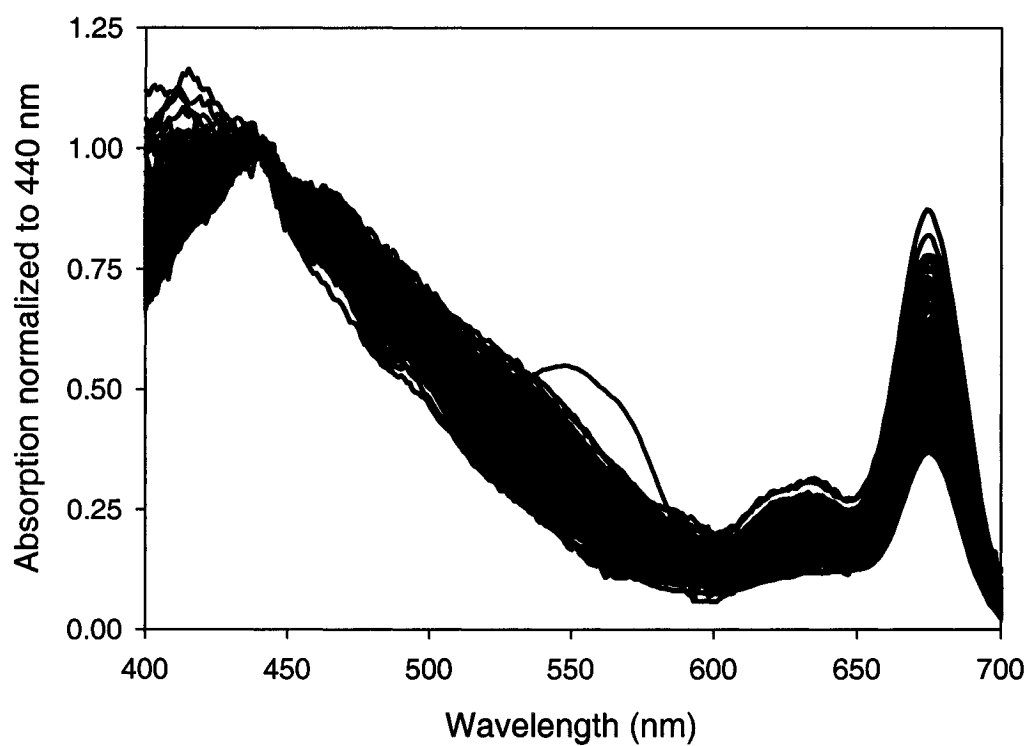
Figure 4.8. Phytoplankton absorption spectra normalised at 440 nm. Samples were collected at 1, 5 and 10 m from March 2000 to April 2001. The red line represents the absorption spectrum of the red tide ciliate *Mesodinium rubrum*.
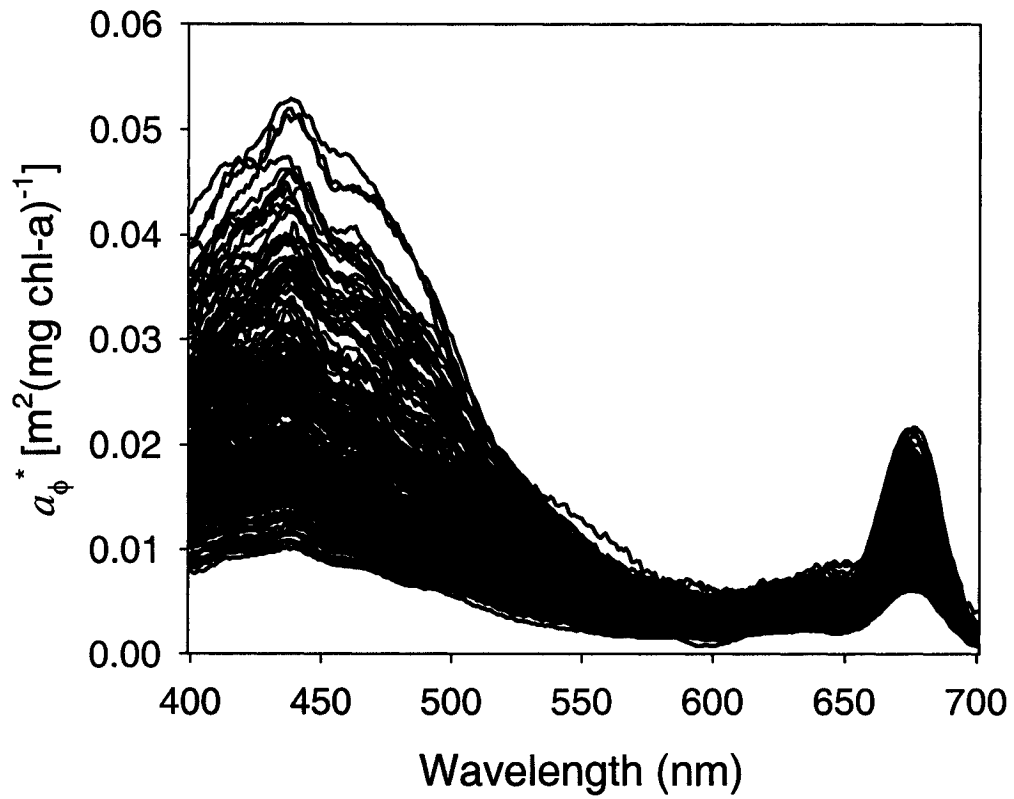
Figure 4.9. Chlorophyll-specific absorption coefficients of phytoplankton obtained from samples collected at 1, 5 and 10 m from March 2000 to April 2001.

presence of phycoerythrin, an indicator pigment for cryptophytes. Although phyco-erythrin cannot be detected by HPLC analysis due to its water-soluble nature, high concentrations of the carotenoid alloxanthin, which is another diagnostic pigment of cryptophyte algae, were also present. Microscopic inspection of water samples detected the presence of the autotrophic ciliate *Mesodinium rubrum*, which contains cryptophyte cells within its cytoplasm. It is not clear whether the relationship between the ciliate and the cryptophyte cells is symbiotic or whether *M. rubrum* is a chimaera which continually ingests algal cells to maintain its photosynthetic machinery (Gustafson et al. 2000). Regardless of its functional classification, *M. rubrum* is known to play an important role in the formation of non-toxic red tides in coastal areas and its associated algae can be significant contributors to primary production in these regions.

In the field of marine optics, developing an appreciation of the main factors governing changes in the relationship between phytoplankton absorption and chloro-phyll concentration is crucial since this relationship is central to the theory behind the retrieval of chlorophyll biomass from ocean-colour data. To examine the seasonal variability in the relationship between phytoplankton absorption and chlorophyll pigment concentration we plotted the chlorophyll-normalised, specific absorption coefficient of phytoplankton at 440 nm ($a^*_\phi(440)$) and 676 nm ($a^*_\phi(676)$) over time. Chlorophyll-a specific absorption coefficients at both wavebands varied strongly throughout the sampling period (Fig. 4.10). Changes in $a^*_\phi(440)$ and $a^*_\phi(676)$ are known to be caused by changes in the size structure of the phytoplankton community (Bricaud et al. 1995). Typically, low chlorophyll-a specific absorption coefficients are characteristic of larger cells (diatoms and dinoflagellates), whereas high chlorophyll-a specific absorption coefficients signify the presence of smaller cells (nanoflagellates and picoplankton). In the Bedford Basin study, bloom events were characterised by low values of both $a^*_\phi(440)$ and $a^*_\phi(676)$, whereas during the summer months, when phytoplankton biomass was low, temperatures were high and water-column stratification was strong, high values of $a^*_\phi(440)$ and $a^*_\phi(676)$ were observed.
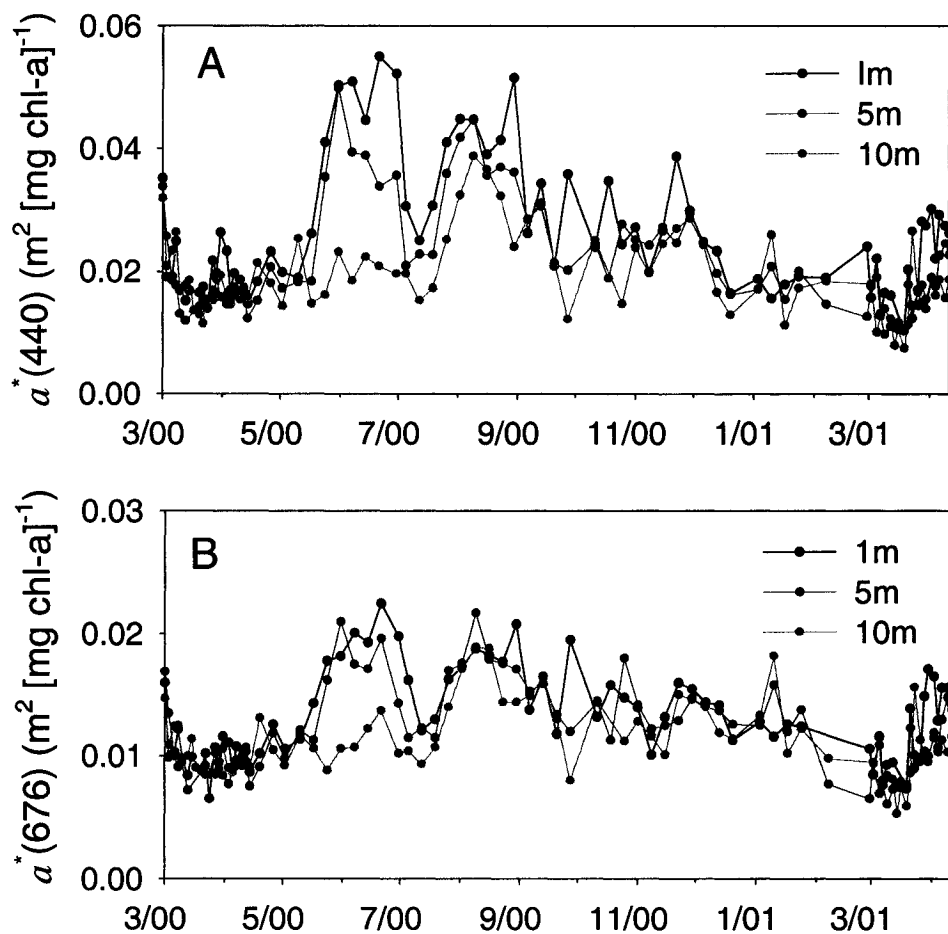
Figure 4.10. Chlorophyll-specific absorption coefficients of phytoplankton at A) 440 nm and B) 676 nm obtained from samples collected at 1 m (black symbols), 5 m (red symbols) and 10 m (green symbols) from March 2000 to April 2001.

Information on the seasonal changes in pigment composition supports the view that changes in both $a_\phi^*(440)$ and $a_\phi^*(676)$ were caused primarily by changes in phytoplankton community structure. Time series observations of the percent contribution of each accessory pigment to the total accessory pigment concentration is shown in Figure 4.11. During the spring bloom in 2000 and the period from mid September 2000 to April 2001, values of both $a_\phi^*(440)$ and $a_\phi^*(676)$ were low (Fig. 4.10), while concentrations of fucoxanthin (an indicator pigment for diatoms) and peridinin, (an indicator pigment for dinoflagellates), were high relative to the other indicator pigments (Fig. 4.11). When values of $a_\phi^*(440)$ and $a_\phi^*(676)$ were high (early June to early July and mid July to early September), however, concentrations of accessory pigments chlorophyll b, 19' hexanoyloxyfucoxanthin and alloxanthin, which are indicator pigments of chlorophytes, prymnesiophytes and cryptophytes respectively, were also high. Since diatoms and dinoflagellates typically fall within the microphytoplankton size range ($> 20\mu$m), whereas chlorophytes, prymnesiophytes and cryptophytes typically fall within the nanophytoplankton size range (2 to 20 μm), there appears to be a strong inverse relationship between the cell sizes of the phytoplankton community and the magnitude of $a_\phi^*(440)$. This relationship is not surprising, since cell size is a contributing factor to the package effect (Morel and Bricaud 1981).

One exception to the strong agreement between pigment complement and the chlorophyll-a specific absorption coefficients at 440 and 676 nm occurred during the period of mid-May to mid-June, when high concentrations of alloxanthin in the 10 m sample were coincident with low $a_\phi^*(440)$ and $a_\phi^*(676)$ values. The complication of using alloxanthin as an indicator of cell size in this marine system is that it is an indicator of both free-living cryptophyte cells (which fall within the nanophytoplankton size range) and of cryptophyte organelles contained within the ciliate M. rubrum (which is in the microphytoplankton size range). Therefore, pigment packaging of a sample dominated by M. rubrum would have been much greater than a sample containing free-living cryptophytes. A study by Kyewalyanga et al.
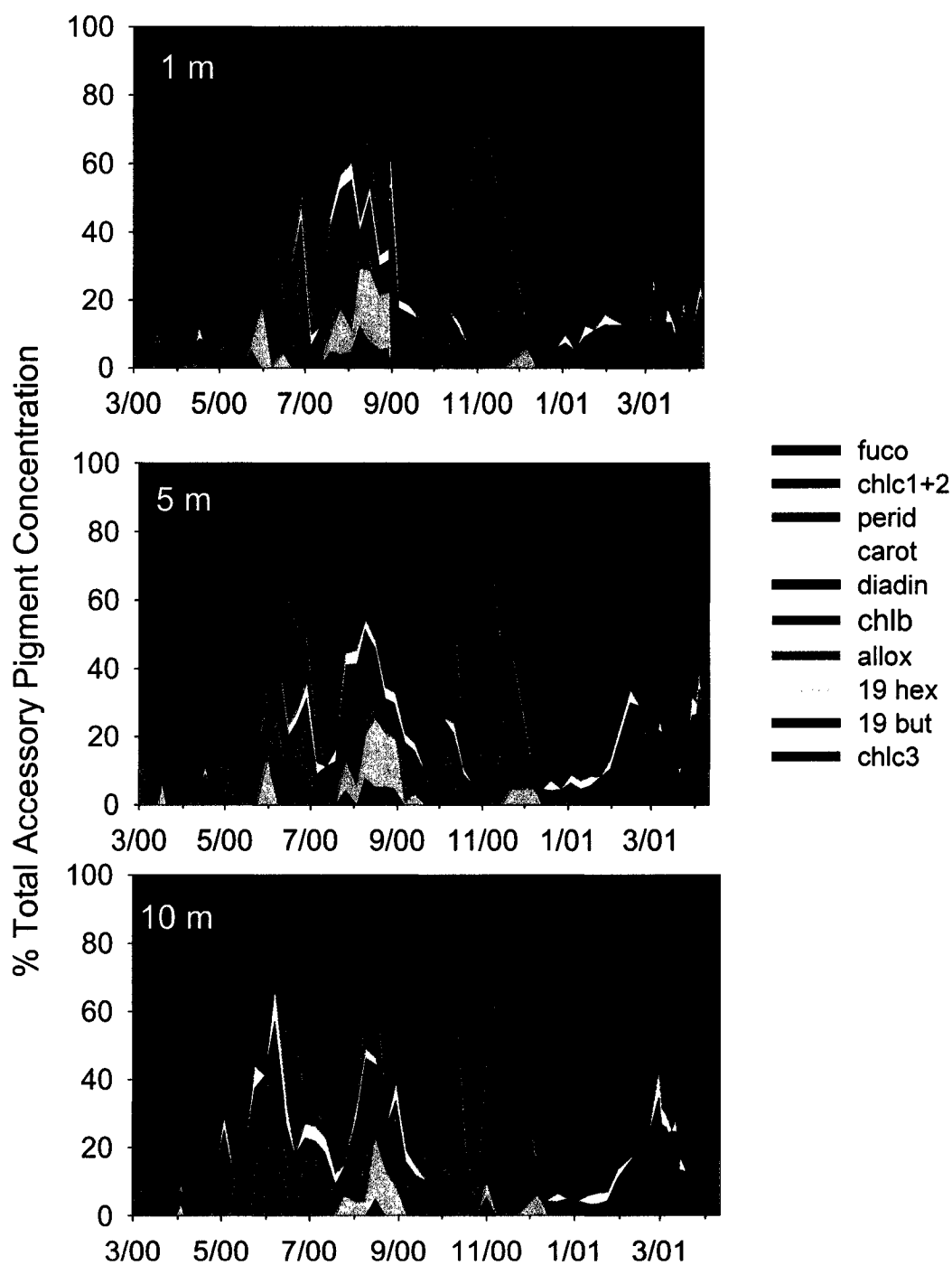
Figure 4.11. Percent contribution of major accessory pigments to the total accessory pigment concentration for samples collected at 1, 5 and 10m during March 2000 to April 2001. Abbreviations for pigments are as follows: Fuco=fucoxanthin, chlc1+2=chlorophyll c1+2, perid=peridinin, carot=α- and β–carotene, diad=diadinoxanthin, chlb=chlorophyll b, allox=alloxanthin, 19hex=19'hexanoyloxyfucoxanthin, 19but=19'butanoyloxyfucoxanthin, chlc3= chlorophyll c3.

(2002) conducted in Bedford Basin reported the lowest values of $\bar{a}_\phi^*$ during a bloom of *M. rubrum*. Another intense bloom of *M. rubrum* was observed in Bedford Basin during September 2000. The bloom was short-lived (2 days) and the cells were concentrated within discrete patches, and confined vertically within a narrow band ranging from approximately 1 to 2 m thick. A series of samples taken during this period shows a negative correlation between the indicator pigment, alloxanthin, and $a_\phi^*(440)$ (Fig. 4.12). Based on these results, one may conclude that the high concentrations of alloxanthin and low values of $a_\phi^*(440)$ observed in the late spring at 10 m were likely caused by the presence of the autotrophic ciliate *M. rubrum*.

4.3.4 Photosynthetic Properties

Photosynthetic performance as indexed by the *P-E* parameters P_m^B and α^B also showed strong seasonal changes (Fig. 4.13). Both parameters were correlated with the mean chlorophyll-a-specific absorption coefficient of phytoplankton, $\bar{a}_\phi^*$, during the period of March to November 2000. Fluctuations in $\bar{a}_\phi^*$ closely resembled those of $a_\phi^*(440)$ during the sampling period (Fig. 4.10), with low values coinciding with the dominance of large cells (diatoms) during bloom events. The correlation of the initial slope, α^B, and $\bar{a}_\phi^*$ is not surprising: α^B is a product of $\bar{a}_\phi^*$ and the maximum quantum yield of carbon fixation (ϕ_m) (Platt and Jassby 1976). Thus if ϕ_m remained relatively constant during the sampling period, changes in α^B would be caused by changes in $\bar{a}_\phi^*$. The strong correlation between $\bar{a}_\phi^*$ and P_m^B is likely the result of both bio-optical properties being influenced by the size and taxonomic structure of the phytoplankton community (Platt and Jassby 1976, Côté and Platt 1983, 1984, Finkel 2002). Within the period of March to December 2000, both photosynthetic parameters were positively correlated with temperature, correlation analysis yielding r-squared values of 0.72 (n=52) for P_m^B and 0.42 (n=52) for α^B. The strong correlation between P_m^B and temperature is in agreement with the findings of Harris (1978), Harrison and Platt (1980) and Côté and Platt (1983, 1984). As mentioned in the previous chapter, this strong correlation has been attributed to
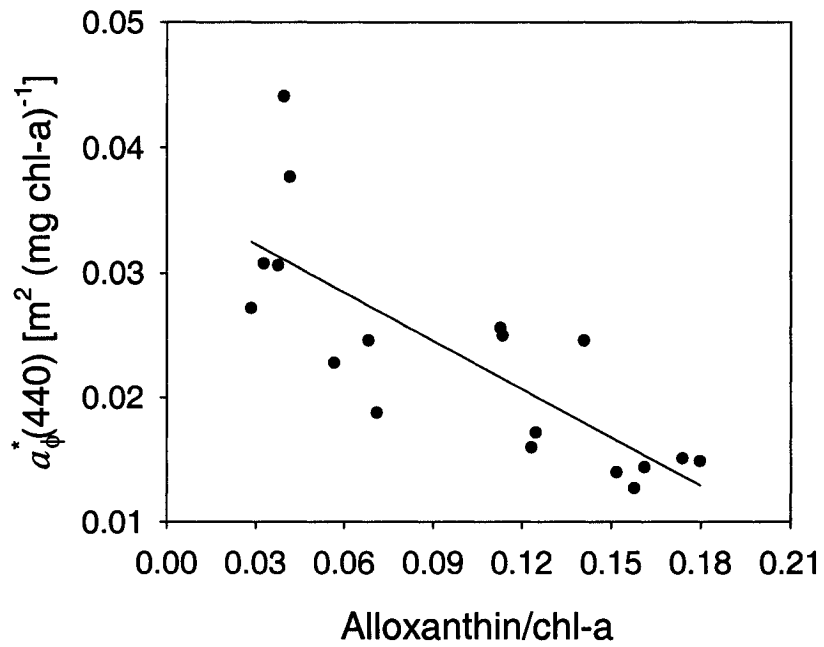
Figure 4.12. The chlorophyll-a-specific absorption coefficient of phytoplankton at 440 nm plotted against the chlorophyll-a normalised alloxanthin concentration.
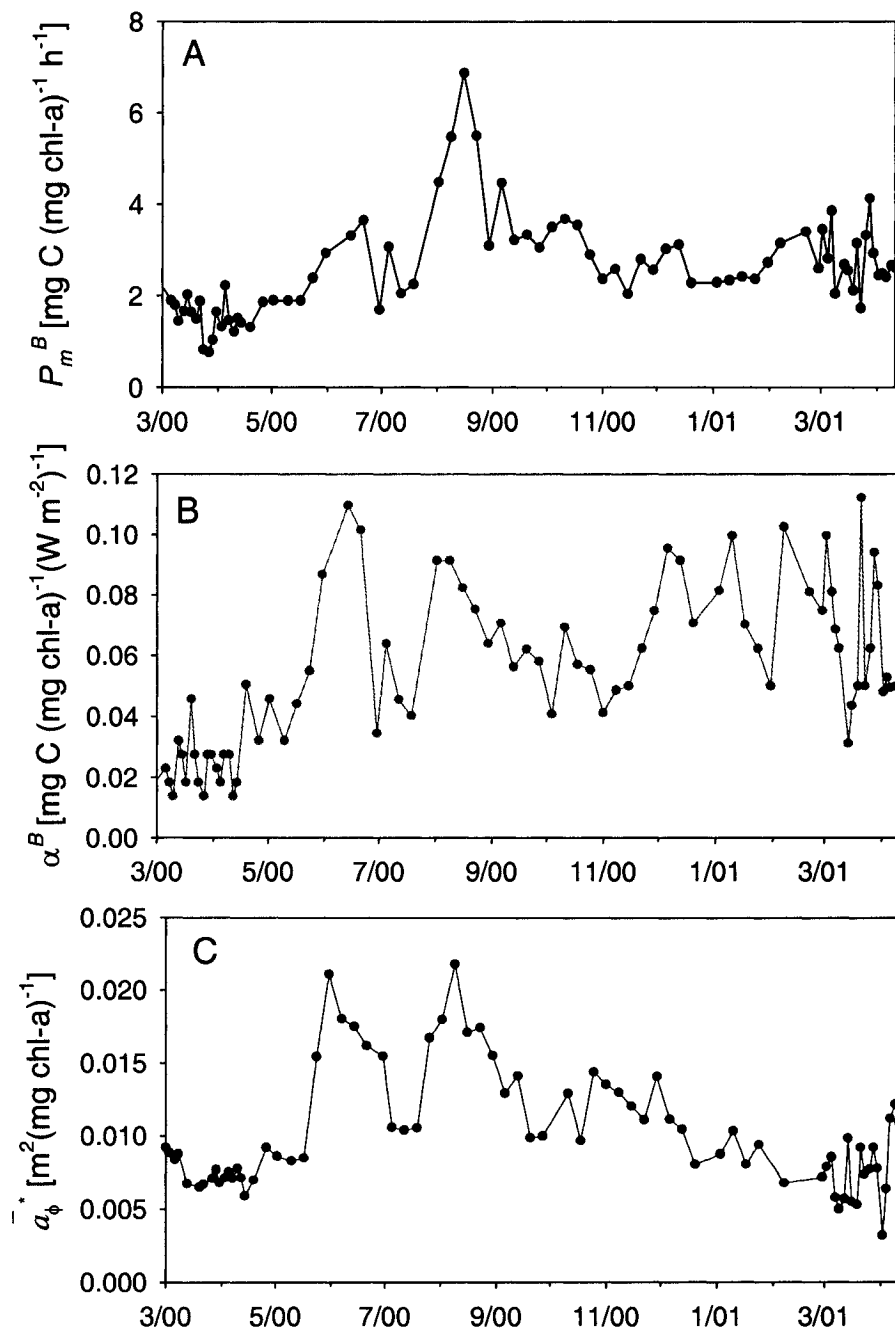
Figure 4.13. Seasonal changes in A) the assimilation number (P_m^B), B) the initial slope of the photosynthesis-irradiance curve (α^B), and C) the mean chlorophyll-a specific absorption coefficient of phytoplankton ($\bar{a}_\phi^*$).

the enzyme mediation of the light-saturated reactions of photosynthesis, but may also be related to the changes in community structure with the change in temperature.

During the winter months, α^B showed a marked increase, whereas $\bar{a}_\phi^*$ and P_m^B remained low. Since, α^B and ϕ_m have been shown to be related to nutrient availability and light history(Geider & Osborne 1992, Babin et al. 1996), the divergence between $\bar{a}_\phi^*$ and α^B may have been caused by the combination of high nutrient and low irradiance conditions during the highly turbulent winter months. The increase in initial slope values during the months of November and December coincided with an increase in silicate and nitrate concentration caused by strong vertical mixing during this period. Another interesting feature of the α^B time-series is the drop in the initial slope values during the diatom bloom in mid-January of 2001, which was coincident with a sharp drop in both nitrate and silicate concentrations. The initiation of the diatom bloom would have required a stabilization of the surface waters, especially given the low incident irradiance, in order for there to be ample light to support rapid algal growth. Thus, the algal cells present during this stratified period would have resided in a markedly different light environment from that present during the conditions of strong vertical mixing, which occurred both before and after this bloom event. Hence, it would appear that during periods of high turbulence, the physiological properties of microalgae are different from those observed under stratified conditions.

In Chapter 3, similar patterns were observed in the relationship between the physical environment, microalgal community structure, the absorptive properties of phytoplankton cells and algal photosynthesis for the Scotian Shelf. Both Bedford Basin and the Scotian Shelf experience the seasonal changes in physical forcing that are typical of temperate marine systems: vernal warming of surface waters and wind-driven mixing. Thus, it should not be surprising that in both systems, shifts in phytoplankton community structure, optical characteristics and photosynthetic response are correlated with sea-surface temperature.

In addition to the seasonal cycle of warming and cooling of the photic zone, however coastal environments are subject to other physical factors to which the open ocean is commonly immune: important among which is the input of freshwater from the land. It not only plays an important role in initiating stability in surface waters, but also brings nutrients into the system, which enhance algal growth. Under conditions in which freshwater inputs are laden with high concentrations of CDOM, terrestrial runoff can also have a negative impact on algal growth, since CDOM competes with phytoplankton for absorption of blue light.

Bedford Basin also differs from the Scotian Shelf in the composition of its algal assemblages. Cell counts obtained on both the Scotian Shelf and in Bedford Basin show that photosynthetic ciliates that are able to migrate vertically through the water column tended to be far more abundant in Bedford Basin compared with the Scotian Shelf. This mobility allows them to accumulate in high numbers at the sea surface, producing red tides. In this study, the red tide organism *Mesodinium rubrum* was frequently observed. This was not the only organism that can produce red tides in this coastal inlet. In September of 1989, a bloom of the red-tide dinoflagellate *Gonyaulax digatale* was also observed in Bedford Basin (Amadi et al. 1992). Also, in the summer of 1993, a dinoflagellate bloom attained the highest chlorophyll-a concentration (109 mg Chl-a m^{-3}) ever recorded in Bedford Basin (Li and Dickie 2001). In all cases the blooms were short lived and attained high chlorophyll-a concentrations, in excess of 40 mg Chl-a m^{-3}. Such blooms can contribute significantly to the productivity of coastal ecosystems. Monitoring programs that have the temporal frequency to detect episodic blooms would help to enhance our understanding of the set of environmental conditions required to initiate their formation and would aid in the development of predictive models of phytoplankton bloom dynamics. Optical sensors will provide biological oceanographers with an invaluable tool to help achieve this goal.

4.4 Concluding Remarks

This study shows that the photosynthetic and absorptive characteristics of the Bedford Basin undergo strong seasonal fluctuations. The variability in the optical properties of the Basin is driven by changes in the physicochemical properties of the water column, such as stability through solar heating, freshwater inputs and wind-driven mixing. Similar to the Scotian Shelf, the Bedford Basin showed a strong relationship between temperature and community structure (indexed by $a_{\phi}^*(440)$). However, the Basin is also subject to episodic fluctuations in both salinity and nutrient concentrations from freshwater inputs from land that strongly influence the dynamics of the phytoplankton community. Fluctuations in CDOM absorption were caused by increases in terrestrial runoff as evidenced by the correlation between absorption by CDOM and salinity. In general, the variability in the optical properties of Bedford Basin results from changes in phytoplankton biomass and CDOM concentration, not by the less variable detrital component. The conservative nature of the spectral shape of absorption by non-algal components, and the covariance between phytoplankton specific absorption and temperature, will aid in the development of ocean-colour algorithms that estimate phytoplankton biomass from spectrally-resolved measurements of total absorption and sea-surface reflectance.

This study also illustrates how the optical and photosynthetic properties of coastal phytoplankton are closely related to changes in the taxonomic and size structure of the phytoplankton community. Correlations between the P-E parameters and the specific absorption coefficients of phytoplankton were also evident on the Scotian Shelf (Chapter 3) . The Bedford Basin and Scotian Shelf datasets also show a strong correlation between P_m^B and temperature. More detailed information on the absorptive properties of phytoplankton will come from the development of optical sensors with greater spectral resolution, and temperature can be easily obtained by both remote sensing and *in situ*. The derived relationships between phytoplankton absorption, temperature and the photophysiological parameters should help assign input parameters of bio-optical models of primary production.

Large variability in α^B was observed during the winter in Bedford Basin. An increase in the initial slope during this period is not unexpected: low irradiance and high nutrient concentrations are known to increase light-limited photosynthesis in culture studies (Geider and Osborne 1992). Published field observations of the photophysiological parameters of phytoplankton during the winter are rare for temperate marine systems. Nevertheless, this study has shown that blooms may occur even during periods of relatively low light and temperature provided that cells are physiologically adapted to these conditions and that the water column is stable enough. In existing models of primary production, the importance of the initial slope is often dismissed, and research is focussed more on explaining variability in the light-saturation parameter P_m^B (e.g. Behrenfeld and Falkowski 1997). This approach is largely based on datasets collected within spring and summer months, however, when the P-E parameters are strongly correlated with each other. To ascertain the contribution of production by phytoplankton to the annual marine carbon cycle, we should increase the number of observations of P-E parameters made during winter.

CHAPTER 5

Summary and Conclusions

5.1 Summary

In this era of optical oceanography, biological oceanographers are able routinely to monitor the state of marine ecosystems over large spatial scales through the use of data from remotely-sensed ocean colour. Although knowledge of radiative transfer theory is necessary to interpret the information obtained by ocean-colour sensors, so too is an understanding of ecological theory (Yentsch and Phinney 1989). Seasonal changes in the taxonomic composition of phytoplankton communities are reflected in the optical characteristics of natural waters (Yentsch and Phinney 1989, Bricaud et al. 1995, Sathyendranath et al. 1999, Stuart et al. 2000). Ignoring the role of community structure on the absorptive properties of aquatic ecosystems may lead to important errors in the estimation of chlorophyll-a using ocean-colour algorithms (Carder et al. 1999, Sathyendranath et al. 1999). One objective of the present work was to investigate the relationship between community structure and the optical properties of marine phytoplankton. Using pigment and flow cytometric data as proxies of community structure, the relationship between community structure and the chlorophyll-a-specific absorption coefficients of phytoplankton was examined for a wide range of oceanic provinces. The results of this analysis, presented in Chapter 2, revealed a strong correlation between phytoplankton community structure and the absorptive properties of marine microalgae. Moreover, a robust relationship was found between temperature and both the taxonomic structure and absorptive properties of microalgal assemblages. The link between phytoplankton community structure and temperature derived from a long-observed trend: as the physical properties of the marine environment change from highly-turbulent to highly-stratified conditions, there is a shift in phytoplankton community structure from one domi-

97

nated by diatoms (microphytoplankton) to one dominated by the smaller nano- and picoplankton (Margalef 1978, Cullen et al. 2002).

The use of temperature as an indicator of the absorptive properties and community structure of phytoplankton proved robust for many of the regions examined in this study, but not for the Arabian Sea. In most ocean regimes, intense wind-mixing entrains cool, nutrient-rich water from depth into the surface layer. In the Arabian Sea, however, high nitrate concentrations were observed at relatively high temperatures ($> 25°C$) during the monsoon period. The phytoplankton was then dominated by diatoms as expected from the high nutrients and not by picoplankton as expected from our general results on temperature. Thus, one should be alert to regional peculiarities and not apply the general results in an unthinking manner.

The relationship between phytoplankton community structure and primary production has been observed in numerous studies of marine and freshwater systems (Platt and Jassby 1976, Harris 1978, Harrison and Platt 1980, Côté and Platt 1983, 1984). Since phytoplankton size and taxonomic structure influence the absorptive properties of marine phytoplankton, as revealed in Chapter 2 and other studies (Yentsch and Phinney 1989, Bricaud et al. 1995, Stuart et al. 1998), and since the absorptive properties of phytoplankton account for most of the variability in the optical signal received by optical sensors mounted on satellites, remote sensing may provide biological oceanographers with information to estimate the physiological parameters required to compute primary production on synoptic scales. Using the Scotian Shelf as a case study, I examined the principal factors governing variability in photosynthetic performance of marine phytoplankton. Regression analysis revealed that the P-E parameters were strongly correlated with both temperature and the specific absorption coefficients of marine phytoplankton.

The strong correlation between P_m^B and temperature has been documented in several studies of natural phytoplankton assemblages (Platt and Jassby 1976, Harris 1978, Harrison and Platt 1980, Côté and Platt 1983, Kyewalyanga et al. 1998). It

has been proposed that this relationship is a consequence of light-saturated photosynthesis being regulated by enzymatic activity, which itself is temperature dependent (Harris 1978, Harrison and Platt 1980, Côté and Platt 1983). In Chapter 3, however, an alternative explanation was presented: that the correlation may be caused by the shift in community structure that accompanies the seasonal change in temperature. This view is supported by data collected in the Arabian Sea, where a poor correlation between the photosynthetic parameters and temperature was found. As demonstrated in Chapter 2, the Arabian Sea is an example of a marine system that experiences large fluctuations in community structure at the high end of the global-ocean temperature range. Using the chlorophyll-a-specific concentration of the accessory pigment fucoxanthin (a diagnostic pigment for diatoms) the relationship between the relative contribution of diatoms to the total algal biomass and P_m^B was examined for both the Scotian Shelf and Arabian Sea datasets. The results suggest that community structure may also play an important role in governing the variability in P_m^B.

In Chapter 4, seasonal changes in the absorptive and photosynthetic characteristics of a coastal inlet were examined. Similar to the results presented in Chapter 3 for the Scotian Shelf dataset, strong correlations between temperature and both phytoplankton absorption and photosynthesis were found during the spring, summer and fall seasons in the Bedford Basin. Changes in $\bar{a}^*$ were the result of shifts in the composition of microalgal communities as revealed by HPLC pigment analysis. The occurrence of a short-lived *Mesodinium rubrum* red tide in late September had a pronounced impact on the optical characteristics of the Basin. This and other episodic blooms, which punctuated the Bedford Basin time series, were likely the result of inputs of nutrients and enhanced vertical stability induced by freshwater runoff. These intermittent fluctuations in the phytoplankton standing stock, which are typical of coastal environments, reinforce the need to use optical technology that can monitor these ephemeral, but often ecologically important, changes in the state of the aquatic ecosystem.

In addition to monitoring changes in phytoplankton absorption, I also examined variations in the absorptive charateristics of non-algal materials, which are known to contribute subtantially to the optical properties of coastal waters. The correlation between salinity and absorption by coloured dissolved organic matter (CDOM) found in this study could be used to assess the contribution of non-algal substances to the absorption budget in this optically-complex system using *in situ* moorings. The conservative nature of the spectral shapes of CDOM and detrital absorption spectra will also aid in determining estimates of algal biomass through inverse models of spectral reflectance.

Although the P-E parameters were strongly correlated with both temperature and phytoplankton absorption in the Bedford Basin during the spring, summer and fall periods, in the winter the initial slope α^B increased markedly, whereas values of both the assimilation number P_m^B and the mean-specific absorption coefficient of phytoplankton $\bar{a}^*$ remained low (Chapter 4). The high-nutrient, low-light conditions characteristic of the winter months are known to favour high α^B values. By not accounting for this increase in α^B in our bio-optical models of photosynthesis, we could incur significant errors in our estimates of daily, water-column primary production during the winter, since a large fraction of the water column is light limited in that season. This observation reinforces the need to increase our understanding of the causes of variability in the P-E parameters during the winter months in both coastal and open-ocean temperate environments, for which the data are extremely sparse at present. By doing so, we may not only improve our modelling of primary production using remote-sensing technology, but gain a broader perspective of the ability of algal cells to acclimate to turbulent mixing and consequently to fluctuations in nutrient and light levels.

5.2 Conclusions

The results presented here show that indices of phytoplankton community structure were highly correlated with temperature for several regions of the world ocean. Temperature is known to be related to the rate of vertical mixing and consequently nutrient availability in many open-ocean systems (Carder et al. 1999, Sathyendranath et al. 1999). Margalef (1979) presented a conceptual model that described the link between phytoplankton community structure and gradients in both turbulence and nutrient status. He proposed that conditions of intense vertical mixing and high nutrient availability would favour the presence of large cells (diatoms), whereas in highly-stratified, nutrient-depleted waters, smaller phytoplankton cells would dominate (nano- and picoplankton). Although the assumption that nutrient supply and turbulence are responsible exclusively for changes in phytoplankton community structure may be oversimplied, the results presented in this study do reveal a strong link between phytoplankton composition (as indexed by pigment, flow cytometry and absorption data) and the physical environment (as indexed by temperature). Since temperature is accessible by remote sensing and has been shown to be correlated with the optical properties of phytoplankton in a broad range of oceanic domains, incorporating information on the sea-surface temperature in existing regional chlorophyll-retrieval algorithms may lead to an improvement in the estimation of pigment biomass. However the case of the Arabian Sea also emphasises that if temperature is to be used in global algorithms, regional differences in the relationship between temperature and absorption should be taken into account.

Phytoplankton community structure and the photosynthesis-irradiance parameters are influenced by the same physicochemical properties of the marine environment: namely light history, nutrient supply and temperature. It is therefore difficult to ascertain whether variability in primary production is caused by changes in environmental factors or whether successional changes in species composition are the principal cause of variations in photosynthetic performance. Results from this

study suggest that the temperature-dependence of light-saturated photosynthesis, that has been shown in numerous studies of the North Atlantic, may be caused by a concomitant change in phytoplankton community structure. When detailed information on the community composition of phytoplankton can be obtained on the same synoptic scales as sea-surface temperature and chlorophyll biomass, the capability of predicting the photosynthesis-irradiance parameters as well as the rate of primary production from remotely-sensed data over large spatial scales may be substantially improved.

Although this study focussed on two potential applications of the links between phytoplankton community structure, ocean optics and the physicochemical environment, namely the improvement in our estimation of pigment biomass and primary production from satellite observations, these relationships may be useful in other research areas. The ability to distinguish populations of large (diatoms) from small (picoplankton) cells may aid in the estimation of the flux of carbon to the deep ocean as well as the cycling of carbon through trophic levels. Furthermore, since the community structure of phytoplankton in temperate regions is often controlled by physical forcing, synoptic fields of phytoplankton absorption may also aid in the monitoring of physical properties, such as the vertical stability of the water column. Such future applications, however, will require further research.

REFERENCES

Allali, K., Bricaud, A., & Claustre, H. 1997. Spatial variations in the chlorophyll-specific absorption coefficients of phytoplankton and photosynthetically-active pigments in the equatorial Pacific. *J. Geophys. Res* **102**: 12413-12423.

Amadi, I., Subba Rao, D. V. & Pan, Y. A. 1992. *Gonyaulax digitale* red water bloom in the Bedford Basin, Nova Scotia, Canada. *Bot. Mar.* **35**:451-455.

Antoine, D., André, J.-M. & Morel, A. 1996. Oceanic primary production 2. Estimation at global scale from satellite (coastal zone color scanner) chlorophyll. *Global Biogechem. Cycles* **10**: 57-69.

Babin, M., Morel, A., Claustre, H., Bricaud, A., Kolber, Z. & Falkowski, P. J. 1996. Nitrogen- and irradiance-dependent variations of maximum quantum yield of carbon fixation in eutrophic, mesotrophic and oligotrophic marine systems. *Deep-Sea Res.* **43**:1241-1272.

Babin, M., Stramski, D., Ferrari, G. M., Claustre, H., Bricaud, A., Obolensky, G. & Hoepffner, N. In press. Variations in the light absorption coefficients of phytoplankton, non-algal particles, and dissolved organic matter in coastal waters around Europe. *J. Geophys. Res.*

Balch, W. , & others. 1992. The remote sensing of ocean primary productivity: Use of new data compilation to test satellite algorithms. *J. Geophys. Res.* **97**:2279-93.

Banse, K. 1976. Rates of growth, respiration and photosynthesis of unicellular algae as related to cell size - a review. *J. Plankton Res.* **12**:135-40.

Barber, R. T., White, A. W. & Siegelman, H. W. 1969. Evidence for a cryptomonad symbiont in the ciliate, *Cyclotrichium meunieri*. *J. Phycol.* **5**: 86-88.

Behrenfeld, M. J. & Falkowski P. G. 1997. Photosynthetic rates derived from satellite-based chlorophyll concentration. *Limnol. Oceanogr.* **42**:1-20.

Behrenfeld, M. J., Marañón, E., Siegel, D. A. & Hooker., S. B. 2002. Photoacclimation and nutrient-based model of light-saturated photosynthesis for quantifying oceanic primary production. *Mar. Ecol. Prog. Ser.* **228**: 103-117.

Bidigare, R. R., Ondrusek, M. E., Marrow, J. H. & Kiefer, D. A. 1988. *In vivo* absorption of algal pigments. *SPIE* **1302**:290-302.

Bouman, H. A., Platt, T., Kraay, G. W., Sathyendranath, S. & Irwin, B. D. 2000. Bio-optical properties of the subtropical North Atlantic. I. Vertical variability. *Mar. Ecol. Prog. Ser.* **200**:3-18.

Bricaud, A., Babin, M., Morel, A. & Claustre, H. 1995. Variability in the chlorophyll-specific absorption coefficients of natural phytoplankton: Analysis and parameterization. *J. Geophys. Res.* **100**: 13321-13332.

Bricaud, A., Morel, A., & Prieur, L. 1981. Absorption by dissolved organic matter of the sea (yellow substance) in the UV and visible domains. *Limnol. Oceanogr.* **26**: 43-53.

Bricaud, A. & Stramski, D. 1990. Spectral absorption coefficients of living phytoplankton and non-algal biogenous matter: a comparison between the Peru upwelling area and the Sargasso Sea. *Limnol. Oceanogr.* **35**:562-582.

Bukata, R. P., Bruton, J. E., Jerome, J. H., Jain, S. C. & Zwick, H. H. 1981a. Optical water quality model of Lake Ontario. 2. Determination of chlorophyll a and suspended mineral concentrations of natural waters from submersible and low altitude remote sensors. *Appl. Optics* **20**: 1704-1714.

Bukata, R. P., Jerome, J. H., Bruton, J. E., Jain, S. C. & Zwick, H. H. 1981b. Optical water quality model of Lake Ontario. 1. Determination of the optical cross sections of organic and inorganic particulates in Lake Ontario. *Appl. Optics* **20**: 1696-1703.

Bukata, R. P., Jerome, J. H., Kondratyev, K. Y. & Pozdnyakov, D. V. 1991. Satellite monitoring of optically-active components of inland waters: an essential input to regional climate change impact studies. *J. Great Lake Res.* **17**: 470-478.

Carder, K. L., Chen, F. R., Lee, Z. P., Hawes, S. K. & Kamykowski, D. 1999. Semianalytic Moderate-Resolution Imaging Spectrometer algorithms for chlorophyll a and absorption with bio-optical domains based on nitrate-depletion temperatures. *J. Geophys. Res.* **104**:5403-21.

Carder, K. L., Steward, R. G., Harvey, G. R., & Ortner, P. B. 1989. Marine humic and fluvic acids: Their effect on remote sensing of ocean chlorophyll. *Limnol. Oceanogr.* **34**: 68-81.

Chisholm, S. W. 1992. Phytoplankton size. *In* Falkowski, P. G. & Woodhead, A. D. [Eds.] *Primary Productivity and Biogeochemical Cycles in the Sea.* Plenum Press, New York, pp.213-37.

Chisholm, S. W., Olson, R. J., Zettler, E. R., Goericke, R., Waterbury, J. B. & Welschmeyer, N. A. 1988. A novel free-living prochlorophyte abundant in the oceanic euphotic zone. *Nature* **334**: 340-343.

Ciotti, A. M., Lewis, M. R. & Cullen, J. J. 2002. Assessment of the relationships between dominant cell size in natural phytoplankton communities and the spectral shape of the absorption coefficient. *Limnol. Oceanogr.* **47**:404-17.

Ciotti, A. M., Cullen, J. J. & Lewis, M. R. 1999. A semi-analytical model of the influence of phytoplankton community structure on the relationship between light attenuation and ocean color. *J. Geophys. Res.* **104**:1559-78.

Claustre, H. M. 1994. The trophic status of various oceanic provinces as revealed by phytoplankton pigment signatures. *Limnol. Oceanogr.* **39**:1206-10.

Cleveland, J. S., Perry, M. J., Kiefer, D. A. & Talbot, M. C. 1989. Maximal quantum yield of photosynthesis in the northwestern Sargasso Sea. *J. Mar. Res.* **47**: 869-886.

Côté, B. & Platt, T. 1983. Day-to-day variations in the spring-summer photo-synthetic parameters of coastal marine phytoplankton. *Limnol. Oceanogr.* **28**: 320-344.

Côté, B. & Platt, T. 1984. Utility of the light-saturation curve as an operational model for quantifying the effects of environmental conditions on phytoplankton photosynthesis. *Mar. Ecol. Prog. Ser.* **18**: 57-66.

Cullen, J. J. & Lewis, M. R. 1988. The kinetics of algal photoadaptation in the context of vertical mixing. *J. Plank. Res.* **10**(5): 1039-1063.

Cullen, J. J., Franks, P. J. S., Karl, D. M. & Longhurst, A. 2002. Physical influences on marine ecosystem dynamics. *In* Robinson A.R., McCarthy J.J. & Rothchild, B.J. [Eds.] *The Sea-Volume 12*, Wiley, New York, pp. 297-336.

Cushing, D. H. 1989. A difference in structure between ecosystems in strongly stratified waters and in those that are only weakly stratified. *J. Plankton Res.* **11**:1-13.

Doerffer, R. & Fischer, J. 1994. Concentrations of chlorophyll, suspended matter, and gelbstoff in case II waters derived from satellite coastal zone color scanner data with inverse modelling methods. *J. Geophys. Res.* **99**: 7457-7466.

Duysens, L. N. M. 1956. The flattening of the absorption spectrum of suspensions as compared to that of solutions. *Biochimica Biophysica Acta* **19**:1-12.

Falkowski, P. G. & LaRoche, J. 1991. Acclimation to spectral irradiance in algae. *J. Phycol.* **27**:8-14.

Finkel, Z. V. 2001. Light absorption and size scaling of light-limited metabolism in marine diatoms. *Limnol. Oceanogr.* **46**:86-94.

Fujiki, T. & Taguchi, S. 2002. Variability in chlorophyll a specific absorption coefficient in marine phytoplankton as a function of cell size and irradiance. *J. Plankton Res.* **24**:859-74.

Garver, S. A. & Siegel, D. A. 1997. Inherent optical property inversion of ocean color spectra and its biogeochemical interpretation. 1. Time series from the Sargasso Sea. *J. Geophys. Res.* **102**: 18607-18625.

Geider, R. J. & Osborne, B. A. 1992. *Algal Photosynthesis: the measurement of algal gas exchange.* Routledge, Chapman and Hall, New York, 256 pp.

Geider, R. J. & Platt, T. 1986. A mechanistic model of photoadaptation in microalgae. *Mar. Ecol. Prog. Ser.* **30**:85-92.

Geider, R. J., Platt, T. & Raven, J. A. 1986. Size dependence of growth and photosynthesis in diatoms: a synthesis. *Mar. Ecol. Prog. Ser.* **30**:93-104.

Goericke, R. 2002. Top-down control of phytoplankton biomass and community structure in the monsoon Arabian Sea. *Limnol. Oceanogr.* **47**:1307-1323.

Gordon, H. R. & Morel, A. 1983. *Remote Assessment of Ocean Color for Interpretation of Satellite Visible Imagery. A Review.* Springer-Verlag, New York. 114 pp.

Gran, H. H. & Braarud, T. 1935. A quantitative study of the phytoplankton in the Bay of Fundy and the Gulf of Maine (including observations on hydrography, chemistry and turbidity). *Jour. Biol. Board of Canada* **1**:279-467.

Gustafson, D. E., Stoecker, D. K., Johnson, M. D., Van Heukelem, W. F. & Sneider, K. 2000. Cryptophyte algae are robbed of their organelles by the marine ciliate *Mesodinium rubrum. Nature* **405**: 1049-1052.

Harris, G. P. 1978. Photosynthesis, productivity and growth: the physiological ecology of phytoplankton. *Arch. Hydrobiol. Beih. Ergeb. Limnol.* **20**:1-171.

Harrison, W. G. & Platt, T. 1980. Variations in assimilation number of coastal marine phytoplankton: Effects of environmental co-variates. *J. Plankton Res.* **2**: 249-260.

Harrison, W. G., Platt, T. & Lewis, M. R. 1985. The utility of light-saturation models for estimating marine primary productivity in the field: A comparison with conventional "simulated" in situ methods. *Can J. Fish. Aquat. Sci.* **42**: 864-872.

Head, E. J. H. & Horne, E. P. W. 1993. Pigment transformation and vertical flux in an area of convergence in the North Atlantic. *Deep-Sea Res.* **40**: 329-346.

Hoepffner, N. & Sathyendranath, S. 1991. Effect of pigment composition on absorption properties of phytoplankton. *Mar. Ecol. Prog. Ser.* **73**: 11-23.

Hoepffner, N. & Sathyendranath, S. 1992. Bio-optical characteristics of coastal waters: Absorption spectra of phytoplankton and pigment distribution in the western North Atlantic. *Limnol. Oceanogr.* **37**: 1660-1679.

Hoepffner, N. & Sathyendranath, S. 1993. Determination of the major groups of phytoplankton pigments from the absorption spectra of total particulate matter. *J. Geophys. Res.* **98**: 22789-22803.

Højerslev, N. K., 1998. Spectral light absorption by gelbstoff in coastal waters displaying highly different concentrations. In *Proceedings, Ocean Optics XIV*, Ackelson, S. G. & Campbell, J. [Eds] Office of Naval Research, Washington, DC.

Holm-Hansen, O., Lorenzen, C. J., Holmes, R. W. & Strickland, J. D. H. 1965. Fluorometric determination of chlorophyll. *J. cons. int. Explor. Mer* **30**: 3-15.

IOCCG. 2000. *Remote Sensing of Ocean Colour in Coastal, and Other Optically-Complex Waters.* Sathyendranath, S. [Ed.], Reports of the International Ocean-Colour Coordinating Group, No. 3, IOCCG, Dartmouth, Canada.

Irwin, B., Caverhill, C., Anning, J., Macdonald, S., Hodgson, M. Horne, E. P. W., & Platt, T. 1989. Productivity localized around seamounts in the Atlantic (PLASMA) during June and July 1987. *Can. Data Rep. Fish. Aquat. Sci.* **732**: 227 pp.

Jassby, A. D. & Platt, T. 1976. Mathematical formulation of the relationship between photosynthesis and light for phytoplankton. *Limnol. Oceanogr.* **21**: 540-547.

Jeffrey, S. W. & Vesk, M. 1997. Introduction to marine phytoplankton and their pigment signatures. *In* Jeffrey, S. W., Mantoura, R. F. C. & Wright, S. W. [Eds.] *Phytoplankton pigments in oceanography.* UNESCO, Paris, pp. 37-84.

Jerlov, N. G. 1968. *Optical Oceanography* Elsevier, Amsterdam, 194 pp.

Jewson, D. H. 1976. The interaction of components controlling net photosynthesis in a well-mixed lake (Lough Neagh, Northern Ireland). *Freshwater Biol.* **6**:551-76.

Johnsen, G., Nelson, N. B., Jovine, R. V. M.& Prézelin, B. B. 1994. Chromoprotein- and pigment-dependent modeling of spectral light absorption in two dinoflagellates, *Prorocentrum minimum* and *Heterocapsa pygmaea. Mar. Ecol. Prog. Ser.* **114**: 245-258.

Karl, D. M. 1999. A sea of change: biogeochemical variability in the North Pacific Subtropical Gyre. *Ecosystems* **2**:181-214.

Kishino, M., Takahashi, M., Okami, N. & Ichimura, S. 1985. Estimation of the spectral absorption coefficients of phytoplankton in the sea. *Bull. Mar. Sci.* **37**: 634-642.

Kirk, J. T. O. 1994. *Light and Photosynthesis in Aquatic Ecosystems.* Cambridge University Press, Cambridge. pp. 509.

Kopelevich, O. V., Lutsarev S. V. & Rodionov, V. V. 1989. Light spectral absorption by yellow substance of ocean water. *Okeanologiya,* **29**: 409-414.

Kyewalyanga, M., Platt, T. & Sathyendranath, S. 1992. Ocean primary production calculated by spectral and broad-band models. *Mar. Ecol. Prog. Ser.* **85**: 171-185.

Kyewalyanga, M. N., Platt, T. & Sathyendranath, S. 1997. Estimation of the photosynthetic action spectrum: implication for primary production models. *Mar. Ecol. Prog. Ser.* **146**:207-223.

Kyewalyanga, M., Platt, T., Sathyendranath, S., Lutz, V. A. & Stuart, V. 1998. Seasonal variations in physiological parameters of phytoplankton across the North Atlantic. *J. Plankton Res.* **20**:17-42.

Kyewalyanga, M., Sathyendranath, S. & Platt, T. 2002. Effect of *Mesodinium rubrum* (= *Myrionecta rubra*) on the action and absorption spectra of phytoplankton in a coastal marine inlet. *J. Plankton Res.* **24**:687-702.

Lazzara, L., Bricaud, A. & Claustre, H. 1996. Spectral absorption and fluorescence excitation properties of phytoplanktonic populations at a mesotrophic and an oligotrophic site in the tropical North Atlantic (EUMELI program). *Deep Sea Res.* **43**: 1215-1240.

Lee, Z. P., Carder, K. L., Peacock, T. G., Davis, C. O. & Mueller, J. L. 1996. Method to derive ocean absorption coefficients from remote-sensing reflectance. *Appl. Optics* **35**: 453-462.

Lee, Z., Carder, K. L., Mobley, C. D., Steward, R. G. & Patch, J. S. 1999. Hyperspectral remote sensing for shallow waters: 2. Deriving bottom depths and waters properties by optimization. *Appl. Optics* **38**: 3831-3843.

Legendre, L. & LeFevre, J. 1989. Hydrodynamical singularities as controls of recycled versus export production in the oceans. *In*: Berger, W. H., Smetacek, V. S. & Wefer, G. [Eds] *Productivity in the Ocean: Present and Past.* John Wiley & Sons, Chichester, p 44-63

Lewis, M. R., Cullen, J. J. & Platt, T. 1984. Relationship between vertical mixing and photoadaptation of phytoplankton: Similarity criteria. *Mar. Ecol. Prog. Ser.* **15**: 141-149.

Li, W. K. W. 1986. Experimental approaches to field measurements: methods and interpretation. *Can. Bull. Fish. Aquat. Sci.* **214**: 251-286.

Li, W. K. W. 1995. Composition of ultraphytoplankton in the central North Atlantic. *Mar. Ecol. Prog. Ser.* **122**:1-8.

Li, W. K. W. 2002. Macroecological patterns of phytoplankton in the northwestern North Atlantic Ocean. *Nature* **419**:154-57.

Li, W. K. W. & Dickie, P. M. 2001. Monitoring phytoplankton, bacterioplankton, and viroplankton in a coastal inlet (Bedford Basin) by flow cytometry. *Cytometry* **44**:236-246.

Li, W. K. W. & Harrison, W. G. 2001. Chlorophyll, bacteria and picophytoplankton in ecological provinces of the North Atlantic. *Deep-Sea Res.* **48**:2271-2293.

Longhurst, A. 1998. *Ecological Geography of the Sea.* Academic Press, San Diego. pp. 398.

Longhurst, A., Sathyendranath, S., Platt, T. & Caverhill, C. 1995. An estimate of global primary production in the ocean from satellite radiometer data. *J. Plankton. Res.* **17**:1245-1271.

Lutz, V. A., Sathyendranath, S. & Head, E. J. H. 1996. Absorption coefficient of phytoplankton: regional variations in the North Atlantic. *Mar. Ecol. Prog. Ser.* **135**: 197-213.

Lutz, V. A., Sathyendranath, S., Head, E. J. H. & Li, W. K. W. 1998. Differences between *in vivo* absorption and fluorescence excitation spectra in natural samples of phytoplankton. *J. Phycol.* **34**: 214-227.

Mackey, M. D., Mackey, D. J., Higgens, H. W. & Wright, S. W. 1996. CHEMTAX- a program for estimating class abundances from chemical markers: application to HPLC measurements of phytoplankton. *Mar. Ecol. Prog. Ser.* **144**:265-283.

Marañón, E. & Holligan, P. M. 1999. Photosynthetic parameters of phytoplankton from 50°N to 50°S in the Atlantic Ocean. *Mar. Ecol. Prog. Ser.* **176**: 191-203.

Margalef, R. 1965. Ecological correlations and the relationship between primary productivity and community structure. it In Goldman, C. R. [Ed.] *Primary Productivity in Aquatic Environments.* University of California Press, Berkley, pp. 355-364.

Margalef, R. 1967. Some concepts relative to the organization of plankton. *Oceanogr. Mar. Biol. Ann. Rev.* **5**:257-289.

Margalef, R.. 1978. Life-forms of phytoplankton as survival alternatives in an unstable environment. *Oceanol. Acta* **1**:493-509.

Margalef, R., Estrada, M. & Blasco, D. 1979. Functional morphology of organisms involved in red tides, as adapted to decaying turbulence. *In*: Taylor, D. T. & Seliger, H. H. [Eds] *Toxic Dinoflagellate Blooms.* Elesvier/North Holland, New York, pp.89-94.

Mitchell, B. G. & Kiefer, D. A. 1988. Chlorophyll a specific absorption and fluorescence excitation spectra for light-limited phytoplankton. *Deep Sea Res.* **35**:639-63.

Moore, L. R., Goericke, R. & Chisholm, S. W. 1995. Comparative physiology of *Synechococcus* and *Prochlorococcus*: Influence of light and temperature on growth, pigments, fluorescence and absorptive properties. *Mar. Ecol. Prog. Ser.* **116**: 259-275.

Morel, A. 1978. Available, usable and stored radiant energy in relation to marine photosynthesis. *Deep Sea Res.* **25**: 673-688.

Morel, A. 1991. Light and marine photosynthesis: a spectral model with geochemical and climatological implications. *Prog. Oceanog.* **26**: 263-306.

Morel, A. 1997. Consequences of a Synechococcus bloom upon the optical properties of oceanic (case 1) waters. *Limnol. Oceanogr.* **42**:1746-1754.

Morel, A. & Bricaud, A. 1981. Theoretical results concerning light absorption in a discrete medium, and application to specific absorption of phytoplankton. *Deep Sea Res.* **28**: 1375-1393.

Morel, A. & Prieur, L. 1977. Analysis of variations in ocean color. *Limnol. Oceanogr.* **22**:709-722.

Odum, E. P. 1959. *Fundamentals of Ecology.* W. B. Saunders Company, Philadelphia. pp. 546.

O'Reilly, J. E. & others 2000. Ocean color chlorophyll a algorithms for Sea-WiFS, OC2, and OC4: Version 4. In: Hooker SB, Firestone ER (eds) SeaWiFS Postlaunch Technical Report Series Volume 11, SeaWiFS Post-launch Calibration and Validation Analyses, Part 3. NASA, Goddard Space Flight Center, Greenbelt, Maryland. p 9-23

Platt, T., Gallegos, C. L. & Harrison, W. G. 1980. Photoinhibition of photosynthesis in natural assemblages of marine phytoplankton. *J. Mar. Res.* **38**: 687-701.

Platt, T. & Jassby, A. D. 1976. The relationship between photosynthesis and light for natural assemblages of coastal marine phytoplankton. *J. Phycol.* **12**: 421-430.

Platt, T., Jauhari, P. & Sathyendranath, S. 1992. The importance and measurement of new production. *In* Falkowski, P. G. & Woodhead, A. D. [Eds.] *Primary Productivity and Biogeochemical Cycles in the Sea.* Plenum Press, New York, 273-284.

Platt, T. & Sathyendranath, S. 1988. Oceanic primary production: Estimation by remote sensing at local and regional scales. *Science* **241**: 1613-1620.

Platt, T. & Sathyendranath, S. 1999. Spatial structure of pelagic ecosystem processes in the global ocean. *Ecosystems* **2**:384-394.

Platt, T. & Subba Rao, D. V. 1975. Primary production of marine microphytes. *In* Copper, J. P [Ed.] *Photosynthesis and Productivity in Different Environments.* Cambridge University Press, Cambridge, pp. 249-280.

Prieur, L. & Sathyendranath, S. 1981. An optical classification of coastal and oceanic waters based on the specific spectral absorption curves of phytoplankton pigments, dissolved organic matter, and other particulate materials. *Limnol. Oceanogr.* **26**:671-689.

Raven, J. A. 1998. The twelfth Tansley Lecture. Small is beautiful: the pico-phytoplankton. *Functional Ecology* **12**:503-513.

Rodriguez, J., Tintore, J., Allen, J. T., Blanco, J. M., Gomis, D., Reul, A., Ruiz, J., Rodriguez, V., Echevarria, F. & Jimenez-Gomez, F. 2001. Mesoscale vertical motion and the size structure of phytoplankton in the ocean. *Nature* **410**:360-363.

Roesler, C. S. & Perry, M. J. 1995. *In situ* phytoplankton absorption, fluorescence emission, and particulate backscattering spectra determined from reflectance. *J. Geophys. Res.* **100**:13279-13294.

Roesler, C. S., Perry, M. J. & Carder, K. L. 1989. Modeling *in situ* phytoplankton absorption from total absorption spectra in productive inland marine waters. *Limnol. Oceanogr.*, **34**: 1510-1523.

Sathyendranath, S., Cota, G., Stuart, V., Maass, H. & Platt, T. 2001. Remote sensing of phytoplankton. pigments: a comparison of empirical and theoretical approaches. *Int. J. Remote Sensing* **22**:249-273.

Sathyendranath, S., Lazzara, L. & Prieur, L. 1987. Variations in the spectral values of specific absorption of phytoplankton. *Limnol. Oceanogr.* **32**: 403-415.

Sathyendranath, S., Longhurst, A., Caverhill, C. M. & Platt, T. 1995. Regionally and seasonally differentiated primary production in the North Atlantic. *Deep-Sea Res.* **42**: 1773-1802.

Sathyendranath, S. & Platt, T. 1988. The spectral irradiance field at the surface and in the interior of the ocean: A model for applications in oceanography and remote sensing. *J. Geophys. Res.* **93**: 9270- 9280.

Sathyendranath, S. & Platt, T. 1989. Computation of aquatic primary production: Extended formalism to include effect of angular and spectral distribution of light. *Limnol. Oceanogr.* **34**: 188-198.

Sathyendranath, S., Platt, T., Horne, E. P. W., Harrison, W. G., Ulloa, O., Outerbridge, R. & Hoepffner, N. 1991. Estimation of new production in the ocean by compound remote sensing. *Nature* **353**: 129-133.

Sathyendranath, S., Stuart, V., Irwin, B. D., Maass, H., Savidge, G., Gilpin, L. & Platt, T. 1999. Seasonal variations in bio-optical properties of phytoplankton in the Arabian Sea. *Deep-Sea Res.* **46**:633-653.

Siegel, D. A. and others 2001. Bio-optical modeling of primary production on regional scales: the Bermuda BioOptics project. *Deep-Sea Res.* **48**: 1865-1896.

Sosik, H. M. 1996. Bio-optical modelling of primary production: Consequences of variability in quantum yield and specific absorption. *Mar. Ecol. Prog. Ser.* **143**: 225-238.

Sosik, H. M. & Mitchell, B. G. 1991. Absorption, fluorescence, and quantum yield for growth in nitrogen-limited *Dunaliella tertiolecta*. *Limnol. Oceanogr.* **36**:910-921.

Sosik, H. & Mitchell, B. G. 1994. Effect of temperature on growth, light absorption, and quantum yield in *Dunaliella tertiolecta* (Chlorophyceae). *J. Phycol.* **30**: 833-840.

Sosik, H. M. & Mitchell, B. G. 1995. Light absorption by phytoplankton, photosynthetic pigments and detritus in the California Current System. *Deep-Sea Res.* **42**: 1717-1748.

Steemann Nielsen, E. 1952. The use of radioactive carbon (^{14}C) for measuring organic production in the sea. *J. Cons. perm. int. Explor. Mer* **18**: 117-140.

Stramski, D., Sciandra, A. & Claustre, H. 2002. Effects of temperature, nitrogen, and light limitation on the optical properties of the marine diatom *Thalassiosira pseudonana*. *Limnol. Oceanogr.* **47**:392-403.

Strom, S. L., Miller, C. B. & Frost, B. W. 2000. What sets lower limits to phytoplankton stocks in high-nitrate, low-chlorophyll regions of the open ocean? *Mar. Ecol. Prog. Ser.* **193**: 19-31.

Stuart, V., Sathyendranath, S., Head, E. J. H., Platt, T., Irwin, B. & Maass, H. 2000. Bio-optical characteristics of diatom and prymnesiophyte populations in the Labrador Sea. *Mar. Ecol. Prog. Ser.* **201**: 91-106.

Stuart, V., Sathyendranath, S., Platt, T., Maass, H. & Irwin, B.D. 1998. Pigments and species composition of natural phytoplankton populations: effect on the absorption spectra. *J. Plankton Res.* **20**:187-217.

Taguchi, S. 1976. Relationship between photosynthesis and cell size of marine diatoms. *J. Phycol.* **12**: 185-189.

Yentsch, C. S. & Phinney, D. A. 1989. A bridge between ocean optics and microbial ecology. *Limnol. Oceanogr.* **34**:1694-1705.